Centro de Investigaciones en Óptica A.C.

TESIS

POLARÍMETRO DE MUELLER COMPLETO BASADO EN RETARDADORES DE CRISTAL LÍQUIDO Y MODULADORES FOTOELÁSTICOS

QUE PARA OBTENER EL GRADO DE:

MAESTRO EN OPTOMECATRÓNICA

PRESENTA

Ing. Alicia Fernanda Torales Rivera

LEÓN, GUANAJUATO, ABRIL 2010

A MIS PADRES

AGRADECIMIENTOS

A mi madre, por siempre creer en mí y alentarme a seguir adelante.

A mi padre, por todo el apoyo que siempre me ha dado durante mi vida y particularmente a lo largo de mis estudios de postgrado.

A mi hermana Ceci, por toda la paciencia y cariño que siempre me ha tenido.

A mis asesores, el Dr. Geminiano Martínez Ponce y la Dra. Cristina Solano Sosa, por todo lo que me enseñaron, su infinita paciencia y muy especialmente por haberme apoyado y creído en mí desde el principio.

A mis sinodales, el Dr. Daniel Malacara Hernández y Dr. Juan Manuel López Ramírez, por muy amablemente haber consentido a revisar y evaluar este trabajo.

Al Dr. Sergio Calixto, por haberme proporcionado un lugar de trabajo cerca de mis asesores y laboratorio, y por todo su apoyo.

Al Consejo Nacional de Ciencia y Tecnología (CONACYT) y el Consejo de Ciencia y Tecnología del Estado de Guanajuato (CONCYTEG) por las becas que me fueron otorgadas durante mis estudios.

INDEX

List of Figures

List of Tables

Thesis Title: “COMPLETE MUELLER POLARIMETER BASED ON LIQUID CRYSTAL VARIABLE RETARDERS AND PHOTOELASTIC MODULATORS”

Candidate: Eng. Alicia Fernanda Torales Rivera
Chairsperson: Dr. Geminiano Martínez Ponce / Dra. Cristina Solano
Program: Masters in Optomechatronics

The implemented Mueller polarimeter works in transmission and is constituted by two modules: a polarisation state generator (PSG) and a polarisation state analyser (PSA). The PSG is based on a dual system of liquid crystal variable retarders (LCVR) set up in accordance to generate any state of polarisation by combining the induced retardance in each. ON the other hand, the PSA is constituted by a dual Photoelastic Modulator (PEM) system which in turn allows for the measurement of the four Stokes parameters without the need to modify the experimental setup.

The measurement for the 16 element Mueller matrix associated to a transparent optical medium is achieved by using a single wavelength (λ = 632.8nm). The procedure consists on propagating a beam of light with four different polarisation states (generated by the PSG) through the sample and to measure the polarisation state in the outcoming beam with the PSA. The aforementioned provides a system of equations which will in turn lead to details on all the sample’s linear anisotropies such as linear and circular birefringence and linear and circular diattenuation. The system uses a silicon photodiode as a means of detecting the incident beam and its behaviour. The photoreceiver encompasses, along with the photodiode, a preamplifying stage and a lock-in amplifier for signal detection and analysis. The system is controlled via a computer and a data acquisition card from National Instruments™. The control program was developed in Labview™ and allows the user to take measurements either manually, step by step or with an automatic sequence.

The applications for this measurement device include material analysis for the development of optical devices, characterisation of optical tissue, detection of polluting substances, and pharmaceutics quality control among many others.

Nombre de la Tesis: “POLARÍMETRO DE MUELLER COMPLETO BASADO EN RETARDADORES DE CRISTAL LÍQUIDO Y MODULADORES FOTOELÁSTICOS”

Defensor: Ing. Alicia Fernanda Torales Rivera
Asesor: Dr. Geminiano Martínez Ponce / Dra. Cristina Solano
Postgrado: Maestría en Optomecatrónica

El polarímetro de Mueller implementado funciona en transmisión y esta compuesto por dos módulos: un generador y un analizador de estados de polarización, PSG y PSA, respectivamente. El PSG está constituido por un sistema dual de placas retardadoras variables de cristal líquido (LCVR) dispuestos de tal manera que pueden generar cualquier estado de polarización al combinar los retardos inducidos en cada una. Por otra parte, el PSA esta formado por un sistema dual de moduladores fotoelásticos (PEM) que permiten la medición de los cuatro parámetros de Stokes sin modificar el arreglo experimental.

La medición de los 16 elementos de la matriz de Mueller asociados a un medio óptico transparente se lleva a cabo utilizando una sola longitud de onda (λ = 632.8nm). El procedimiento consiste en propagar un haz de luz con cuatro estados de polarización diferentes generados por el PSG a través de la muestra y medir los estados de polarización en el haz transmitido empleando el PSA. Lo anterior proporciona un sistema de ecuaciones que llevará a la obtención de todas las anisotropías lineales de la muestra bajo estudio (birrefringencia lineal / circular, diatenuación lineal / circular). El sistema utiliza como dispositivo de detección un fotodiodo de silicio con etapa de preamplificación y un amplificador de amarre de fase para el análisis de la señal. El sistema es controlado por medio de una computadora y una tarjeta de adquisición de datos de National Instruments™. El programa de control desarrollado en la plataforma Labview™ permite al usuario tomar las mediciones de manera manual, paso a paso, o con una secuencia automática.

Las aplicaciones en donde las bondades de este instrumento de medición son de gran utilidad incluyen el estudio de materiales para el desarrollo de dispositivos ópticos, la caracterización de tejido biológico, la detección de contaminantes, el control de calidad de fármacos, entre otros muchos.

Chapter 1
Introduction

1.1 On Polarisation and its importance in Science

Light polarisation is widely acknowledged to be one of the most important properties of light (Collet, 2005), being broadly used in several applications in a wide variety of fields, including Medicine, Holography, Biology, Pharmaceutics, and Food Processing. This property has led to numerous discoveries and technological breakthroughs all the way back to the 1600s (Goldstein, 2003).

According to Maxwell's theory, light, as an electromagnetic wave, presents both an oscillating electric field and an oscillating magnetic field. The former oscillating at the same frequency than the latter, but with a perpendicular orientation. Only the electrical field is considered when determining the polarisation state of light.

1.2 Polarisation and Coherence

In 2005, Nobel Laureate R.J. Glauber proposes that the coherence condition is fulfilled only if the light is totally polarised (Réfrégier, 2007). Additionally, Emil Wolf (Pye, 2001) stated that there is an intimate relationship between polarisation properties of a random electromagnetic beam and its coherence properties.

Assuming that monochromatic light travels in sinusoidal waves, the amplitude and phase of such waves can only be maintained constant throughout certain amount of time. Afterwards, the amplitude is bound to vary the further it travels. The period of time in which the phase of a light wave remains on average, constant is known as coherence time.

Given that it is possible to define a polarisation state only when both components of light maintain the same relative phase one with respect to the other, it is possible to say that polarisation of light is only possible when the light is coherent.

Furthermore, a single ray of light consists of two independent oppositely polarised rays. When passed through a birefringent (doubly refractive) crystal, such as calcite, two emerging rays can be observed. This is due to the fact that in a birefringent crystal, these two rays experience different refractive indexes.
If then, a second crystal is used through which both rays pass through, by means of rotation one of the beams can be completely extinguished, whereas the other one's intensity is maximised. By rotating the second crystal again, another 90°, the first ray reappears at maximum intensity and the second one vanishes. Finally, if the crystal is to be reoriented at an angle of 45°, the

intensities of the two rays are equal. These two rays are then said to be polarised (Collet, 2005).

The two rays represent the “S” and the “P” polarisation states. The S and P notations come from the German words for parallel (*paralelle*) and perpendicular (*senkrecht*). This way, a light beam can be represented by two components, the P polarisation component, usually denoted as E_y and the S polarisation component, denoted as E_x.

As a wave, light propagates sinusoidally throughout space at an angular frequency ω. If we represent the maximum amplitudes of the two components as E_{ox} and E_{oy} and the phases as ϕ_x and ϕ_y, a beam of light can be represented by the following equations:

$$E_x(z,t) = E_{ox} \cos(\omega t - kz + \phi_x)$$
$$E_y(z,t) = E_{oy} \cos(\omega t - kz + \phi_y)$$

Where $k = 2\pi/\lambda$, which is the wave number magnitude.

In the case in which the components have identical phases, one can obtain linearly polarised light in several directions. It is possible to combine the orthogonal components of linearly polarised light so as to produce other types of polarised light.

Another case worth noting is when the components’ phases are 90° out of phase with each other, whereas the amplitudes are exactly the same. This results in circularly polarised light.

If neither of the conditions described above is met, then the light will present an elliptical polarisation, which is considered to be the most general case. In order to analitically visualise the above description, we shall briefly develop some theory.

1.2.1 Linear Polarisation

Considering light as an electric field whose magnitude oscillates through time and which is oriented along the polarisation axis, the polarisation is linear. Thus, for light propagating along the z axis, it is possible to describe linearly polarised light along the x axis as:

$$E_x = E_{ox} \sin[\omega t - kz + \phi_o] \mathbf{i} \qquad (1.1)$$

And along the y axis as:

$$E_y = E_{oy} \sin[\omega t - kz + \phi_y] \mathbf{j} \qquad (1.2)$$

Where:

$E_{ox,oy}$ → Amplitude (electric field magnitude)

i → Unit vector along the x axis

j → Unit vector along the y axis

$\omega = 2\pi\nu$ (ν = wave frequency)

$k = 2\pi/\lambda$ (λ = wavelength)

ϕ_o = absolute phase

Hence, the electric field of linearly polarised light may be described as the vector sum of E_x and E_y.

$$E = E_x + E_y$$

$$= \{E_{ox} \mathbf{i} + E_{oy} \mathbf{j}\} \sin[\omega t - kz + \phi_o] \qquad (1.3)$$

This configuration may be better visualised in the following figure, in which the two orthogonal components are represented in blue and the resulting polarisation in red.

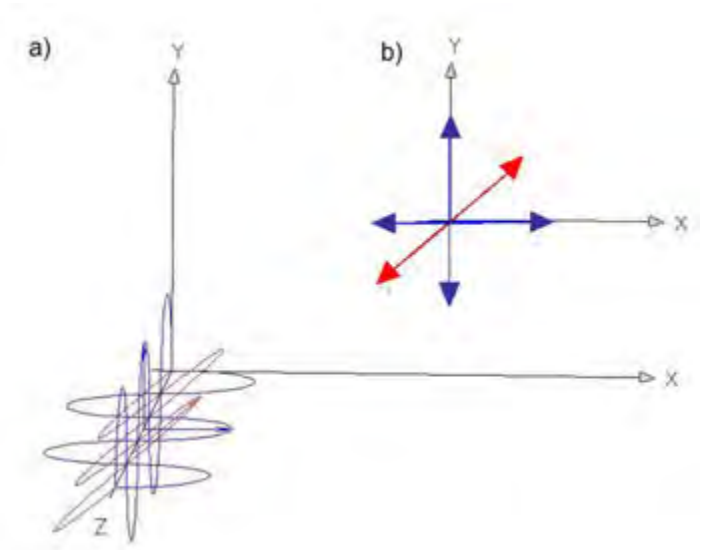

Figure 1.1. Representation of linearly polarised light at 45°. a) isometric view. b) frontal view.

1.2.2 Circular Polarised Light

Consider the case in which both components are equal in magnitude, but 90° ($\pi/2$ rad) apart from each other in phase.

$$E_{rcp} = E_o\{\sin[\omega t - kz + \phi_o]\ \mathbf{i} + \sin[\omega t - kz + \phi_o + \pi/2]\ \mathbf{j}\}$$
$$= E_o\{\sin[\omega t - kz + \phi_o]\ \mathbf{i} + \cos[\omega t - kz + \phi_o]\ \mathbf{j}\} \quad (1.4a)$$

$$E_{lcp} = E_o\{\sin[\omega t - kz + \phi_o]\ \mathbf{i} + \sin[\omega t - kz + \phi_o - \pi/2]\ \mathbf{j}\}$$
$$= E_o\{\sin[\omega t - kz + \phi_o]\ \mathbf{i} - \cos[\omega t - kz + \phi_o]\ \mathbf{j}\} \quad (1.4b)$$

This configuration results in circularly polarised light, which can be better visualised in the following figure:

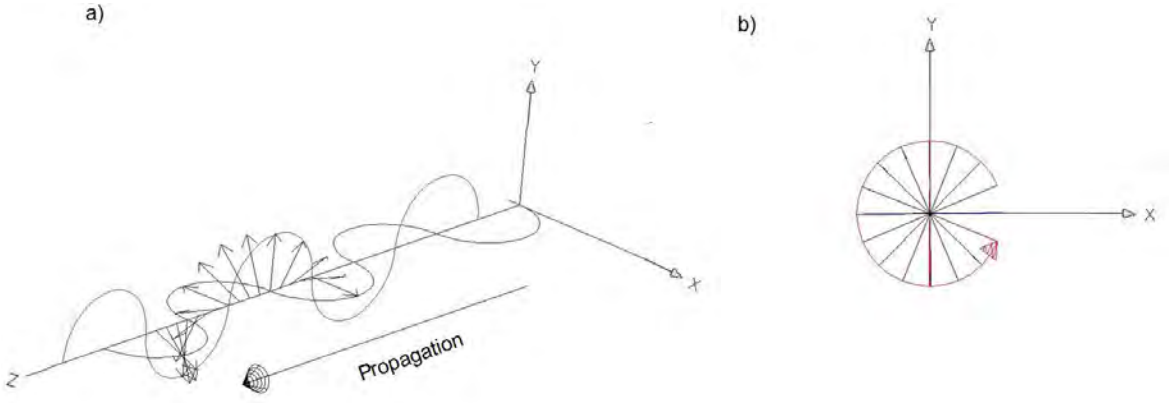

Figure 1.2. Representation of circularly polarised light (represented by the arrows). a) isometric view. b) frontal view.

As seen from the z axis, the electric field-representing vector has a constant magnitude, but its orientation changes over time in such a way that the vector's head describes a circular route over time. Thus, the vector in the z=0 plane seems to draw a circle clockwise when seen from the z+ side in front of the origin.

Hence, this polarisation is called "left circularly polarised light".

1.2.3 Elliptically Polarised Light

Elliptically polarised light may be considered as the general case of polarisation. Again, if the phases are separated 90° from each other, but the component $E_y \neq 0$ and $E_y < E_x$, then the light will be elliptically polarised, with the major axis of the ellipse directed along the x axis. If, on the other hand, $E_x \neq 0$ and $E_x < E_y$, the major axis of the ellipse will be along the y axis. Hence, the ellipticity and orientation of the polarisation ellipse will depend on the relative values of E_x and E_y and on their respective relative phases.

Similarly to circularly polarised light, the electric field vector of elliptically polarised light forms an ellipse through time as seen from the z axis. It would appear like a flattened spiral when seen from the xy plane (figure 3).

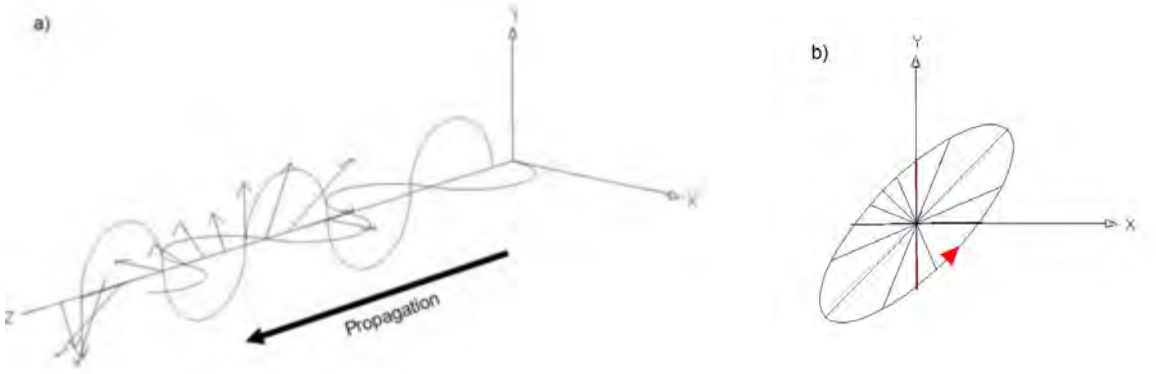

Figure 1.3. Representation of elliptically polarised light (represented by the arrows). a) isometric view. b) frontal view.

Another possible way of obtaining elliptically polarised light is with different phases of 0°, 90°, 180° and 270°, despite having equal amplitudes. Also if $E_x \neq E_y$ and $\phi_x \neq \phi_y$.

1.3 Polarising Elements

1.3.1 Linear Polarisers

Linear polarisers can transmit light, whose electric field vector oscillates within the plane that contains the polariser's axis. This plane's orientation can be varied by rotating the polariser. If the plane is horizontal, the polariser is called a horizontal linear polariser. If the electric field of the light passing through the polariser's got a component that is orthogonal to the polariser's transmission axis, it will suffer attenuation of said component.

Whenever a linear polariser is placed in front (or behind) another linear polariser, both of them with their axes placed orthogonally to each other (crossed polarisers), all light should ideally be extinguished.

1.3.2 Glan Thompson Prism

The Glan Thompson prism configuration is shown in figure 1.4. The prism is polished in such a way that the optical axis is located in the plane of the entrance face as well as parallel to the diagonal cut. This prism has several advantages. Since light enters the crystal normal to the surface and to the optic axis, both the ordinary and the extraordinary rays move normal to the surface, without deviating. For traditional Glan-Thompson prisms, both halves are glued

together. Note that the separating material between both halves of the prism does not necessarily have to have a refraction index which is intermediate to the ordinary and extraordinary rays. What is required is that the angle is such that one of the two rays suffers total internal reflection and the other one does not.

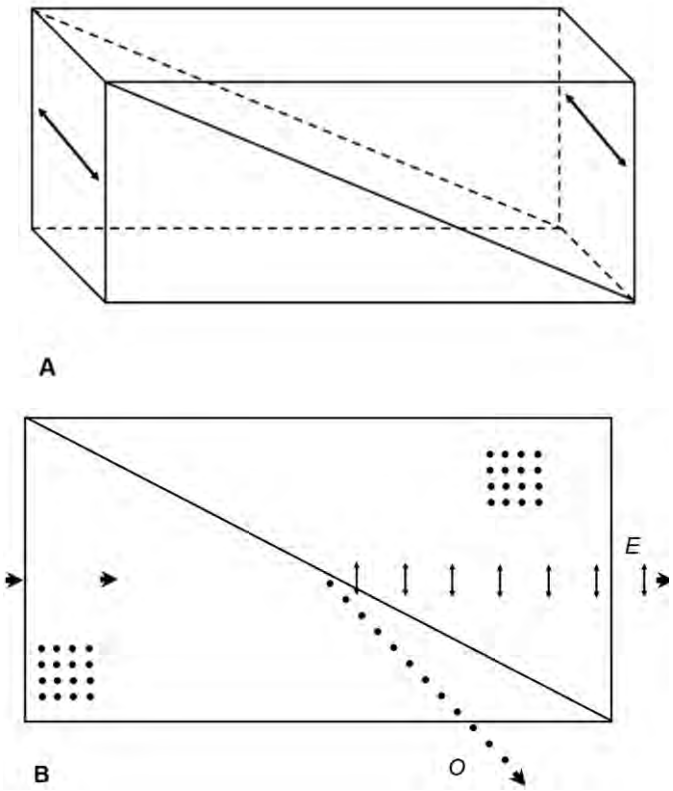

Figure 1.4 – Glan-Thompson prism. Perspective (A) and cross-sectional (B). The optic axis is shown by the double headed arrows in (A) and by the matrix of points in (B).

1.3.3 Dichroic Sheet Polariser

In dichroic sheet polarisers, the molecules within a plastic sheet are re-orientated in such a way that their transition dipole moments are aligned along a specific axis. Thus, light polarised in this same axis is absorbed whereas light polarised orthogonally is transmitted.

1.3.4 Retarders

Retarders make the absolute phases of two orthogonal polarisation components to be varied after propagation, as a function of thickness. A common example is the quarter wave plate retarder ($\lambda/4$), which increases by 90° the phase of a linear polarisation relative to another.

Retardance is an effect caused by the refractive index. As light is transmitted from vacuum to another material, the speed of light is reduced by a factor of 1/n, where n is the refractive index of the material. Since the frequency remains constant when the light passes from one medium to another, this results in a faster variation of the phase angle of light within a body than in vacuum. Consequently, any transparent body increases the phase of light in comparison to the one it has outside the body.

A body that provokes retardation between orthogonal components in the same degree, for any given polarisation, regardless of the orientation of propagation, is said to be isotropic in nature.

1.3.5 Birefringent Plate Retarders

Birefringent plate retarders can cause a phase difference between two orthogonal polarisations.

It is also possible to modify the polarisation state using anisotropic absorption elements.

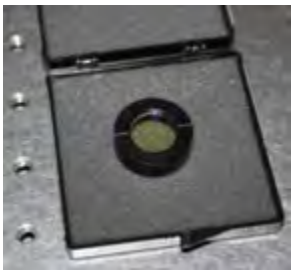

Figure 1.5 – A quarter waveplate retarder.

Consider a linearly polarised light beam that passes through a birefringent crystal or waveplate. Given that linearly polarised light is formed by two components (Eq. 1.3), this causes the two components to experience slightly different refractive indexes.

If we have a plate of thickness d and assuming that the wavelength λ remains the same before and after passing through the medium, the wavelength in the crystal may be defined as λ/n, where n is the crystal's index of refraction. Thus, the total number of waves in the plate is $d/(\lambda/n)$. If each of the mutually orthogonal components is affected by a different refraction index, the phase difference after exiting the plate can be defined as:

$$\delta = 2\pi \frac{d(n_i - n_j)}{\lambda} \qquad (1.5)$$

Where n_i and n_j are the two different refractive indexes affecting the components, hence causing for them to pass through the plate at different speeds (Tompkins, 2005).

1.3.6 Liquid Crystal Variable Retarder (LCVR)

Liquid crystal variable retarders are real-time, continuously tunable waveplates. An LCVR is composed of two plates separated by a few micrometers. This space is filled with nematic liquid crystal, which is a birefringent material whose birefringence can be adjusted by means of a variating applied voltage.

Electrodes are located in specific places among the retarder, so as to enable an electric field to be applied between both plates and hence, the liquid crystal.

Upon application of the voltage, the molecules within the liquid crystal gradually reorientate themselves until they are perpendicular to the plates. As the voltage increases, the molecules continue reorientating, causing a reduction in birefringence and consequently, in retardation (Meadowlark, 2009).

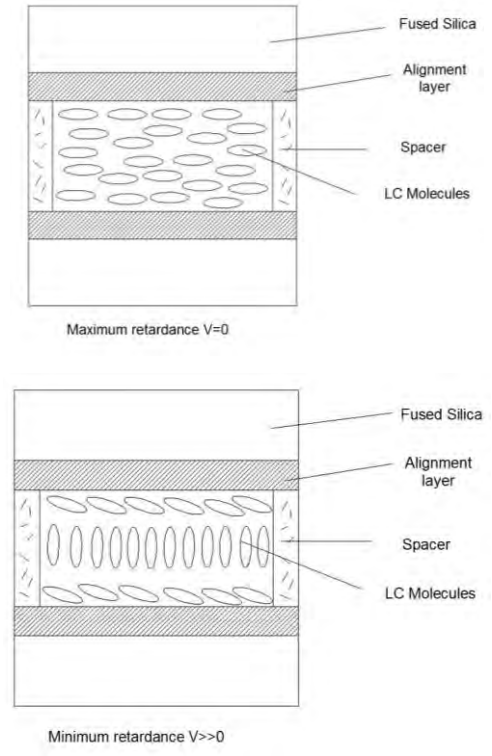

Figure 1.6 – Schematic representation of the principle of operation of an LCVR

1.3.7 Photoelastic Modulator (PEM)

A photoelastic modulator causes a phase shift between the orthogonal components of a light beam to change sinusoidally as a function of time. This phase shift is obtained by making the two perpendicular components of light pass through a waveplate at different speeds. This is achieved by inducing a time-varying birefringence by way of a time-varying stress in a normally isotropic material. An isotropic material will become anisotropic when stressed and will thus induce the same kind of birefringence as an anisotropic crystal like calcite.

A picture of the constituting elements of a photoelastic modulator is shown in figure 1.7. A piezoelectric transducer is a block of crystalline quartz cut at a specific orientation (-18°, Xcut).

A metal electrode is deposited on each of two sides and the transducer is cut in such a way that it resonates at a specified frequency F. The resonance is uniaxial and is directed along the long axis of the crystal. A block of fused quartz is cemented to the end of the transducer. The length of the fused quartz is such that it also has F as the fundamental longitudinal resonance. When both elements are cemented together, resonance of the transducer causes a periodic strain in the fused quartz (Jellison, 2005).

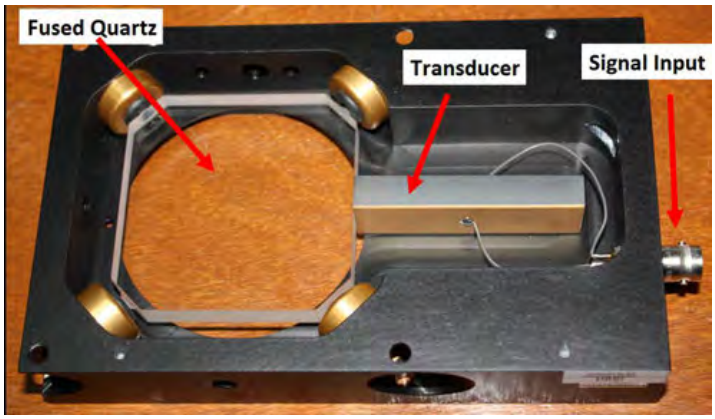

Figure 1.7 – The components of a photoelastic modulator

1.4 Dual PEM Systems in Polarimetry

A dual Photoelastic modulator system can obtain all 16 elements of the Mueller Matrix (provided the four incident polarisation states of the incoming beam are known), which describes the polarisation properties of a material (Goldstein, 2003). The typical configuration for such an ellipsometer would be tuning the first PEM, P1, at frequency F_1 and orientation of 0°, and the second PEM (P2) tuned at frequency F_2 (where F_2 is slightly different from F_1). Furthermore, P2 must have an orientation of 45°. P2 is then followed by a linear polariser at 0°, as shown in figure 1.8.

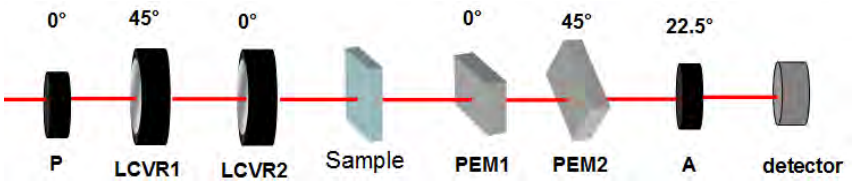

Figure 1.8 – Polarimetric system based on photoelastic modulators(PEM_1 y PEM_2). A is a linear polariser (analyser).

1.4.1 Applications of a Dual Modulator System

Whether in transmission or reflection, certain materials can affect the polarisation state of light that interacts with them. This is due to intrinsic qualities and properties of said materials such as optical activity, chirality and reflectivity.

Applications for Dual PEM Systems range from the medical to the military.

Depending on the wavelength and other parameters, the system enables analysis and characterisation of different materials (most of them organic in nature, but also certain reflecting materials). Such materials are used in medical analysis, holography, food processing and pharmaceutics, among others.

Dual PEM polarimeters are used in astronomy to study light polarisation from nearby stars and sunspots.

Another useful application of this system is in optical fibres. When a fibre is bent, it generates mechanical stress, which in turn causes the polarisation state of the light travelling through the fibre to change. Light polarisation may also vary depending on the environment the fibre is in. Polarimeters are hence used to monitor the polarisation state of light coming out of the fibre (Hinds Instrument, 2005).

Intrinsic qualities of materials have an effect on the way light interacts with them. Properties and characteristics such as stress, defects, reflectivity, and polarisation loss may be determined with the instrument by measuring the polarization state of light after passing through a material.

Other applications include thin film characterisation as well as laser test and measurement.

1.5 Polarisation in Nature

1.5.1 Why is the sky blue?

In other planets and satellites in outer space, the sky appears black and the stars are visible throughout all day, regardless of the position of the Sun.

Nevertheless, here on Earth, the daytime sky appears blue and stars are not visible. Whereas during night when the Sun is set, the stars are clearly visible and the sky appears to be black. Why is this?

John Tyndall explained this phenomenon by showing that scattering of sunlight, thus polarising it to a certain degree, takes place in the upper atmosphere (Pye, 2001). Furthermore, he demonstrated that small particles in the atmosphere scatter light of short wavelengths more strongly than those of larger wavelengths. Thus, the blue color is predominantly scattered rather than say, the red one. Lord Rayleigh further estimated that the atmosphere need not necessarily contain solid or liquid particles for the scattering to occur. A large enough amount of gas molecules will also suffice for blue light to be scattered.

As it may be surmised, UV light, being shorter in wavelength than blue, is scattered even more strongly, and although the human eye cannot see it, several other animals are able to detect near-UV light and use it for different survival purposes.

1.5.2 Seeing Polarisation

Besides UV-light, certain animals, mostly insects, are also able to detect polarisation. Fifty years ago, Karl von Frisch studied the bees' navigation abilities. He discovered that bees used the orientation from the sun to tell their kin the location of food sources. When an explorer bee leaves the hive in search of food, it locates the position of the sun and can travel relatively large distances up to nearly 4 hours away from the hive before heading straight back. Nevertheless, the Sun's position will obviously change throughout that period of time. In addition, Frisch also noted that bees are able to navigate accurately even when the Sun is covered by a cloud or mountain, thus realising the Sun's position isn't the bees' true compass, but rather the polarisation pattern in the sky, determined in turn, by the Sun itself.

Through experimentation with Polaroid film, Frisch was able to prove his theory, and proposed that each segment in the eight-segmented bee eye is more sensitive to one specific direction of polarisation, thus enabling the bees to detect different orientations.

Ants are also able to discriminate polarisation in sunlight (Pye, 2001). Experiments on desert ants have been carried out in their natural habitat. These insects often forage wide desertic areas in search of food, with no landmarks to guide them back to their nest. If, for instance, the entire sky is to be obscured by a cardboard box, the ants' pathway becomes erratic, rendering the insects unable to find their way back. In other experiments, the sunlight was shielded from the ants, and in its stead, a reflection of the sun was projected toward the insects. The result was a direction reversal of their course.

It is not only insects that can see polarisation and use it in their daily lives. Research with molluscs has also been carried out with results suggesting they are also able to detect it. Exactly what use polarisation is to them is as yet unknown, but scientists have theorised it may be used to their advantage in spotting food. Some small fishes they feed on, have reflecting scales, imitating the reflections of light in water, rendering them nearly invisible to most predators. However, these reflections in the fishes' scales do not match in terms of polarisation, to the scattering produced by incident light on water, thus enabling the octopus to distinguish its prey with relative ease.

Finally, a crustacean species, commonly known as "Peacock Mantis Shrimp" has been reported to be able to detect circularly polarised light, better in fact, than any man-made optical device currently in existence (Matson, 2009).

1.5.3 Polarisation in Medicine

Applications in tissue studies

Biological media comprise two large categories in which the different tissues and fluids may be divided (Tuchin, 2006). The first one, known as "Weakly Scattering Media", which transparent tissues and fluids such as cornea, vitreous humour and crystalline lens. The second one, the "Strongly Scattering Media" includes opaque or turbid tissues and fluids like the skin, brain, blood and lymph.

Biological tissues are rendered transparent in the near-infrared (NIR) region of the spectrum, due to the absence of absorbing chromophores in this spectral range. A chromophore is a chemical and part of a molecule that absorbs light "with a characteristic spectral pattern" (Tuchin, 2006), hence being responsible for the molecule's color.

However, biological tissues produce rather strong scattering in this spectral region, making it difficult to obtain clear images of inhomogeneties within the sample, making them hard to localise. Due to this, classic imaging is virtually useless for studying this kind of media and specialised techniques need to be used when analysing biological tissues.

In certain tissues for example, the degree of polarisation of transmitted or reflected light is measurable regardless of the tissue's thickness, whereas in other media, reflected or transmitted light depolarises much too fast for obtaining useful information out of it degree of polarisation. Still, information about the structure and birefringence of its components may be obtained by measuring the degree of depolarisation of initially polarised light passing through a tissue sample.

However, it is not only from these polarisation properties that useful information can be obtained. Several tissues, retina and tooth enamel among them, present properties such as linear birefringence and optical activity due to their composition and nature. Collagen, keratin or glucose being present in them.

Considering all the aforementioned, it is safe to say that biological tissues and fluids are, in most cases, polarising materials to some extent. These properties are expected to enhance the improvement of the current techniques in medical tomography and other diagnostic methods (Tuchin, 2006).

Other important medical applications which use polarisation include glucose and bacteria sensing.

This work will not delve on the history of polarisation studies, but rather in the nature of the phenomenon and its applications.

Chapter 2
Review of Literature

2.1 Introduction

Several instruments for measuring polarisation of light, i.e., polarimeters and ellipsometers, have been proposed throughout the years (Guo, 2007; Wang, 2005; Oakberg, 2005; Giudicotti, 2007; Aspnes, 1976, Azzam, 1977; Ord, 1977). This kind of systems, in which this work will focus, enable measurement of light polarisation properties *before* and *after* light has gone through or has been reflected by a sample.

Polarimeters also enable the study and analysis of parameters such as the complex refractive index and thickness of thin films.

The term "*Polarimetry"* describes the polarisation properties of light. Hence, a polarimeter measures and analyses such properties from a beam of light. In its simplest form, a polarimeter is composed of a polarisation state generator and a polarisation state analyser. Together, they constitute a closed-loop system, in which control and feedback is provided to and from the system. For this project, we will use the terms "polarimeter" and "ellipsometer" as equivalent.

In addition, polarimeters may also be classified as Stokes Polarimeters and Mueller Matrix Polarimeters. The former merely describes the polarisation state of light through the Stokes Parameters, whereas the latter, enables the description of the polarisation properties of a material in reflection or transmission.

The Stokes vector is a set of four parameters which together define the polarisation state of a given beam of light. The vector is defined as follows:

$$\begin{pmatrix} S_0 \\ S_1 \\ S_2 \\ S_3 \end{pmatrix} \qquad (2\text{-}1)$$

Where S_0 represents the total light intensity of the beam, regardless of the polarisation state, S_1 refers to the linearly polarised components either vertically or horizontally oriented. S_2 also refers to the linearly polarised components but with ±45° of orientation, and finally S_3 represents the right and left circularly polarised components.

Furthermore, from these parameters it is possible to obtain the degree of polarisation, ellipticity and orientation of the analysed beam.

Besides there being different measuring systems, there are also different components and configurations used in them (Aspnes, 1976). These mainly include modulating elements, detection devices and data processing systems. All of them with both advantages and disadvantages.

An analysis of the most commonly used systems and elements is presented. Note that only the systems that are able to measure all four Stokes components will be mentioned.

Furthermore, besides the polarimetry system itself, an appropriate data processing system ought to be implemented in order to interpret the results correctly, calculate the Mueller Matrix and finally obtain the polarisation state and properties from the sample under study.

2.2 Polarimeters that enable measurement of the 4 Stokes Parameters

2.2.1 Rotating element polarimeters

The elements that constitute these systems are all linear retarders and polarisers .

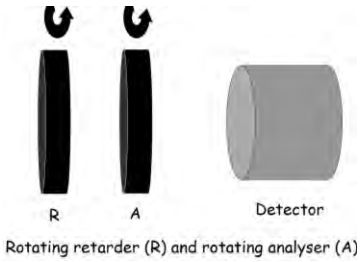

Fig. 2.1 – Example of a rotating-element polarimeter

These elements are usually rotated by mechanical or electromechanical means. Measurements need to be forcibly taken periodically with a rotation at a continuous speed or making pauses at periodic intervals to take each measure. The former method is undeniably the most accurate and fastest one, as it provides a greater number of measurements, but the detection and data acquisition need to have a very fast response.

Stepper motors or servo motors are often the preferred choice for these polarimeters, though systematic errors and encoder performance may affect the precision and reliability of the obtained data (Giudicotti, 2007). Different mechanical

setups have been used, usually involving a quarter-wave plate retarder and/or an analyser mounted on a rotation stage, driven by a motor. Two of these setups are shown below on figure 2. The mechanism on the left shows a motor-band system that enables automatic rotation of the base in which the waveplate is mounted. The second mechanism proposes a system of two gears. One of them is mounted on the motor, whereas the second one serves the double purpose of rotating stage and mount for the retarder. Needless to say, the latter example is more accurate, as long as both gears are perfectly compatible in matter of diameter/number of teeth relationship. Nevertheless, at least the gear in which the waveplate is mounted ought to be custom – made for the plate to fit properly in the exact centre. Mini-steppers have also been used successfully, providing greater accuracy in the measurements (Ord, 1977).

The measurements are then taken using the angular position of the transmission axis of the rotating element as reference, hence determining the initial point of the graphic generated by the acquired data, thus simplifying the mathematical analysis.

Whenever more than one element is rotating, they must both do so at the same frequency (Azzam, 1977).

The mathematical analysis for these type of system usually encompasses Fourier analysis of the recorded signal (Goldstein, 2003), though a weighted least-square best fit has also been proven efficient (Giudicotti, Brombin, 2007).

Finally, it must be stated, that when these systems are used as ellipsometers, they are of no real use for samples undergoing rapid changes.

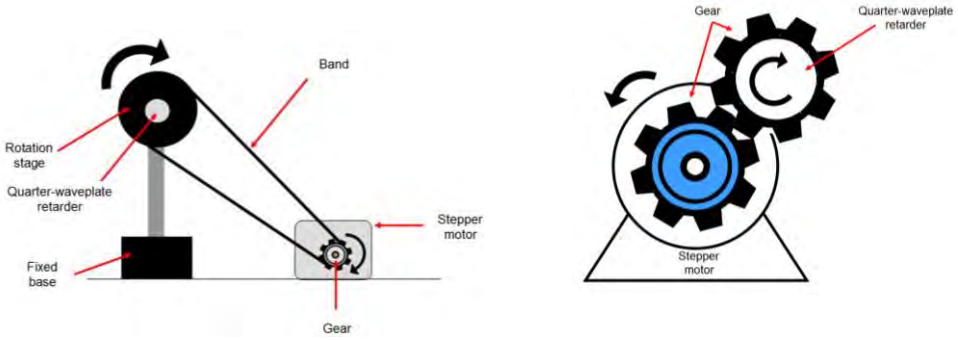

Fig. 2.2 - Two mechanical rotation setups suitable for rotation of elements in a polarimeter.

2.2.2 Oscillating element polarimeters

These systems rotate the polarisation of light using an electro or magneto-optical device such as a Faraday cell (Goldstein, 2003). If the plane of polarisation is

rotated in the cell, the effect would be the same as mechanically rotating the elements in a rotating element polariser by a proportional angle.

As stated in last chapter, these cells may be driven by a periodic voltage signal, thus forcibly requiring a signal generator. The most widely used devices are the liquid crystal variable retarders (LCVRs).

For the specific case of LCVRs, two of them are required to measure all four Stokes parameters (Meadowlark optics, 2005).

These systems provide for a significantly faster response than those previously described, thus proving far more efficient when used with rapid-changing samples (Aspnes, 1976). Nevertheless, when calibrating and taking measurements, care must be taken to preserve a constant temperature level, since liquid crystals are sensitive to temperature variations and may affect the obtained results (Carey, 1996).

2.2.3 Phase modulation polarimeters

These systems use modulators that are controlled by an electrical signal. The most commonly used element is the photoelastic modulator (PEM). The system presented here is of this type. It consists basically of a dual phase modulator and a fixed analyser. A diagram of the element setup is presented in the following figure:

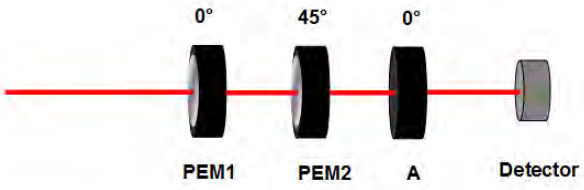

Fig. 2.3 – Dual PEM Stokes polarimeter, which measures all four Stokes parameters, where PEM1 and PEM2 are photoelastic modulators and A denotes an analyser.

The two photoelastic modulators in the polarisation analyser are operated at slightly different resonant frequencies, thus generating a “beat signal” that modulates the polarised component of the incident light. Typically, these frequencies are in the range of tens of kilohertz.

One of the main advantages of this system over both rotating and oscillating element polarimeters is speed. Although they all require an electrical signal for control and acquisition purposes, the response of PEMs is significantly faster than any motor or liquid crystal cell. Nevertheless, the overall cost of the device increases significantly given the high cost of each modulator.

These systems, though popular as a dual PEM system, are used in different physical setups involving axis orientation.

2.3 The Mueller Matrix

Consider the Stokes vector from equation (2-1), with its four parameters represented by:

$$\begin{pmatrix} S_0 \\ S_1 \\ S_2 \\ S_3 \end{pmatrix}$$

which together represent the polarisation properties of a given light beam.

Let us now assume that the beam interacts with a polarising medium whose characteristics are at present unknown. The emerging beam will then be represented by a new Stokes vector, which we shall represent by:

$$\begin{pmatrix} S_0' \\ S_1' \\ S_2' \\ S_3' \end{pmatrix} \qquad (2\text{-}2)$$

If we represent each of the S_i' (where i = 0,1,2,3) parameters as a linear combination of the original S_i parameters, we may obtain the following relations (Goldstein, 2003):

$$S_0' = m_{00}S_0 + m_{01}S_1 + m_{02}S_2 + m_{03}S_3 \qquad (2\text{-}3a)$$
$$S_1' = m_{10}S_0 + m_{11}S_1 + m_{12}S_2 + m_{13}S_3 \qquad (2\text{-}3b)$$
$$S_2' = m_{20}S_0 + m_{21}S_1 + m_{22}S_2 + m_{23}S_3 \qquad (2\text{-}3c)$$
$$S_3' = m_{30}S_0 + m_{31}S_1 + m_{32}S_2 + m_{33}S_3 \qquad (2\text{-}3d)$$

In matrix form, (2-3) can also be expressed as,

$$\begin{pmatrix} S_0' \\ S_1' \\ S_2' \\ S_3' \end{pmatrix} = \begin{pmatrix} m_{00} & m_{01} & m_{02} & m_{03} \\ m_{10} & m_{11} & m_{12} & m_{13} \\ m_{20} & m_{21} & m_{22} & m_{23} \\ m_{30} & m_{31} & m_{32} & m_{33} \end{pmatrix} \begin{pmatrix} S_0 \\ S_1 \\ S_2 \\ S_3 \end{pmatrix} \qquad (2\text{-}4)$$

or

$$S' = MS \tag{2-5}$$

Where S and S' are the Stokes vectors and M is the 4 x 4 matrix known as the Mueller Matrix.

Whenever an optical beam interacts with matter, whatever the media, its polarisation state nearly always suffer changes. Depending on specific properties of the material, the polarisation state of the incident beam varies accordingly. Some of these variations in polarisations state include changes in the amplitude, phase, direction of the orthogonal field components, and transference of energy from polarised states to the unpolarised state (Goldstein, 2003). Each of these elements may be in turn, represented by a particular Mueller Matrix.

For instance, a linear polariser, with its axes along the x and y directions may be represented by the following Mueller Matrix:

$$M_p = \frac{1}{2}\begin{pmatrix} p_x^2 + p_y^2 & p_x^2 - p_y^2 & 0 & 0 \\ p_x^2 - p_y^2 & p_x^2 + p_y^2 & 0 & 0 \\ 0 & 0 & 2p_x p_y & 0 \\ 0 & 0 & 0 & 2p_x p_y \end{pmatrix} \tag{2-6}$$

where, $0 \le p_{x,y} \le 1$

and p_x and p_y are the attenuation coefficients of the polariser.

For simplification purposes, an alternate notation may also be used, where the same Mueller Matrix defined in (2-6) can be rewritten as:

$$M_p = \begin{pmatrix} A & B & 0 & 0 \\ B & A & 0 & 0 \\ 0 & 0 & C & 0 \\ 0 & 0 & 0 & C \end{pmatrix} \tag{2-7}$$

Where,

$$A = \frac{1}{2}(p_x^2 + p_y^2) \quad \text{(2-7a)}$$

$$B = \frac{1}{2}(p_x^2 - p_y^2) \quad \text{(2-7b)}$$

$$C = \frac{1}{2}(2p_x p_y) \quad \text{(2-7c)}$$

Furthermore, each of the Mueller Matrix elements describes a different property of the material it represents. Among such properties, it is possible to determine the diattenuation (differential attenuation of orthogonal polarisations for both linear and circular polarisation states), depolarisation coefficient, and linear retardance assuming a thin film. Thus, the properties are represented as follows (Tuchin, 2009; Kim, 1987):

$$m = \begin{bmatrix} p & -(LD_0) & -(LD_{45}) & (CD) \\ -(LD_0) & p & (CB) & (LB_{45}) \\ -(LD_{45}) & -(CB) & p & -(LB_0) \\ (CD) & -(LB_{45}) & (LB_0) & p \end{bmatrix} \quad \text{(2-8)}$$

Where,

P = Isotropic Absortion
LD_0 = Linear Diattenuation (0° or 90°)
LD_{45} = Linear Diattenuation (±45°)
CD = Circular Diattenuation
CB = Circular Birefringence
LB_0 = Linear Birefringence (0° or 90°)
LB_{45} = Linear Birefringence (±45°)

However, not all materials alter polarisation in the same way or indeed, in the same degree. When it is required to analyse the polarising properties of a specific material, a Mueller Matrix polarimeter is then used, which enables the measurement of the different elements that constitute the Mueller Matrix that represents said material, thus providing useful information on properties and characteristics of the sample under study.

2.4 Mueller Matrix Polarimeters

Mueller Polarimeters aim to measure the elements from the 4x4 Mueller Matrix of a given sample either in reflection or transmission. A polarimeter is said to be

complete if it measures all 16 elements from the matrix, whereas an incomplete polarimeter merely measures a part of the matrix. Given that different elements from the Mueller Matrix represent different properties of the material under study, it is sometimes unnecessary to measure all 16 elements, and thus, an incomplete polarimeter may be used for such cases.

In order to have a complete measuring system, the instrument must encompass two stages, both functioning in strict synchronicity. The first stage consists of a complete polarisation state analyser (PSA) and the second, a complete polarisation state generator (PSG). The reason for both stages is clear: it is necessary to know which polarisation state is entering the sample as well as which state is exiting it, thus enabling calculation of which polarisation changes occurred during the process.

As in the case of Stokes polarimeters, there are different elements available for both the PSA and PSG stages, these being either rotating elements or phase-modulating devices. As in the previous section, only complete Mueller polarimeters will be mentioned.

2.4.1 Rotating element polarimeter

A rotating element polarimeter capable of measuring all 16 elements of Mueller matrix is formed by a fixed polarimeter, followed by a rotating retarder, which together constitute the PSG stage. The sample is located in the middle of both PSG and PSA stages. The PSA stage is similarly formed by a rotating retarder, followed by a fixed analyser. The following diagram illustrates this setup:

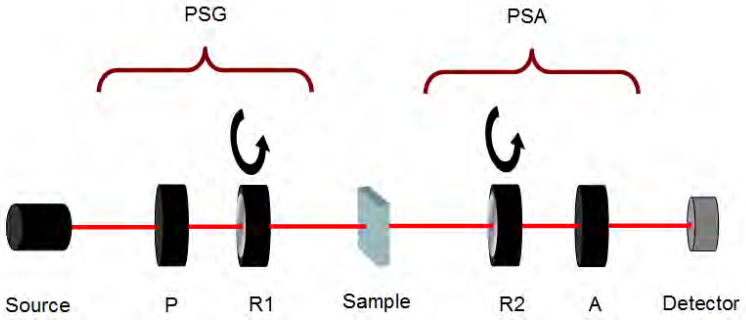

Fig. 2.4 – Rotating element Mueller polarimeter, where "P" denotes the polariser, "A" is an analyser, and R1 and R2 are retarders.

2.4.2 Phase-Modulating Polarimeter

This system uses photoelastic modulators (PEM) as a means for controlling and determining the state of polarisation of a light beam. The arrangement consists on a fixed polarimeter oriented at 0°, a PEM oriented at 45°, followed by a second PEM oriented horizontally. These elements together constitute the PSG stage of the system. Again, the sample is located between the PSG and PSA. The PSA

then follows the sample with a PEM oriented horizontally, a second PEM at 45° and finally, a fixed analyser at 0°.

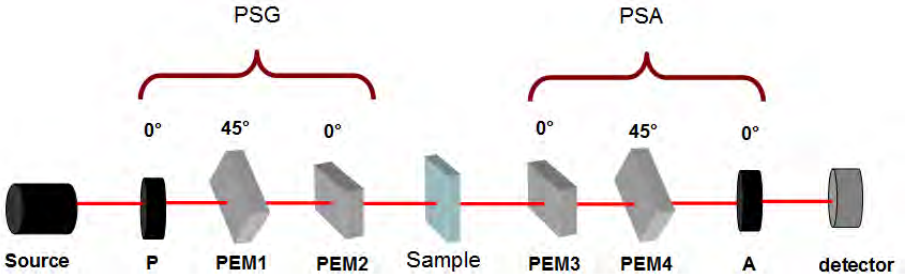

Fig. 2.5 – Complete Mueller polarimeter based on photoelastic modulators. The same notation as in the previous figure is used for the constituting elements.

2.4.3 Oscillating Element Polarimeter

Yet another setup for measuring the Mueller matrix has been proposed based on the use of four LCVRs (De Martino, 2003; Uberna, 2006). Although still under development, the results obtained thus far seem promising. The PSG stage generates a sequence of four different retardations before the beam enters the sample. Different retardation values have been tested, each based on the work of different authors and criteria. A set of four values has been proposed by the authors, with which the most accurate results have been obtained. The experimental setup for the instrument is presented as follows,

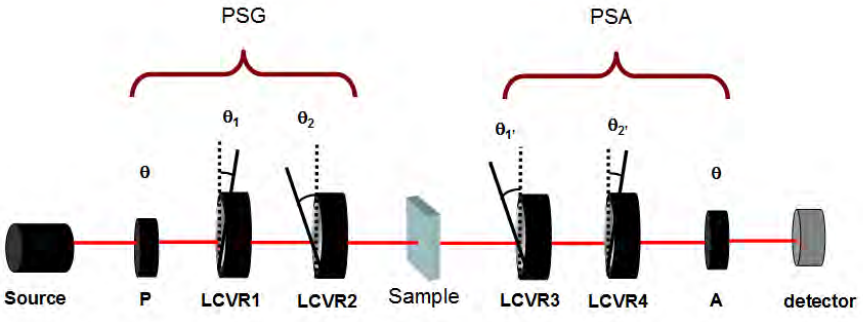

Fig. 2.6 – Complete Mueller polarimeter based on liquid crystal variable retarders (LCVR). θ and its different subindexes represent various possible orientations of the elements.

2.4.4 Applications of a Mueller Polarimeter

Whether in transmission or reflection, certain materials can affect the polarisation state of light that interacts with them. This is due to intrinsic qualities and properties of said materials such as optical activity, chirality and reflectivity.

Applications for Dual PEM Systems range from the medical to the military.

Depending on the wavelength and other parameters, the system enables analysis and characterisation of different materials (most of them organic in nature, but also certain reflecting materials). Such materials are used in medical analysis, holography, food processing and pharmaceutics, among others.

Dual PEM polarimeters are used in astronomy to study light polarisation from nearby stars and sunspots.

Another useful application of this system is in optical fibres. When a fibre is bent, it generates mechanical stress, which in turn causes the polarisation state of the light travelling through the fibre to change. Light polarisation may also vary depending on the environment the fibre is in. Polarimeters are hence used to monitor the polarisation state of light coming out of the fibre (Hinds Instrument, 2005).

Intrinsic qualities of materials have an effect on the way light interacts with them. Properties and characteristics such as stress, defects, reflectivity, and polarisation loss may be determined with the instrument by measuring the polarisation state of light after passing through a material.

Other applications include thin film characterisation as well as laser test and measurement.

2.5 Detection Devices: Different Types of Photon Detectors

2.5.1 The Photomultiplier Tube

A typical photomultiplier tube consists of a vacuum tube containing a photosensitive cathode followed by a series of electrodes (known as dynodes) that collect and multiply the photocurrent generated in the cathode (Jonasz, 2009). A voltage of the order of hundreds of volts is distributed between the electrodes of the multiplier by a voltage divider network. A photon that strikes the photocathode ejects an electron with the quantum efficiency of less than one fourth. Such electron is then accelerated by the potential differences between the cathode and the following electrode. The impact with said electrode results in the ejection of several next-generation electrons. This electron multiplication continues for each of the following dynodes, ending up in the anode, where the electrons are collected. The overall process hence provides for an approximate of 10^6 electron gain.

2.5.2 Photodiodes

Sensing devices for polarisation measuring systems require a high-speed, low-noise response. Since the system presented in this work is to measure a single light beam, we will focus on photodiodes as the preferred means of measuring light intensity.

Photodiodes generate a small electrical current, which is proportional to the level of the illumination incident on its surface.

There are two types of photodiode available for this kind of application: the PIN photodiode, which can detect signals within a significantly wide spectral band, and the avalanche photodiode, which has a faster response (Graeme, 1995). Nevertheless, controlling the second type presents a somewhat greater challenge.

The photodiode to be used must be carefully selected in accordance to the signal characteristics, such as amplitude and frequency. Not all photodiodes will be able to detect a signal at a high frequency, nor will they be equally sensitive to all wavelengths. Also, operation conditions should be taken into account so as to minimise possible electrical noise and temperature variations during measurements.

The main properties to keep in mind while choosing a suitable photodiode are junction capacitance (C_j), dark current, spectral range, active area, and response time (Graeme, 1995).

Spectral Response

The current generated by a given level of incident light varies with wavelength. The relation between photoelectric sensitivity and wavelength is referred to as the spectral response of the photodiode.

The operating wavelength for this stage of the project is that of λ = 632.8nm, which corresponds to the red color. Bearing this in mind, a silicon photodiode was chosen due to its high sensitivity to red light.

In the following figure, a typical spectral response curve of photodiodes made of different materials is presented (Johnson, 2004), in which the diode's sensitivity along a specific range of the spectrum may be seen. Notice that, according to the graph, silicon photodiodes provide a fairly good responsivity along the red part of the spectrum, making them suitable for the application at hand.

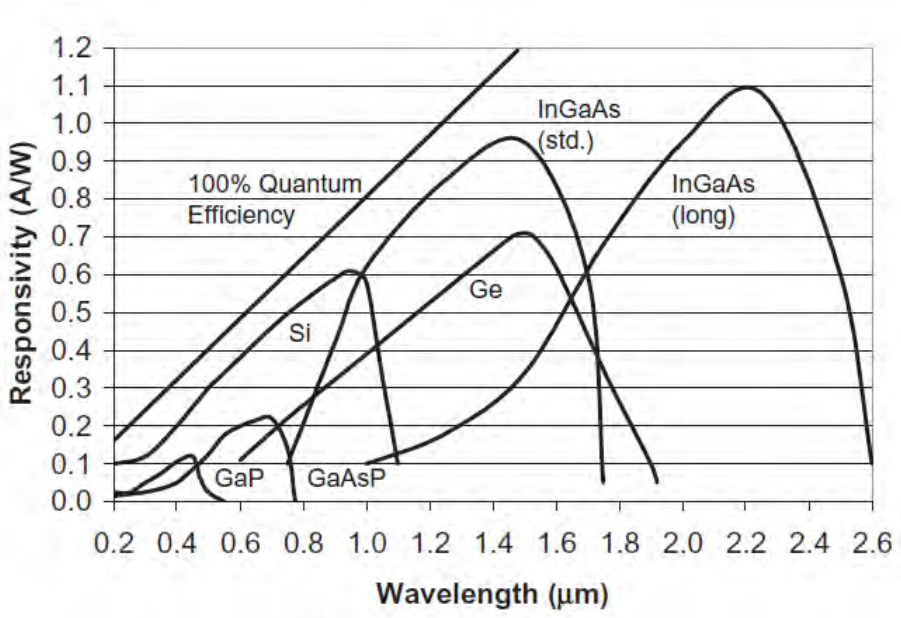

Figure 2.7 – Typical spectral response of a silicon photodiode.

Dark Current

It is a small current that flows when a reverse voltage is applied to a photodiode, i.e. when the diode is used in photoconductive mode, even when no illumination is incident on the diode. This current adds noise to the overall signal and must therefore be minimised as much as possible.

Active Area

Physically, the active area refers to the amount of surface in the photodiode that detects illumination. It is directly related to yet another characteristic, which is the junction capacitance (c_j). The smaller the active area is the smaller the junction capacitance, which in turn provides for a greater frequency bandwidth (Graeme, 1995).

Mode of Operation

Any photodiode may be used in one of two different operating modes, the photovoltaic and the photoconductive. In the former one, the photodiode functions as a current source, simply changing light to an electric signal. On the other hand, the photoconductive mode requires an inverse voltage to be applied to the diode. This mode provides a greater linearity and frequency response, but is more susceptible to noise and dark current (Jung, 2002). By applying and inverse polarisation to the photodiode, the junction capacitance is reduced, which in turn

will improve the diode's response time (Rashid, 1999). This mode is generally used for applications requiring a fast response. Furthermore, the photoconductive mode usually requires a preamplifier, which encompasses a current to voltage converter. Thus, the linearity is lost after the conversion.

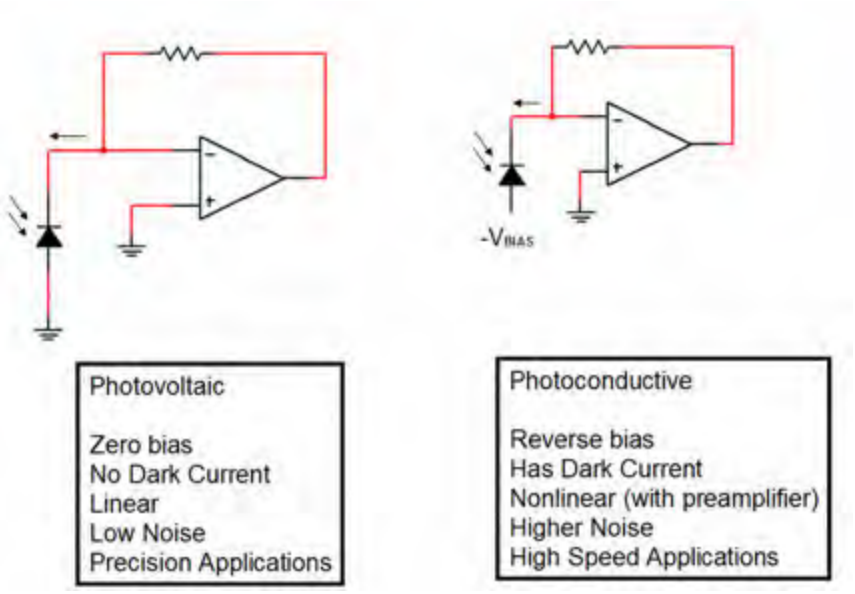

Figure 2.8 – Photodiode operating modes

In the photoconductive mode, it is possible to read either a voltage or current signal. However, the generated electrical current is a linear function of the light intensity, as opposed to the voltage response. Since most devices are designed to reading voltage rather than current, in most cases a preamplifier stage in order to obtain suitable readings in volts.

The preamplifier stage, as the name indicates, encompasses an operational amplifier used as a current-to-voltage converter, which basically takes the generated current from the photodiode and converts it to voltage. This stage also functions as a filter, which aims to minimise the noise effects of the dark current generated by the diode.

A careful selection of the constituting elements as well as an in depth analysis of the overall circuit must be carried out in order to meet the system requirements and obtain usable and reliable data out of the measurements.|

The main characteristic to bear in mind for this kind of application is bandwidth. Which means one must be sure to select an appropriate photodiode with a high enough response speed and low junction capacitance. As for the operational amplifier to be used, it must also provide the necessary bandwidth one requires for the application at hand. This opamp is usually selected with the highest unity gain

bandwidth product to input capacitance as possible (Graeme, 1995). The unity gain bandwidth refers to the frequency at which unity gain occurs (Neiswander, 1975).

A more detailed description of analysis and design of the preamplifier stage will be presented later on.

It has also been proposed (Neiswander, 1975, Fjarlie, 1977) that under harsh environmental conditions, such as airborne or space borne monitoring, it might be advisable to cool the entire circuit, diode and preamplifier stage included up to 200K. It has been reported that by doing this, dark current and other noise sources may be actively suppressed.

2.6 Data Processing System

A Lock-in Amplifier (LIA) is a filtering system designed to acquire a particular AC signal buried in noise or other signals and "extract" it from the rest, providing its amplitude and phase. A reference sinusoidal signal, tuned to frequency and phase of the desired one must be used.

Though signal generators or oscillators provide a reasonably stable signal, the generated frequency varies by a few hertz through time. For this application, this variation will not do, since we are aiming to "lock" the signal that is buried in noise. Therefore, a phase locked loop (PLL) is also required to ensure that the reference signal is precisely tuned and whose frequency is continuous. Basically, the PLL, along with passive components with calculated values, is fed the sinusoidal signal at a specific frequency. The circuit then feeds back the signal to the PLL and stabilizes the frequency, so as to ensure that it is fixed at the desired value.

Care must be taken to select the adequate values for the passive components. Otherwise, the obtained frequency will not match the desired one. Formulae have been provided for this purpose, and whenever the results render a non commercial value for resistors and/or capacitors, trimpots are often advisable to ensure frequency accuracy.

2.6.1 Lock-in Amplifier: Principle of Operation

The reference signal is fed to the lock in via one input channel and to a phase locked loop, whereas the noisy signal and fed to another one. The noisy signal then enters an optional amplifying stage (because usually the amplitude of the desired signal is too small, usually in the range of mili or nanovolts). After the amplification, the signal is sent to two separate stages. One stage directly multiplies (or mixes) the noisy signal with the reference signal. The other one also multiplies the noisy signal, but this time with the reference signal 90° out of phase. So for instance, if the reference signal is a Sine, this other signal would be a Cosine.

Both outputs are then fed to low-pass filters, tuned to eliminate all AC components, and keep only those with frequencies close to zero, which would be the DC component.

The actual process and complete circuit is somewhat more complex than the description above. Since the signal may be buried in several others with various frequencies, both greater and smaller, more than one filter may be required, either low-pass or high-pass after the gain stage and others just before the final output. Finally, a band-suppressing notch filter is sometimes recommended to be used right after the amplifying stage to eliminate a reduced range of specific frequencies whose amplitude is greater or equal to the one that is being extracted, yet significantly apart in frequency terms from the desired signal (otherwise, one might accidentally eliminate the signal along with the unwanted noise).

It must also be noted that the process of phase-sensitive detection demands an exact phase synchronisation between the reference signal and the modulation of the light beam (Chabay, 1975). With this in mind, it is advisable to use the very same electrical signal that is driving the photoelastic modulators as the reference for the lock-in.

A block diagram of the main stages of a lock-in amplifier is presented in figure 1.9:

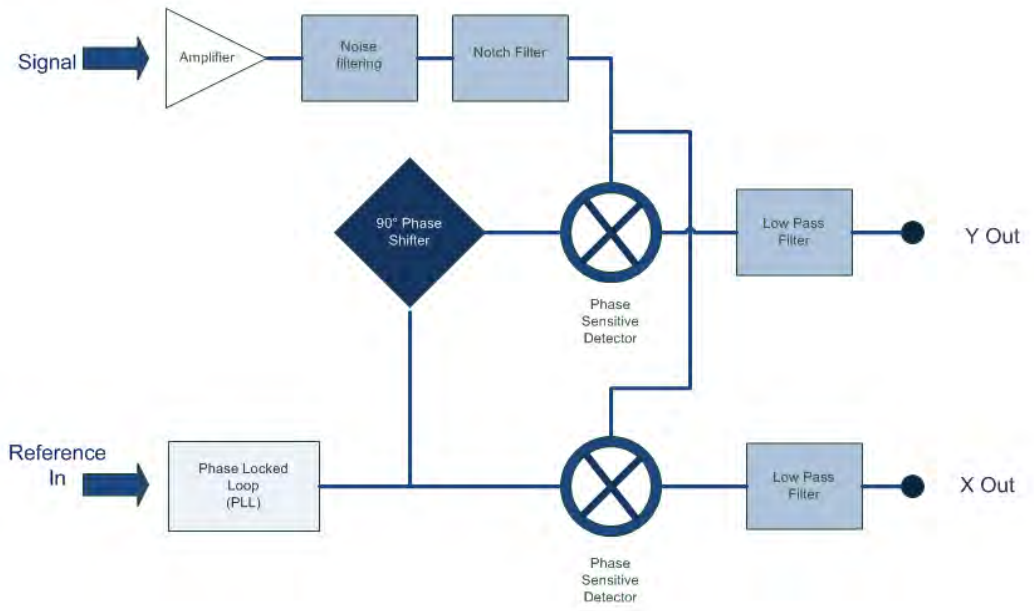

Fig. 2.9 - Lock-In Amplifier Functional Block Diagram

Phase sensitive detectors, shown in the above figure, measure the phase difference between two signals of the *same frequency*. It does so by multiplying

both signals and thus obtaining a DC signal proportional to the phase difference between the signals. For two square signals at a low frequency, an XOR gate will suffice to achieve this. Nevertheless, for higher frequencies in sinusoidal waveforms, a more specialised circuit is required. The IC AD633 is an analog multiplier designed for this purpose.

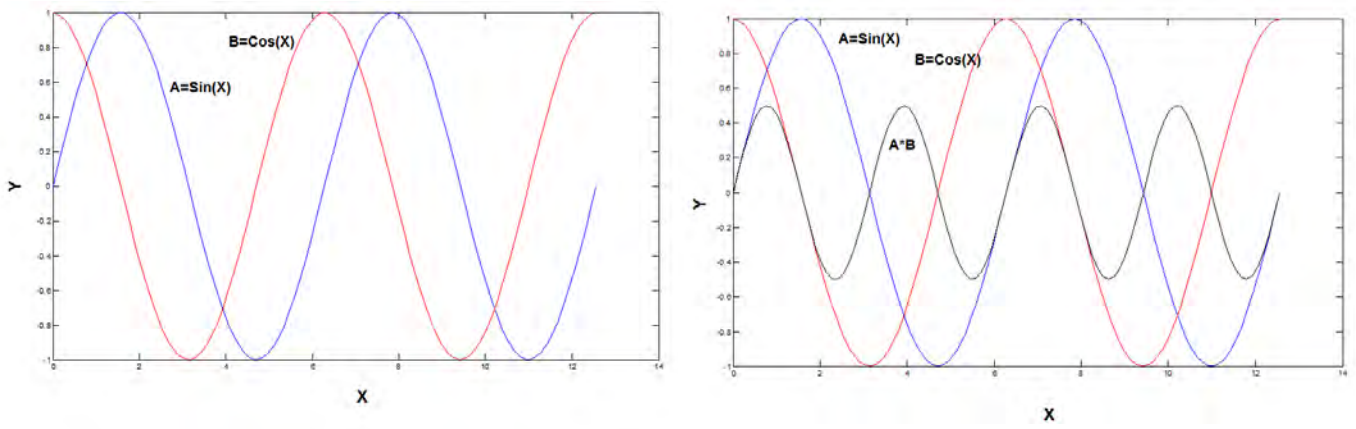

Figure 2.10 - Graphical representation of two sinusoidal signals with a phase difference of 90° (left) and the resulting multiplication (right).

2.6.2 Basic Theory

Mathematically speaking, if we express the desired signal as,

$$V_{sig}Sin(\omega_r t + \theta_{sig}) \qquad (2\text{-}9)$$

Where V_{sig} is the amplitude of the signal.

And the reference signal as,

$$V_L Sin(\omega_L t + \theta_{ref}) \qquad (2\text{-}10)$$

By multiplying both signals, we get:

$$V_{PSD} = V_{sig}V_L Sin(\omega_r t + \theta_{sig})Sin(\omega_L t + \theta_{ref}) \qquad (2\text{-}11)$$

$$= \frac{1}{2}V_{sig}V_L Cos([\omega_r - \omega_L]t + \theta_{sig} - \theta_{ref}) - \frac{1}{2}V_{sig}V_L Cos([\omega_r + \omega_l]t + \theta_{sig} + \theta_{ref})$$

The output is then passed through a low pass filter to remove all AC components, keeping solely the DC one, which is proportional to that of the signal. Thus,

$$V_{PSD} = \frac{1}{2} V_{sig} V_L Cos(\theta_{sig} - \theta_{ref}) \quad (2\text{-}12)$$

Assuming that $\theta_{sig} = \theta_{ref}$, then $(\theta_{sig} - \theta_{ref}) = 0$ and cos $(\theta_{sig} - \theta_{ref}) = 1$. Resulting in,

$$V_{PSD} = \frac{1}{2} V_{sig} V_L \quad (2\text{-}13)$$

If, on the other hand, $(\theta_{sig} - \theta_{ref}) = 90°$, the output would be zero.

In short, a lock-in with just one PSD renders an output of $V_{sig}Cos\theta$.

Since we are looking for the value of V_{sig}, the phase dependency needs to be eliminated. This can be achieved by adding a second PSD, and using the same reference signal, but shifted 90° with respect to the previous one. Thus, after low-pass filtering the second output,

$$V_{PSD2} = \frac{1}{2} V_{sig} V_L Sin(\theta_{sig} - \theta_{ref}) = V_{sig} Sin(\theta) \quad (2\text{-}14)$$

Conventionally, this last expression is referred to as “Y”, or “in-phase component”, whereas the expression $V_{sig}Cos\theta$ is called “X”, or “quadrature component”.

Having both X and Y, it is now possible to obtain both the amplitude (R) and the phase (θ) of the signal by:

$$R = \left(X^2 + Y^2\right)^{1/2} \rightarrow V_{sig} \quad (2\text{-}15)$$

and

$$\theta = \tan^{-1}\left(\frac{Y}{X}\right) \quad (2\text{-}16)$$

Thus obtaining the required information from the signal.

It must be noted that LIA’s output is given in RMS, so a factor of $(2)^{1/2}$ must be considered during calculations.

Also, in order to minimise ambient noise and light intensity fluctuation, a chopper may be added to the optical system, rotating at a much lower frequency (around 500 Hz), thus providing for a greater signal-to-noise ratio (Guo, 2007).

2.6.3 Why design and implement a LIA when there are commercial ones available?

There is a wide variety of commercially available lock-in amplifiers that work within a specific frequency range. Although it is advisable to use a commercial LIA for calibrating and testing the instrument, it is nevertheless important that the final installment of the complete system include its own LIA.

Design and construction of a lock-in specifically for the application at hand may be more desirable for a number of reasons.

Firstly, the cost of a commercial lock-in is significant, and by purchasing it, the total cost of the instrument under development is consequently increased. Also, when working with a specific set of single values, precious time and calibration procedure may be saved with a circuit built to the exact instrument's specifications, whereas with a commercial lock-in a lengthy procedure involving warm-up, adjustment and calibration must take place before any actual measurements can be obtained.

Finally, the whole automation process may be hindered or negatively affected by the limitations of the commercial lock-in. Although most of these devices have a built-in system for computer interfacing and programming, the port or other specifications and protocols might not necessarily be the most convenient for the system at hand. In contrast, when a lock-in is developed specifically for an application in mind, it is possible to consider the available and most suitable resources for interfacing and to effectively establish communication with the computer or any third party equipment that is needed by the instrument, thus allowing for the engineer to choose the hardware and software to use, at least to some extent. Needless to say, this significantly simplifies the overall implementation of the complete system.

2.7 Analysis of Different System Configurations based on PEM devices

The appropriate orientation of the PEMs varies depending on the application at hand. In imaging applications, specifically while using a spectropolarimetric camera, a dual system with both PEM retardance axes aligned and the modulators used in tandem proved successful, the experimental setup being as follows:

One setup involves a quarter waveplate retarder with its fast axis oriented at -45°, followed by both PEMS oriented horizontally and finally a second quarter waveplate retarder oriented at 45°. This setup provided for a circular retarder that modulates the Q and U parameters. Since measurement of the parameter V (circular polarisation) was not required for the specific application, it sufficed for satisfactory measurement of only 3 of the 4 Stokes parameters, I, Q and U (Diner, 2007). Nevertheless, if it were required to fully measure the degree of polarisation of incident light, this system would not be adequate by itself.

Yet another configuration, proposed by Hinds Instruments (Wang, 2005) involves one of the modulators oriented at 45° and the second one horizontally, followed by an analyser oriented at 22.5°.

Chapter 3

Methods

3.1 Introduction

The full Mueller Matrix polarimeter described here is based on both dual Liquid Crystal Variable Retarders (LCVR) and Photoelastic Modulator (PEM) systems. The instrument is constituted by two stages: a polarisation state generator (PSG) and a polarisation state analyser (PSA). The first controls and feedbacks the polarisation state of an incoming red beam at a wavelength of λ=632.8 nm while the second is a full Stokes polarimeter.

As above mentioned, the polarisation state of a beam emitted by a continuous wave He-Ne laser is controlled by means of a set of two LCVRs, each driven by a periodic voltage signal. These signals are computer generated and fed to the phase modulating elements through a Data Acquisition Card. The voltage amplitudes are combined according to the desired polarisation state, thus, providing full knowledge of the initial polarisation state of the light beam before entering the sample under study.

On the other hand, the full Stokes polarimeter measures the four parameters describing the polarisation state of the outgoing beam once it has gone through the sample being analysed. The PSA is based on two PEMs and an analyser, followed by a photoreceiver that in turn send the information to a Data Analysis system in order to determine the beam's state of polarisation.

After collecting a number of measurements, they are sent to the computer in order to be analysed, so as to determine the full Mueller Matrix of the sample and hence, useful information on the material's optical properties.

This chapter will thus focus on the methodology and tools used to control and enable correct performance of the overall system.

3.2 Optical Measurement System Description

In Fig. 3.1 the overall measurement system is presented schematically. The device will enable the calculation of the 16 coefficients from the Mueller matrix and hence, different optical properties of the material under analysis. LCVRs are 1' diameter scientific grade elements from Arcoptix™. On the other hand, PEMs are made of fused silica (IISF42 and IISF47) and provided by Hinds Instruments™.

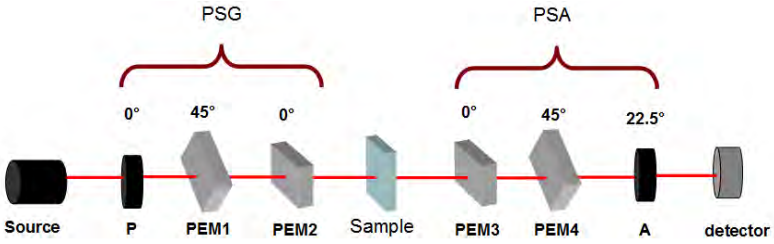

Fig. 3.1 – Full Mueller polarimeter. "P" and "A" denote polariser and analyzer, respectively; PEM 1, 2, 3, and 4 are photoelastic modulators.

3.2.1 Constituting elements

- Liquid Crystal Variable Retarders

The polarisation state generator is constituted by a linear polariser (P1) with its transmission axis at 0°, followed by two liquid crystal retarders (LCVR1 and LCVR2) oriented at 45° and 0° respectively.

Both LCVRs are controlled by means of a 1KHZ square wave signal of variable amplitude, generated by a function generator and controlled via software. Depending on the amplitudes of both signals, the LCVRs induce a retardation in the light, and hence, a change in polarisation. Specific amplitude values are to be sent to the retarders in order to induce a known polarisation state.

By applying a series of square signals at different amplitudes and combinations between both LCVRs, the required voltage values for achieving the six main polarisation states from an incident linearly polarised beam oriented at 0°, were determined. The set of voltages fed to the LCVRs and the generated polarisation state in the probe beam are shown on Table 3.1.

Polarisation State	Voltage LCVR 0° (V)	Voltage LCVR 45° (V)
Linear 0°	4.9	0.98
Linear 90°	1.599	2.873
Right Circular	2.92	2.245
Left Circular	1.457	4.68
45°	5.25	2.227
-45°	5.4	4.75

Table 3.1. Applied voltages to both LCVRs required to obtain all six main polarisation states.

- Photoelastic Modulators

Initial tests were carried out using only one of the modulators, evaluating the correct performance of both, modulator and detector against the computer generated curves. The set-up to examine the functionality of the elements consists on pair of linear polarisers oriented perpendicularly with respect from one another (null system), and a PEM, fast axis oriented horizontally, between both of them. The PEM modulation is controlled with a square signal at a frequency of 47 KHz, with different phase retardances that can be modified by the users via a control provided by the PEM manufacturer.

An important property of these photoelastic modulators is that the beam must enter the PEM at the precise centre of the crystal, given that, according to the manufacturer, the modulation varies sinusoidally throughout the crystal as it moves away from the centre. This was tested, and proved to be correct. Thus, if the beam enters the crystal in some other point that is not the centre, the obtained curves will not be the ones expected. For this reason, a black cardboard mask was made for both modulators that cover the windows the crystals are in and with a small orifice in the exact centre so as to ensure the incident beam enters the PEM at the right point.

Using a mathematical analysis software, in this case Mathcad™, the ideal light intensity transmission curves corresponding to several different polarisation states passing through the system were estimated, in order to predict the response that was to be obtained during experimental trials.

The experimental setup for these tests is shown in Fig. 2.

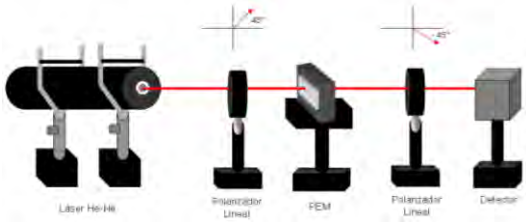

Fig. 3.2 – Experimental setup used for the characterisation of the photoelastic modulator.

Two of the ideal curves are presented in figure 3.3, for two different amplitude phase retardations: half- and 1.5-wave.

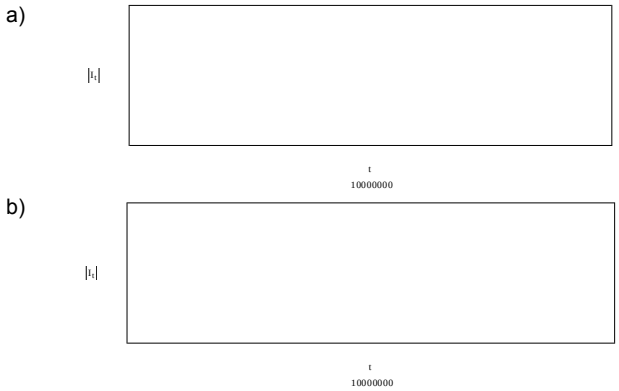

Fig. 3.3 – Ideal output of system for a retardance of a) half a wave ($\Delta=\pi$) and b) 1.5 waves ($\Delta=3\pi$).

Using a commercial photoreciever, New Focus Model 1801, the above signals can be obtained using the experimental setup shown in figure 3.2.

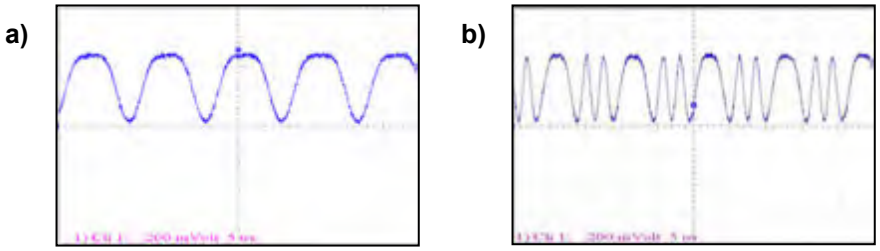

Fig. 3.4 – Output signals obtained using a New Focus photodetector with a retardance of a) half a wave ($\Delta=\pi$) and b) 1.5 waves ($\Delta=3\pi$).

- **Detector**

Since the instrument ought to be independent from commercial equipment besides the modulators, a photodetector system was to be developed in order to detect the signal. The design was based on the performance characteristics from the commercial one.

The photodetecting system consists in itself on different stages, which shall now be analysed separately the better to describe its overall operation.

As stated in the previous chapter, a silicon PIN photodiode was selected for this system due to its spectral response, more specifically, to its high sensitivity to red light.

Considering the operating frequency of both photoelastic modulators, 45 KHz and 47 KHz respectively, it is advisable that the response speed of the detector be several times these frequencies. Since the response of PIN photodiodes is

fast enough for this case, and for simplicity purposes, it was decided to use this type of diode in the project.

Two different photodiode models were tested, whose characteristics are shown on Table 3.2. Let it be noted that the response time of both diodes, while different, is brief enough for the application at hand. Nevertheless, the Melles Griot diode is not only faster, but its junction capacitance (and thus the active area) is significantly smaller, providing a greater bandwidth.

Manufacturer	Advanced Photonix	Melles Griot
Model Number	SD 445-11-21-305	13 DSH 005
Junction Capacitance (C_j) @ 10V	350pf	5.5pf
Dark Current	30nA	0.25nA
Spectral Range	350 - 1100nm	350 - 1100nm
Active Area	107.2mm2	1.57mm2
Response Time @ 10V	13ns	2.5ns

Table 3.2 – Technical specifications for silicon photodiodes

Once the photodiode had been selected, tests with different electronic designs for the preamplifier stage were made, as well as with different models of operational amplifiers (Opamps) available on the market. Naturally, integrated circuits specifically designed for instrumentation applications were selected, which provide for a more efficient design, together with less noise susceptibility.

For the initial tests, an instrumentation amplifier model AD624AD was used along with a basic design, involving a current to voltage converter, as that shown in figure 3.5. However, the bandwidth this model offers proved to be insufficient for this application, making it necessary to test other options.

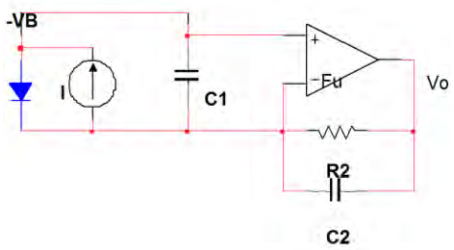

Fig. 3.5 – Basic current to voltage converter

Starting from the same design of a current to voltage converter, the transference function and necessary equations to determine the minimum and

maximum frequencies the circuit could handle, were obtained. In the circuit in figure 3.4, C_1 denotes the net capacitance ($C_{photodiode}$ + C_{opamp}) and f_u is the Unitiy Gain-Bandwidth product (GBW), which determines the frequency at which the unity gain occurs.

Analysing the circuit the following equations may be obtained,

$$f_1 = \frac{1}{2\pi R_2 C_1} \quad , \tag{3.1}$$

$$f_2 = \frac{1}{2\pi R_2 C_2} \quad , \tag{3.2}$$

$$f_2 = \sqrt{f_1 f_u} \quad , \tag{3.3}$$

$$C_2 = \sqrt{\frac{C_1}{2\pi R_2 f_u}} \quad . \tag{3.4}$$

Combining equations (3.1) and (3.2),

$$f_2 = \sqrt{\frac{f_u}{2\pi R_2 C_1}} \quad . \tag{3.5}$$

Thus, knowing the characteristics for both the photodiode and the operational amplifier, it is possible to determine the bandwidth of the circuit.

From equation 3.5, it may be established that in order to maximise f_2, the opamp must have a high f_u as well as a low C_{IN}. Thus, the relationship f_u/C_{IN} allows for an adequate selection of an operational amplifier. With this in mind, and after having evaluated different models, the AD823 IC, whose main characteristics are shown in Table III, was selected.

AD823		
GBW (f_u) (MHz)	**Capacitance (C_{IN}) (pF)**	**f_u / C_{IN} (MHz / pF)**
16	1.8	8.9

Table 3.3 – Technical specifications for the AD823 Opamp

The obtainable bandwidth using the AD823 IC and the Melles Griot diode can be calculated using equations 3.1 to 3.5. Thus, the resulting bandwidth is 1.65 MHz. with a maximum frequency of 1.868 MHz. Since the diode will be inversely polarised, some amount of dark current, and hence a certain amount of noise, is unavoidable. Adding a second photodiode D2 to the circuit can reduce the error this generates. It must be noted that D2 ought to have the same characteristics as the first diode D1, inversely polarised with the same

voltage as D1 so that it conducts a dark current of approximately the same magnitude through a 100 KΩ resistor, thus suppressing the effects of D1's dark current. The following figure shows a diagram of the circuit.

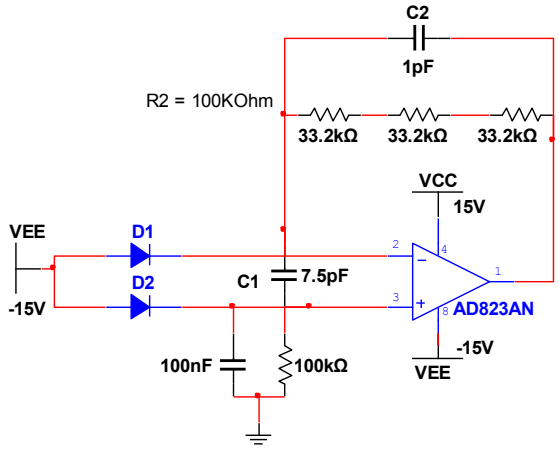

Fig. 3.6 – Current to voltage converter with a bandwidth of BW = 1.65 MHz and dark current compensation.

In order to minimise the undesirable effects of electrical noise, the circuit was encased in a metal box.

The complete element list constituting the preamplifier is as follows,

- IC AD823AN
- 2 Identical Photodiodes
- (3) 33.2 KW resistors
- (2) 100 KW resistor
- 1pF capacitor
- 7.5 pF capacitor
- 100 nF capacitor
- Power Source (±15 V)
- Metallic encasing for the circuit in order to minimize noise

With the photodetector finished, several tests for performance and accuracy were carried out. For comparison purposes, a commercial detector was initially used (New Focus, Model 1801), and its response was then verified by the computer generated simulation, henceforth ensuring the accuracy of the experimental system previously shown in figure 3.2.

The following images were taken using an oscilloscope connected to the two photodetectors. The results for both the commercial and the developed detectors are presented.

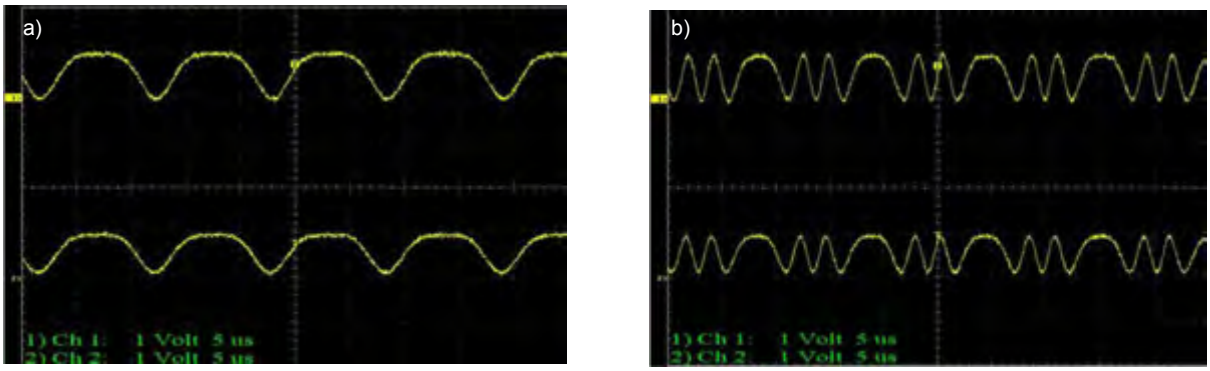

Fig. 3.7 – Signals obtained with the developed detector (upper curves) and the commercial one (lower curves) for a retardance of a) 0.5λ and b) 1.5λ

If we compare the above curves to the ideal ones in figure 3.3, it is possible to conclude that the developed photoreceiver functions correctly, and that its performance and bandwidth are suitable for the application at hand.

- NI Data Acquisition Card

The bidirectional communication between the system and the computer is controlled via a National Instruments Data Acquisition Card model NI DAQ USB 6229.

Figure 3.8 – NI DAQ USB 6229 Data acquisition card from National Instruments.

The technical characteristics for this card are stated in the following table:

NI DAQ USB 6229	
Analog Inputs	32
Analog Outputs	4
Analog - Resolution (bits)	16
Digital I/O	48
Digital - Resolution (bits)	32
Input Max Rate (S/s)	250 K
Output Max Rate (S/s)	833 K
Range (V)	±10

Table 3.4 – Technical specifications for National Instruments data acquisition card

- Commercial Lock-in Amplifier

Characteristics

The lock-in amplifier from Stanford Research Systems, model SR830 was used for measuring the different components of the output signal, read and sent by the photodetector.

The LIA can communicate bidirectionally with the computer via the serial port (rs232) and a series of commands in ASCII characters.

The SR830 has a 256 input character buffer, and different commands may be sent in quick succession so that the buffer lines them up and the device performs them in the order they were received (FIFO). Some examples of the main instructions used for these particular applications are presented on table V.

These commands are either for an action to be performed by the amplifier or for monitoring the LIA's status, such as locked and overloaded states in order to prevent any measurement errors. All commands must end with a carriage return in order that the device "knows" the instruction line is over.

Command	Description
*IDN?	Queries the device identification
PHAS x	Sets the phase to the value of x, where x is expressed in degrees.
IGND 1	Specifies the input shield grounding to the "Ground" state.
OFLT i	Sets the time constant to the value of i, where I ranges from 10us to 30 Ks.
APHS	Performs the autophase function.
OUTP 1	Reads the current value of X

Table 3.5 – Sample list of ASCII commands for the Lock-in amplifier

- Optical Chopper

In order to accurately measure the dc signal with synchronous detection using a lock-in amplifier, in an analogous way as the ac signals are measured, it is desirable to minimise the effects of light intensity fluctuation and normalise the total light intensity of the incoming beam.

For this purpose, a mechanical chopper was added to the system, whose rotation takes place at a regular frequency F (of 500 Hz. in this case) and

locking the chopped intensity signal at this frequency using the lock-in amplifier once again (Guo, 2007).

The optical chopper model SR540 from Stanford Research Systems can provide a chopping frequency from 4Hz to 3.7 KHz. The chopper consists of a disc with a series of equidistant apertures. The disc is divided in two sets of apertures, the "inner" series, which is closes to the disc's centre chops the beam with one specific frequency f_i while the "outer" series (farther from the centre) chops at a different frequency f_o. A self explanatory diagram of these divisions is shown below:

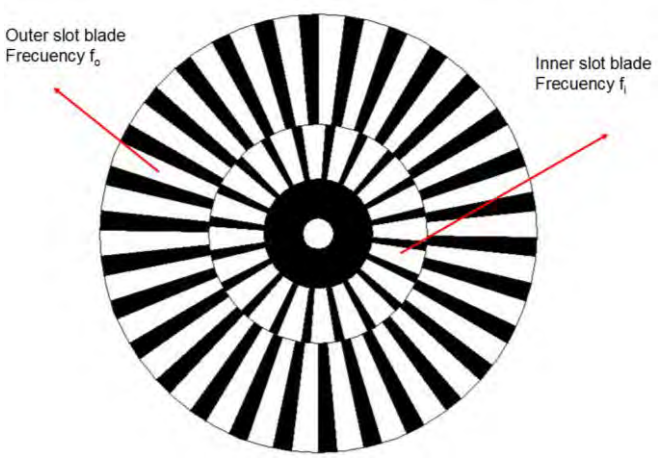

Figure 3.9 – Diagram of slot blade disc used for the chopper (unscaled)

The controller for the chopper, besides sending the signal to the motor, also has two analog outputs in which different reference signals may be read, including the square signal that matches the chopping frequency, twice the frequency and the sum and difference of the inner and outer frequencies.

3.2.2 Full-Stokes polarimeter: Mathematical Analysis and Interpretation

Consider the following optical setup,

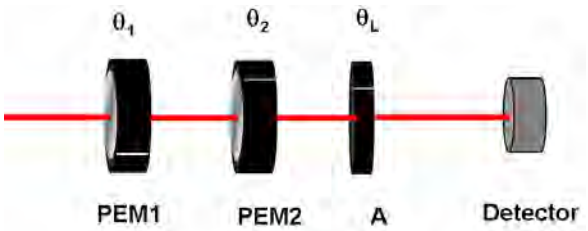

Figure 3.10 – Schematic of the dual-photoelastic based full-Stokes polarimeter

In which A represents a linear polariser and θ_1, θ_2 and θ_L represent the orientation angle of the PEM1, PEM2 and A respectively, and the incident monochromatic beam is polarised with a specific orientation and ellipticity.

Then, the transmitted beam has a Stokes vector $I_o = \{I_o, Q_o, U_o, V_o\}$ given by:

$$I_o = L(\theta_L)P_2(\theta_2)P_1(\theta_1)I_i, \tag{3.6}$$

where,

$$P_1(\theta_1) = R(\theta_1)P_1R(-\theta_1),$$

$$P_2(\theta_2) = R(\theta_2)P_2R(-\theta_2),$$

$$L(\theta_L) = R(\theta_L)LR(-\theta_L),$$

and

$$L = \frac{1}{2}\begin{pmatrix} 1 & 1 & 0 & 0 \\ 1 & 1 & 0 & 0 \\ 0 & 0 & 0 & 0 \\ 0 & 0 & 0 & 0 \end{pmatrix},$$

$$P = \begin{pmatrix} 1 & 0 & 0 & 0 \\ 0 & 1 & 0 & 0 \\ 0 & 0 & C_{\phi i} & S_{\phi i} \\ 0 & 0 & -S_{\phi i} & C_{\phi i} \end{pmatrix},$$

$$R(\pm\theta) = \begin{pmatrix} 1 & 0 & 0 & 0 \\ 0 & C_{2\theta} & \pm S_{2\theta} & 0 \\ 0 & \mp S_{2\theta} & C_{2\theta} & 0 \\ 0 & 0 & 0 & 1 \end{pmatrix},$$

i=1,2. **R** is the Mueller rotation matrix. ϕ_I is the retardance induced by the i-th photoelastic modulator and S_x and C_x represent the sin x and cos x respectively.

The signal collected by the photoreceiver D is proportional to the light intensity, which is given by the first row of I_o,

$$I_D \propto I_o = \frac{1}{2}\left(A_0 I_i + A_1 Q_i + A_2 U_i + A_3 V_i\right) \tag{3.7}$$

where

$$A_0 = 1,$$
$$A_1 = C^2_{\phi/2}\left[C_{2\theta_1} C_{2(\theta_1-\theta_L)} + C_{\phi_1} S_{2\theta_1} S_{2(\theta_1-\theta_L)}\right] - S_{\phi_1} S_{\phi_2} S_{2\theta_1} S_{2(\theta_2-\theta_L)} + S^2_{\phi/2}\left[C_{2\theta_1} C_{2(\theta_1-2\theta_2+\theta_L)} + C_{\phi_1} S_{2\theta_1} S_{2(\theta_1-2\theta_2+\theta_L}\right],$$
$$A_2 = C^2_{\phi/2}\left[-S_{2\theta_1} C_{2(\theta_1-\theta_L)} + C_{\phi_1} C_{2\theta_1} S_{2(\theta_1-\theta_L)}\right] - S_{\phi_1} S_{\phi_2} C_{2\theta_1} S_{2(\theta_2-\theta_L)} + S^2_{\phi/2}\left[-S_{2\theta_1} C_{2(\theta_1-2\theta_2+\theta_L)} + C_{\phi_1} C_{2\theta_1} S_{2(\theta_1-2\theta_2+\theta_L}\right],$$
$$A_3 = C^2_{\phi/2} S_{\phi_1} S_{2(\theta_1-\theta_L)} + S_{\phi_2} C_{\phi_1} S_{2(\theta_2-\theta_L)} + S^2_{\phi/2} S_{\phi_1} S_{2(\theta_1-2\theta_2+\theta_L)}$$

It can be seen from equation 3.7 that each term is proportional to one Stokes parameter at the input.

The phase retardation values ϕ_1 and ϕ_2 induced by the propagation through P_1 and P_2 respectively, may be expressed as,

$$\phi_i = \delta_i \sin(\omega_i t), i = 1,2, \tag{3.8}$$

where δ_I is the phase retardation amplitude and ω_I is the modulation angular frequency. Using equation 3.8, equation 3.7 is often rewritten by means of the Fourier expansion in terms of the first class Bessel functions,

$$\sin(\delta_i \sin \omega_i t) = 2\sum_{k=1}^{\infty} J_{2k-1}(\delta_i) \sin(2k-1)\omega_i t, \tag{3.9}$$

and

$$\cos(\delta_i \sin \omega_i t) = J_0(\delta_i) + 2\sum_{k=1}^{\infty} J_{2k}(\delta_i) \cos 2k\omega_i t, \tag{3.10}$$

In practice, the angles $[\theta_1,\theta_2,\theta_L]$, the retardation amplitudes (δ_1,δ_2), and the index order k of the Bessel function expansion are chosen conveniently to simplify the analysis of I_o.

Special Case: Circular Polarisation Sensitivity

Full Stokes polarimeters may be classified in accordance to their sensitivity to either linear or circular polarisation. In this project, we shall focus on the latter.

One set of conditions to be met for obtaining circular polarisation sensitivity in the system are as follow: $\theta_1 = \pi/4$, $\theta_2 = 0$, $\theta_L = \pi/8$, $J_0(\delta_1) = J_0(\delta_2) \approx 0$, and k = 1. These settings correspond to an already commercially available dual-PEM polarimeter.

After using equations 3.9 and 3.10, equation 3.7 can be further simplified as:

$$I_o = \frac{1}{2} I_i + \frac{\sqrt{2}}{2}(J_2(\delta)\cos(2\omega_1 t) - J_1(\delta)^2\{\cos[(\omega_1+\omega_2)t] - \cos[(\omega_1-\omega_2)t]\})Q_i - \frac{\sqrt{2}}{2} J_2(\delta)\cos(2\omega_2 t)U_i + \frac{\sqrt{2}}{2}(J_1(\delta)\sin(\omega_1 t) - J_1(\delta)J_2(\delta)\{\sin[(2\omega_1+\omega_2)t] - \sin[2\omega_1-\omega_2)t]\})V_i, \quad (3.11)$$

where $\delta = \delta_1 = \delta_2$.

From equation 3.11, it is possible to obtain an approximate value I_{ap} for I_i by using a lock in amplifier tuned and synchronised at the adequate frequencies. If these conditions are met, the Stokes parameter I_{ap} is proportional to the DC term in the I_D signal obtained by the photoreceiver. Q_{ap} can be found from the amplitudes of the signals at frequencies $2\omega_1$ and $\omega_1 \pm \omega_2$. U_{ap} is proportional to the amplitude of the signal at frequency $2\omega_2$. Finally, V_{ap} is calculated using the amplitudes of the signals at frequencies ω_1 and $2\omega_1 \pm \omega_2$. These amplitudes are obtained from,

$$I_{ap} = 2I(0), \quad (3.12)$$

$$Q_{ap} = \frac{\sqrt{2}}{J_2(\delta)}\frac{\mathrm{Re}\{I(2\omega_1)\}}{I_{ap}} = \mp\frac{\sqrt{2}}{J_1(\delta)^2}\frac{\mathrm{Re}\{I(\omega_1 \pm \omega_2)\}}{I_{ap}}, \quad (3.13)$$

$$U_{ap} = -\frac{\sqrt{2}}{J_2(\delta)}\frac{\mathrm{Re}\{I(2\omega_2)\}}{I_{ap}}, \quad (3.14)$$

$$V_{ap} = \frac{\sqrt{2}}{J_1(\delta)} \frac{\mathrm{Im}\{I(\omega_1)\}}{I_{ap}} = \mp \frac{\sqrt{2}}{J_1(\delta) J_2(\delta)} \frac{\mathrm{Im}\{I(2\omega_1 \pm \omega_2)\}}{I_{ap}}, \quad (3.15)$$

where,

$$I(\omega) = \frac{1}{\Delta t} \int_{-\Delta t}^{\Delta t} I_D \exp(i\omega t) dt, \quad (3.16)$$

$2\Delta t$ is the integration time and $i = \sqrt{-1}$.

Numerical Evaluation

The numerical evaluation of the full Stokes polarimeter was made using Mathcad. The modulator frequencies have been set at $f_1 = 42KHz$ and $f_2 = 47KHz$, where $\omega_1 = 2\pi f_i$. The integration time of the lockin was set at $\Delta t = 0.2ms$.

A criterion for selecting the frequencies at which the lock in amplifier should be tuned is to identify the stronger signals through the analysis of the Fourier spectrum of equation 3.11. In figure 3.11a, the figure spectra of the signals when linearly polarised with orientation $\psi = 0$ and $\pi/4$, and right circularly polarised light are shown. From this, it is evident that Q_{ap} and V_{ap} will be obtained from equations 3.13 and 3.15 respectively. It can also be concluded that this configuration will have a larger sensitivity towards circularly polarised light.

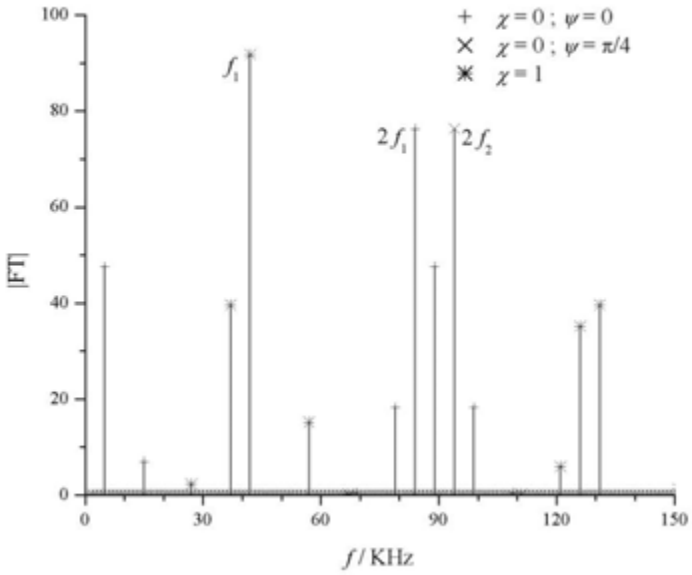

Figure 3.11 – Fourier spectrum of the modulated intensity signal using the circular polarisation sensitive configuration for three different states of polarisation: linearly polarised light and right circularly polarised light.

Afterward, the ellipticity of the incident polarisation was varied whilst keeping the orientation constant $(\psi = 3\pi/8)$. Figure 12a illustrates the error in calculating I_i from equations 3-12 to 3-15. In this case, the Stokes parameter for circularly polarised light (V) is recovered better than those for linearly polarised light (Q and U). This result is to be expected because the sensitivity to circular polarisation of the configuration. The largest error is that of Q.

To obtain the results shown in figure 3.12b, the orientation ψ of elliptically polarised light was changed while keeping the ellipticity constant: $\chi = 0.5$. The error for the calculated Stokes parameters behaves exactly as in the previous analysis. Thus, it may be stated that the system detects the Stokes parameter V with higher accuracy.

a)

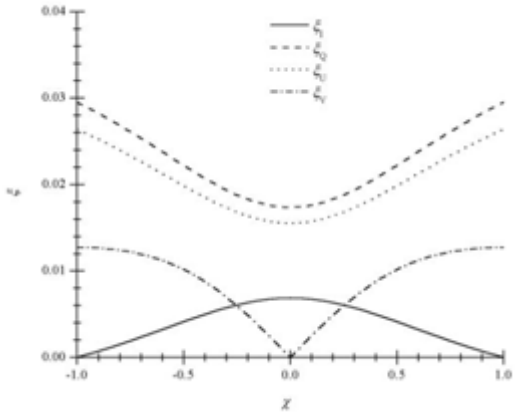

b)

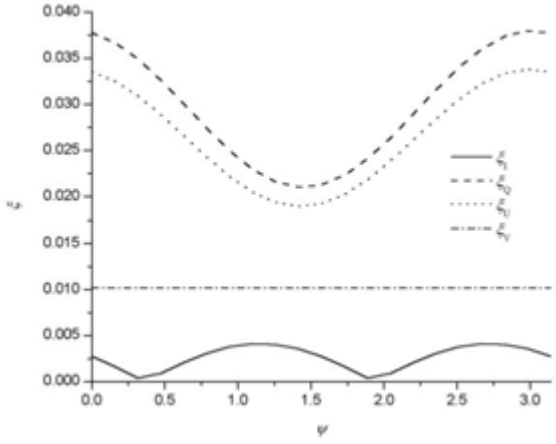

Figure 3.12 – Difference between calculated and incidence Stokes parameters while varying a) the ellipticity and b) the orientation of the incident light beam.

3.3 Control and Communication

3.3.1 LCVR Control

Each LCVR is driven by a square signal with variable amplitude that ranges from 0 to ±8 V rms and a frequency of 1KHz. Great care must be taken not to apply any DC voltage to the LCVR, for it could cause irreversible damages to its chemical constitution. Therefore, when a square wave signal of at least 1 KHz is not being applied, the voltage must be that of 0 V.

With this in mind, a LabView program was developed for characterisation and control of the retarders. This program is explained in greater detail in the section below.

- Program control VI

Since there are two LCVRs to be controlled, two independent analog outputs were required. Given that the necessary frequency is not too high, the performance that the NI DAQ 6229 (see previous section) provides was more than enough for the feat to be achieved.

A recently implemented feature of the Labview platform enables the user to output two analog signals (either with the same or different characteristics) simultaneously. Hence, synchronous control of both LCVRs was possible.

A sequence of two analog outputs with varying amplitude (from 0 to 8 V) was developed in order to monitor and determine the required amplitude values to obtain the main six polarisation states. These states include:

- Linear polarisation at 0° (Horizontally polarised light)
- Linear polarisation at 90° (Vertically polarised light)
- Linear polarisation at 45°
- Linear polarisation at -45°
- Circular right polarisation
- Circular left polarisation

The monitoring procedure consisted in fixing one of the LCVRs at a specific amplitude of the square signal while sequentially varying the other and registering the resulting polarisations states of the outcoming beam, knowing beforehand the polarisation state of the incoming beam. The same process was then repeated with the other LCVR.

The resulting table provided the required information, and the determined amplitude values required to achieve the aforementioned states of polarisation were hence implemented in the program.

A screenshot of the control program is shown below. The amplitude values and their respective resulting polarisation state with an incoming horizontally polarised beam are shown.

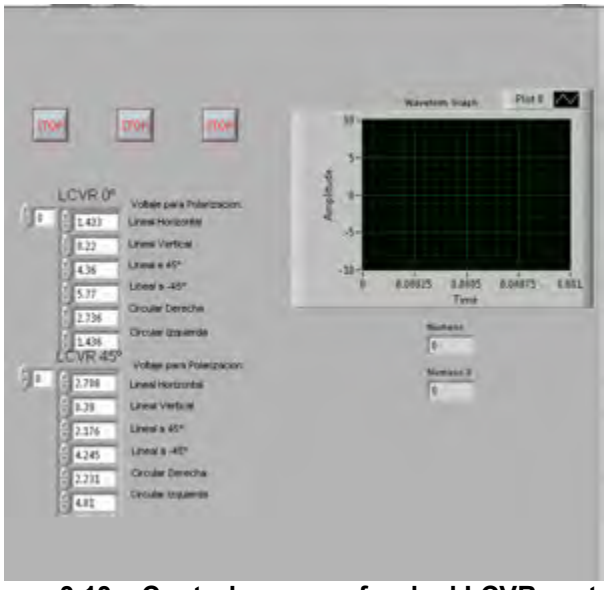

Figure 3.13 – Control program for dual LCVR system

After having the amplitude values determined, four out of these six polarisation states were selected and a new program, generating all four states sequentially was made.

3.3.2 PEM Control

- Switch Control

Given that four different signals must be used as reference for the lock-in amplifier to detect and measure the necessary amplitudes for the signal analysis. As previously mentioned, the photoelastic modulators are each controlled by separate device, provided by the manufacturer along with the PEMs.

Since the reference signal used to locate a specific component of the system's output signal, it follows that the reference must have the same frequency as the one we wish to measure. Furthermore, the reference must be perfectly synchronised to the other for the "lock-in" to happen.

Fortunately, each PEM controller has two signal outputs, which are the square signal at which the PEM is being driven, with a frequency f, and a second square signal at twice the frequency f.

Thus, we have therefore a total of four signals: f_1, $2f_1$, f_2, and $2f_2$. The subindexes 1 and 2 refer to the two PEMs, one driven at 45Hz and the other at 47Hz.

Finally, the chopping frequency must also be taken into account, given that it is modulating the signal as well, though in this case, in matter of amplitude.

A switching device was hence developed intended to be controlled by the computer and sequentially switch among all four signals to be fed to the lock-in amplifier for the different amplitudes to be measured and sent in turn to the computer. Simply put, the device feed the different reference signals to the lock-in amplifier, one at a turn, through one same output.

Figure 14 shows the schematic diagram for a single switch. The switching device is constituted by five of this.

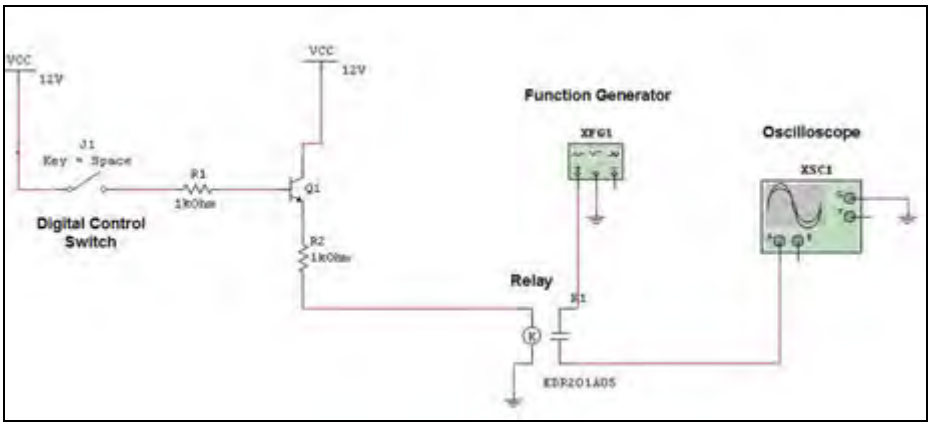

Figure 3.14 – Digital switch used to control the input of the reference signal for the lock-in amplifier

The "digital control switch" from figure 14 represents a simple digital switch that, in this case, will be one of the acquisition cards digital outputs. Five of these terminals were used for each of the signals. The relay is fed by a 12 V source, the same as the detector, so that no additional voltage sources are required. The function generator emulates the reference signal from the PEM controller and the response was monitored in an oscilloscope. A computer simulation using Multisim™ is shown in the figure below in both the ON and OFF state.

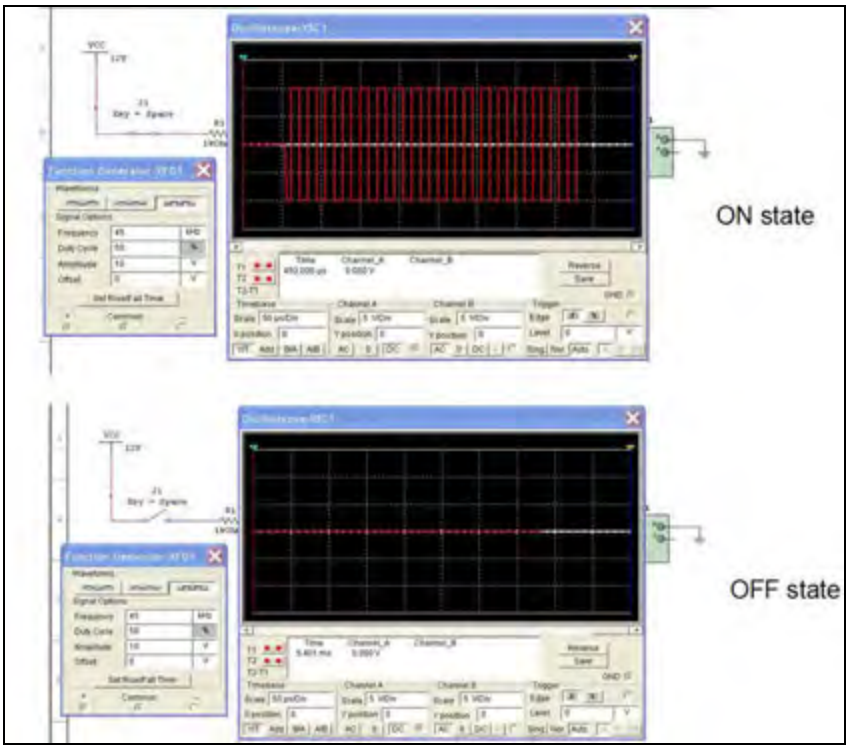

Figure 3.15 – Software simulation for the switching device.

Finally, the overall connection diagram, including LCVRs, PEM controllers, switch, DAQ, source, and detector is depicted in figure 3.16.

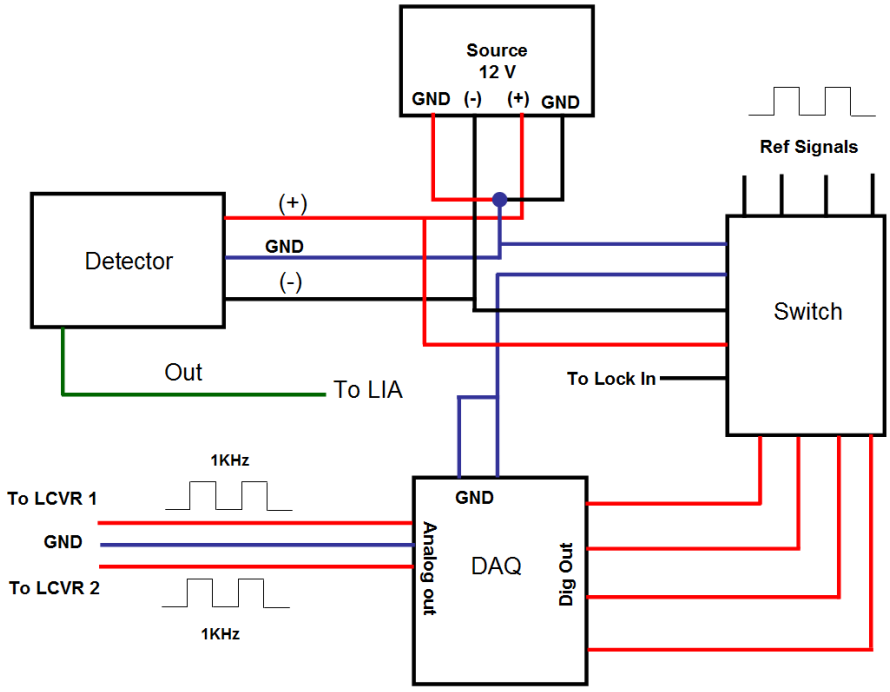

Figure 3.16 – Connection diagram for the system.

3.3.3 Signal Analysis

- RS-232 Interface Control Program

Basic Serial Write and Read.vi

The program enables data communication in and out of the serial rs232 port, allowing the user to control the transmission rate, number of bits to read or write and the port number to use. The program is already an example from the Labview library and merely used as an addition to the overall program for communication with the lock-in amplifier. The program is called as a subvi from different parts of the main programs.

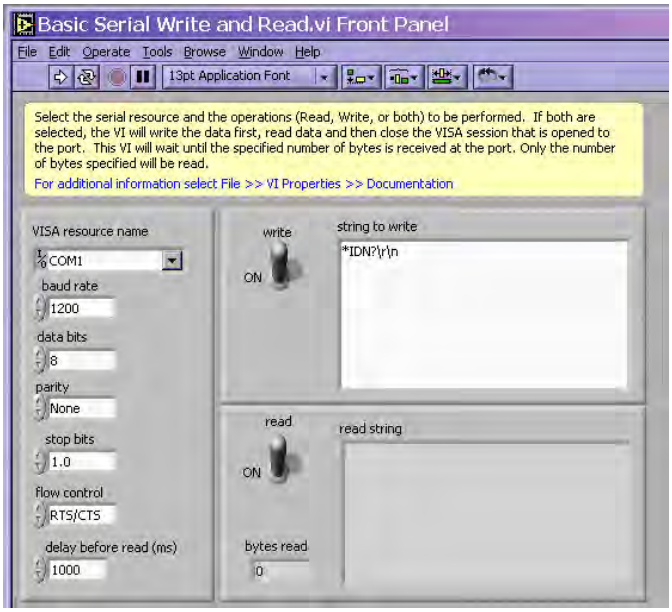

Figure 3.17 – Control window for Basic Serial Write and Read.vi

- Calculations and Ellipse Simulation programs

The calculations from the "Analysis" section from this chapter were implemented in a Labview program. Basically, the program receives the data measured by the lock-in amplifier and sent via the serial port. This information includes amplitude and phase for the different components of the output signal.

The calculations provide the full Stokes vector as well as polarisation state, orientation, ellipticity and degree of polarisation.

The Elipse.vi program gathers the calculations form the previous program, draws and displays the corresponding polarisation ellipse from the specified data and sends it back to the main program for the user to better visualise the readings.

3.4 Main Labview Program and User Interface

The program may be divided in two parts: the manual and the automatic.

The manual part comprises Boolean and numeric controls for direct communication with the LIA. The amplifier's manual provides the user with a set of instructions for different adjustments, measurements and specifications that can be controlled during a measurement. These commands were implemented in the program by means of the "Basic serial write and read.vi" (see previous section). These controls include manipulation of sensitivity, time constant, filters, reference (floating or grounded), reference signal (internal or external), reset, autophase, autoreserve, and autogain. These last three are of

particular importance since all three must be pressed in sequence autoreserve-autogain-autophase for the lock-in to perform the measurement accurately. The rest of the aforementioned controls are mainly used to avoid overloading and minimise noise.

Furthermore, the program reads and monitors the LIA's state (overload, unlocked) upon pressing a Boolean control, and displays the information by means of text-boxes or Boolean indicators depending on the data type. The user also has the option of sending the readings to a data log, either creating the file or writing in an already existing one.

Finally, the control window also includes a set of buttons for controlling the switching device through the DAQ card and hence, the reference signals for the system.

Figure 3.18 – Control panel for manual operation of system

The automatic option of the program enables the user to specify how many measurements to take and performs a sequence, for the specified number of times, switching among the four different signal references, reading each of the amplitudes from the lock-in and calling upon the different calculation programmes to obtain the polarisation state of the incident beam. Note that after each measurement, the program pauses and displays a message to the user, asking him or her to realign the elements for the next measurement. The program waits until the user presses the "OK" button before continuing with the next measurement until the specified number of readings has been completed.

After each measurement, the polarisation ellipse, Stokes vector, ellipticity, and orientation are displayed for the user to see.

Figure 3.19 – User interface for automatic measurement sequence

Once the measurements are finished, the program displays the readings in a data table for perusal whilst sent to a data log (ASCII or TXT file). The different columns containing information on the four Stokes parameters are also drawn in graphics for better analysis and simplicity purposes.

Nevertheless, the above program is only one half of the entire project since the measuring stage must work in synchronicity with the state generator, constituted by the already mentioned LCVRs.

Thus, the state-generating program - which sequentially generates four of the six fundamental polarisation states – was implemented in the main program. As each of the four states is generated, the resulting Stokes vector is measured, resulting in a series of four measurements.

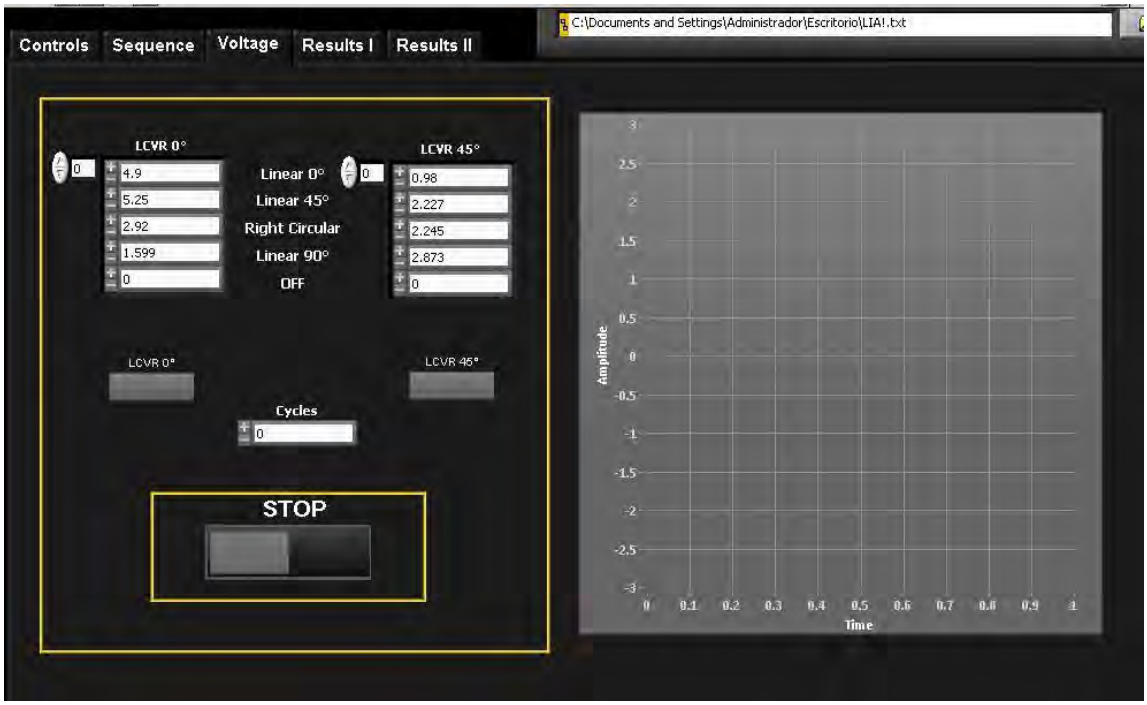

Figure 3.20 – Implementation and control panel of the voltage sequence for the LCVRs

Finally, the sample to be analysed was added to the experimental setup. Since the incident light upon the material under study has a known polarisation state (due to the LCVRs system), the sole unknown information is the polarisation state of the outcoming state, which is in turn measured by the dual-PEM system and detector.

All in all, the system constitutes a closed loop given that the input is controlled by the PC and the output is fed onto it.

Finally, with the required information from both the system's input and output, it is possible to calculate the Mueller Matrix of the sample.

The calculation of the Mueller Matrix by the labview program is as follows.

Suppose that a medium can be represented by the Mueller matrix

$$M = \begin{bmatrix} m_{00} & m_{01} & m_{02} & m_{03} \\ m_{10} & m_{11} & m_{12} & m_{13} \\ m_{20} & m_{21} & m_{22} & m_{23} \\ m_{30} & m_{31} & m_{32} & m_{33} \end{bmatrix} \tag{3.17}$$

On way of finding the 16 constituting elements is propagating a light beam with four different known states of polarisation and by analysing the changes the beam suffers upon exiting the sample. Thus, the incident polarisation states are:

$$I_{LH}^{i} = \begin{bmatrix} 1 \\ 1 \\ 0 \\ 0 \end{bmatrix};\ I_{45}^{i} = \begin{bmatrix} 1 \\ 0 \\ 1 \\ 0 \end{bmatrix};\ I_{RC}^{i} = \begin{bmatrix} 1 \\ 0 \\ 0 \\ 1 \end{bmatrix};\ I_{LV}^{i} = \begin{bmatrix} 1 \\ -1 \\ 0 \\ 0 \end{bmatrix}, \tag{3.18}$$

and the polarisation states after having exited the medium,

$$I_{LH}^{o} = \begin{bmatrix} I_{LH}^{o} \\ Q_{LH}^{o} \\ U_{LH}^{o} \\ V_{LH}^{o} \end{bmatrix};\ I_{45}^{o} = \begin{bmatrix} I_{45}^{o} \\ Q_{45}^{o} \\ U_{45}^{o} \\ V_{45}^{o} \end{bmatrix};\ I_{RC}^{o} = \begin{bmatrix} I_{RC}^{o} \\ Q_{RC}^{o} \\ U_{RC}^{o} \\ V_{RC}^{o} \end{bmatrix};\ I_{LV}^{o} = \begin{bmatrix} I_{LV}^{o} \\ Q_{LV}^{o} \\ U_{LV}^{o} \\ V_{LV}^{o} \end{bmatrix}, \tag{3.19}$$

The 16 elements are obtained by solving the linear equations system,

$$\begin{bmatrix} 1 & 1 & 0 & 0 & 0 & 0 & 0 & 0 & 0 & 0 & 0 & 0 & 0 & 0 & 0 & 0 \\ 1 & 0 & 1 & 0 & 0 & 0 & 0 & 0 & 0 & 0 & 0 & 0 & 0 & 0 & 0 & 0 \\ 1 & 0 & 0 & 1 & 0 & 0 & 0 & 0 & 0 & 0 & 0 & 0 & 0 & 0 & 0 & 0 \\ 1 & -1 & 0 & 0 & 0 & 0 & 0 & 0 & 0 & 0 & 0 & 0 & 0 & 0 & 0 & 0 \\ 0 & 0 & 0 & 0 & 1 & 1 & 0 & 0 & 0 & 0 & 0 & 0 & 0 & 0 & 0 & 0 \\ 0 & 0 & 0 & 0 & 1 & 0 & 1 & 0 & 0 & 0 & 0 & 0 & 0 & 0 & 0 & 0 \\ 0 & 0 & 0 & 0 & 1 & 0 & 0 & 1 & 0 & 0 & 0 & 0 & 0 & 0 & 0 & 0 \\ 0 & 0 & 0 & 0 & 1 & -1 & 0 & 0 & 0 & 0 & 0 & 0 & 0 & 0 & 0 & 0 \\ 0 & 0 & 0 & 0 & 0 & 0 & 0 & 0 & 1 & 1 & 0 & 0 & 0 & 0 & 0 & 0 \\ 0 & 0 & 0 & 0 & 0 & 0 & 0 & 0 & 1 & 0 & 1 & 0 & 0 & 0 & 0 & 0 \\ 0 & 0 & 0 & 0 & 0 & 0 & 0 & 0 & 1 & 0 & 0 & 1 & 0 & 0 & 0 & 0 \\ 0 & 0 & 0 & 0 & 0 & 0 & 0 & 0 & 1 & -1 & 0 & 0 & 0 & 0 & 0 & 0 \\ 0 & 0 & 0 & 0 & 0 & 0 & 0 & 0 & 0 & 0 & 0 & 0 & 1 & 1 & 0 & 0 \\ 0 & 0 & 0 & 0 & 0 & 0 & 0 & 0 & 0 & 0 & 0 & 0 & 1 & 0 & 1 & 0 \\ 0 & 0 & 0 & 0 & 0 & 0 & 0 & 0 & 0 & 0 & 0 & 0 & 1 & 0 & 0 & 1 \\ 0 & 0 & 0 & 0 & 0 & 0 & 0 & 0 & 0 & 0 & 0 & 0 & 1 & -1 & 0 & 0 \end{bmatrix} \begin{bmatrix} m_{00} \\ m_{01} \\ m_{02} \\ m_{03} \\ m_{10} \\ m_{11} \\ m_{12} \\ m_{13} \\ m_{20} \\ m_{21} \\ m_{22} \\ m_{23} \\ m_{30} \\ m_{31} \\ m_{32} \\ m_{33} \end{bmatrix} = \begin{bmatrix} I_{LH}^{o} \\ I_{45}^{o} \\ I_{RC}^{o} \\ I_{LV}^{o} \\ Q_{LH}^{o} \\ Q_{45}^{o} \\ Q_{RC}^{o} \\ Q_{LV}^{o} \\ U_{LH}^{o} \\ U_{45}^{o} \\ U_{RC}^{o} \\ U_{LV}^{o} \\ V_{LH}^{o} \\ V_{45}^{o} \\ V_{RC}^{o} \\ V_{LV}^{o} \end{bmatrix} \tag{3.20}$$

The solution for the elements of **M** is,

$$\begin{bmatrix} 0.5 & 0 & 0 & 0.5 & 0 & 0 & 0 & 0 & 0 & 0 & 0 & 0 & 0 & 0 & 0 & 0 \\ 0.5 & 0 & 0 & -0.5 & 0 & 0 & 0 & 0 & 0 & 0 & 0 & 0 & 0 & 0 & 0 & 0 \\ -0.5 & 1 & 0 & -0.5 & 0 & 0 & 0 & 0 & 0 & 0 & 0 & 0 & 0 & 0 & 0 & 0 \\ -0.5 & 0 & 1 & -0.5 & 0 & 0 & 0 & 0 & 0 & 0 & 0 & 0 & 0 & 0 & 0 & 0 \\ 0 & 0 & 0 & 0 & 0.5 & 0 & 0 & 0.5 & 0 & 0 & 0 & 0 & 0 & 0 & 0 & 0 \\ 0 & 0 & 0 & 0 & 0.5 & 0 & 0 & -0.5 & 0 & 0 & 0 & 0 & 0 & 0 & 0 & 0 \\ 0 & 0 & 0 & 0 & -0.5 & 1 & 0 & -0.5 & 0 & 0 & 0 & 0 & 0 & 0 & 0 & 0 \\ 0 & 0 & 0 & 0 & -0.5 & 0 & 1 & -0.5 & 0 & 0 & 0 & 0 & 0 & 0 & 0 & 0 \\ 0 & 0 & 0 & 0 & 0 & 0 & 0 & 0 & 0.5 & 0 & 0 & 0.5 & 0 & 0 & 0 & 0 \\ 0 & 0 & 0 & 0 & 0 & 0 & 0 & 0 & 0.5 & 0 & 0 & -0.5 & 0 & 0 & 0 & 0 \\ 0 & 0 & 0 & 0 & 0 & 0 & 0 & 0 & -0.5 & 1 & 0 & -0.5 & 0 & 0 & 0 & 0 \\ 0 & 0 & 0 & 0 & 0 & 0 & 0 & 0 & -0.5 & 0 & 1 & -0.5 & 0 & 0 & 0 & 0 \\ 0 & 0 & 0 & 0 & 0 & 0 & 0 & 0 & 0 & 0 & 0 & 0 & 0.5 & 0 & 0 & 0.5 \\ 0 & 0 & 0 & 0 & 0 & 0 & 0 & 0 & 0 & 0 & 0 & 0 & 0.5 & 0 & 0 & -0.5 \\ 0 & 0 & 0 & 0 & 0 & 0 & 0 & 0 & 0 & 0 & 0 & 0 & -0.5 & 1 & 0 & -0.5 \\ 0 & 0 & 0 & 0 & 0 & 0 & 0 & 0 & 0 & 0 & 0 & 0 & -0.5 & 0 & 1 & -0.5 \end{bmatrix} \begin{bmatrix} I^o_{LH} \\ I^o_{45} \\ I^o_{RC} \\ I^o_{LV} \\ Q^o_{LH} \\ Q^o_{45} \\ Q^o_{RC} \\ Q^o_{LV} \\ U^o_{LH} \\ U^o_{45} \\ U^o_{RC} \\ U^o_{LV} \\ V^o_{LH} \\ V^o_{45} \\ V^o_{RC} \\ V^o_{LV} \end{bmatrix} = \begin{bmatrix} m_{00} \\ m_{01} \\ m_{02} \\ m_{03} \\ m_{10} \\ m_{11} \\ m_{12} \\ m_{13} \\ m_{20} \\ m_{21} \\ m_{22} \\ m_{23} \\ m_{30} \\ m_{31} \\ m_{32} \\ m_{33} \end{bmatrix} \quad (3.21)$$

Hence, one last program was implemented onto the main one, which merely gathers the data and calculates the Mueller Matrix of the material under analysis (figure 21), displaying the results for the user's perusal (figure 22) and sending it as well to a datalog should the user wish to import the results to a spreadsheet later on.

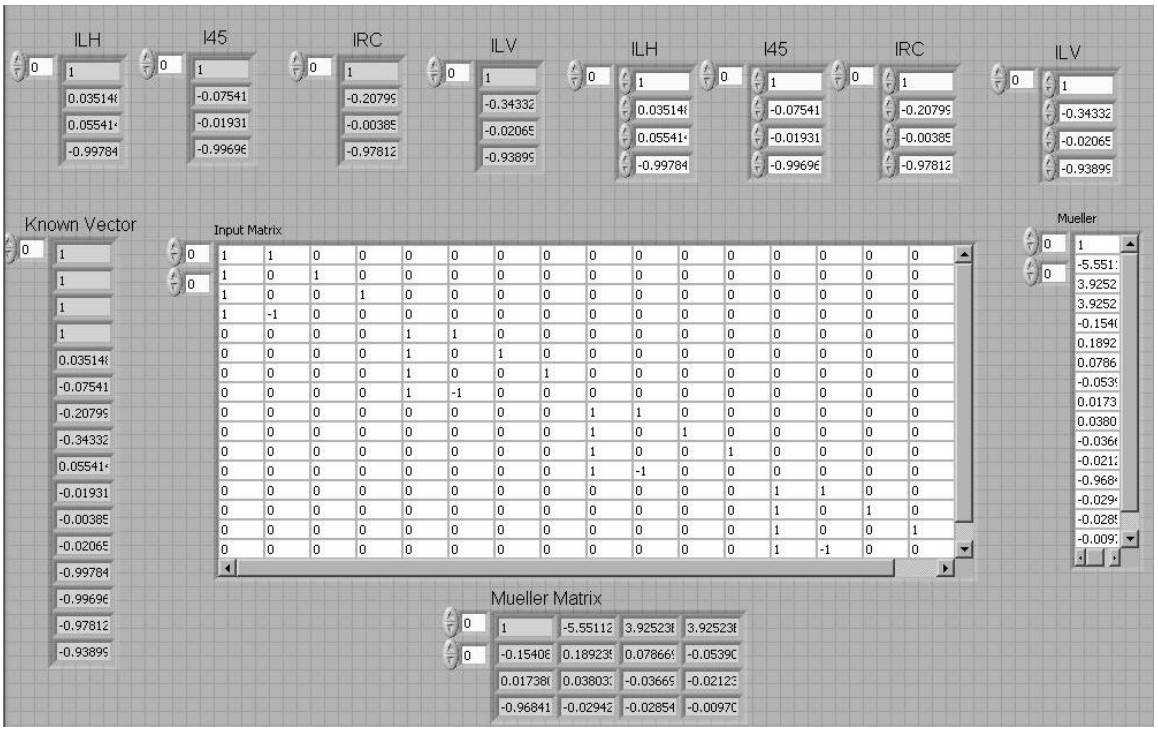

Figure 3.21 – Subvi which calculates the Mueller matrix from a given set of four Stokes vectors

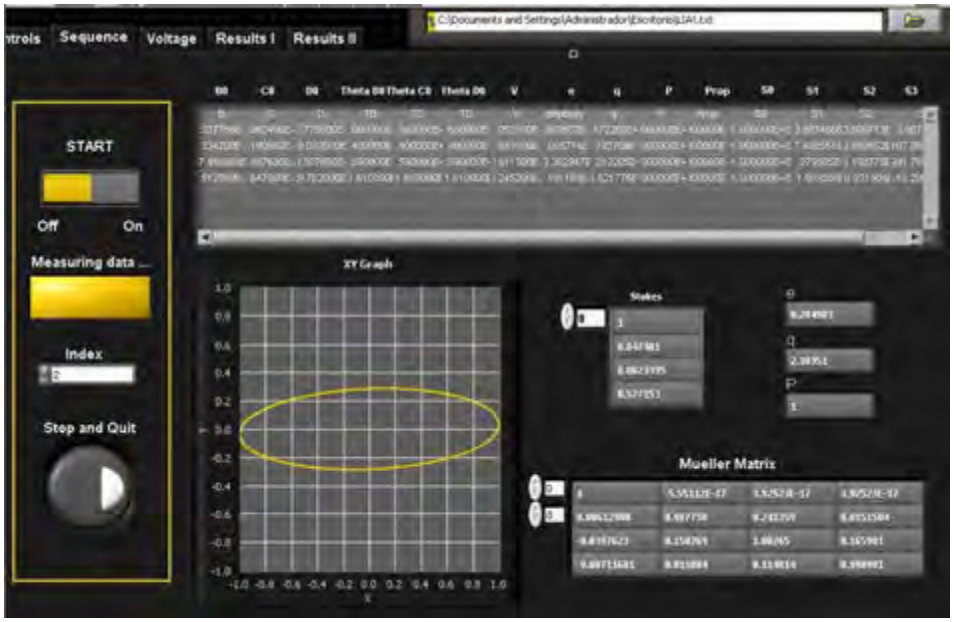

Figure 3.22 – Automatic measurement user panel, displaying the Mueller matrix of the sample under study.

Chapter 4
Results

4.1 Characterisation of elements and system

4.1.1 LCVR characterisation

Given that the polarisation state generator (PSG) is one of the two main stages in the project, it is of vital importance to ensure that its constituting elements are functioning correctly for the generated states to be as precise as possible. This is why, before attempting to make the PSG, it was necessary to analyse both LCVRs' responses and compare them. Given that both LCVRs are the same brand and model, in this case the manufactures being ARCoptix, it is to be expected that both their responses are the same or, at least, very similar.

The selected procedure for these characterisations is simple, though the process might be lengthy. Using a Helium-Neon laser, whose wavelength is approximately λ = 633 nm. and a commercial polarimeter from Thorlabs™, this characterisation was possible.

First off, the necessary electrical connections to control each LCVR were made. For this particular model, the retarder has two banana type connectors with independent voltage polarisation, i.e. it is irrelevant which terminal is connected to ground and which to positive voltage.

The LCVR ought to be oriented with its fast axis at a 45° angle with respect to the incoming laser beam polarisation. Thus, the incoming beam was oriented at 45°, whereas the LCVR remained horizontal.

Using a data acquisition card from National Instruments (NI DAQ USB-6229), a Labview program was developed in order to inject the LCVR with a square 1 KHz signal at a specific voltage, which the user was to vary from 0 to 10 volts.

In the following figure, a screenshot of said program is presented:

Figure 4.1 – Labview program for controlling the input square signal used to characterise the LCVR

Two sets of measurements were performed, one for each of the two retarders to analyse.

The results for the measurement are listed on the following table:

LCVR2			LCVR1 (2nd measurement)		
Amplitude	Orientation	Ellipticity	Amplitude	Orientation	Ellipticity
0.00	47.35	-0.3	0,0000	44.52	-0.33
0.5	47.35	-0.29	0,5000	44.55	-0.33
1.00	47.4	0.00	10,000	45.75	-0.04
1.5	142.16	-0.2	15,000	152.89	-0.28
2.00	48.22	0.17	20,000	45.03	0.26
2.50	141.04	0.52	25,000	152.67	0.38
3.00	141.86	-0.04	30,000	151.73	-0.11
3.50	143.84	-0.35	35,000	154.37	-0.39
4.00	147.1	-0.57	40,000	160.49	-0.6
4.5	154.73	-0.76	45,000	174.4	-0.74
5.00	178.49	-0.87	50,000	15.53	-0.76
5.5	26.3	-0.82	55,000	28.99	-0.7
6.00	35.45	-0.73	60,000	35.08	-0.63
6.5	39.03	-0.66	65,000	38.2	-0.57
7.00	40.85	-0.6	70,000	40.03	-0.52
7.5	41.96	-0.54	75,000	41.15	-0.47
8.00	42.6	-0.5	80,000	41.99	-0.44
8.5	43.04	-0.46	85,000	42.35	-0.41
9.00	43.5	-0.43	90,000	43	-0.38
9.5	43.71	-0.4	95,000	43.15	-0.35
10.00	43.91	-0.38	100,000	43.44	-0.33

Table 4.1 – Results for LCVR characterisation

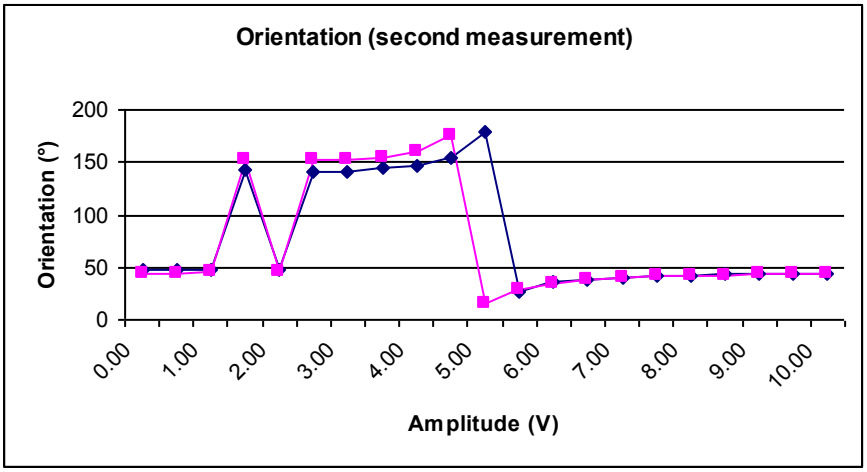

Figure 4.2. Comparison between the obtained curves for orientation. The lilac curve corresponds to LCVR1 and the blue curve to LCVR2.

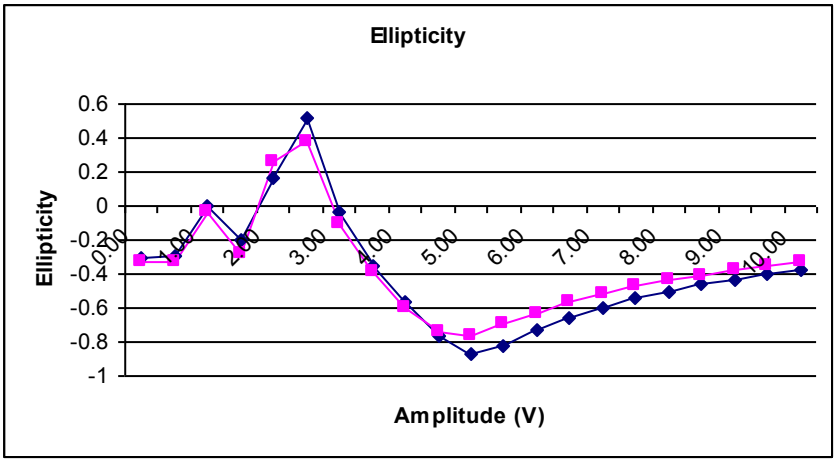

Figure 4.3. Comparison between the obtained curves for ellipticity of outcoming beam. The lilac curve corresponds to LCVR1 and the blue curve to LCVR2.

Although a slight phase difference is evident, one can also clearly see that both curves are very similar to each other. However, it must be noted that even a slight deviation in alignment and orientation may cause a certain amount of error in the obtained data.

Once having established the correct performance of both LCVRs, the stage for the polarisation state generator was set up. As stated in previous chapters, this stage consists on a linear polariser followed by two LCVRs, the first oriented at 45° and the other at 0°. A picture of the setup for the PSG may be seen in Fig. 4.4.

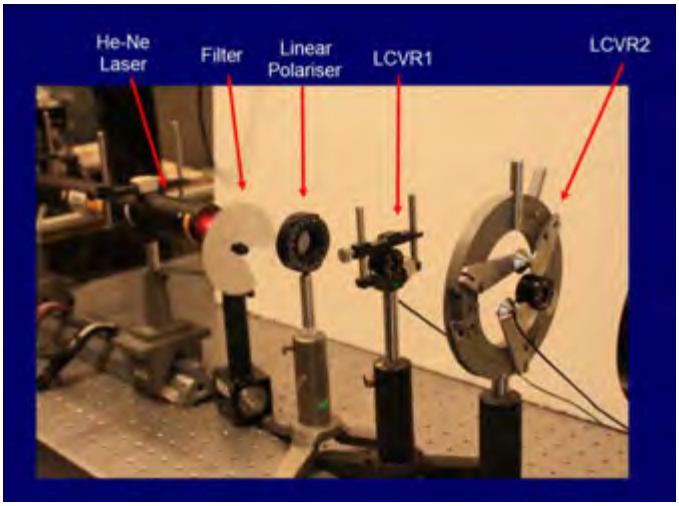

Figure 4.4 Experimental setup for the polarisation state generator based on two liquid crystal variable retarders.

4.1.2 Characterisation of Polarisation State Generator

With all the constituting elements working as a single system, the next step is to test and make the appropriate measurements in order to ensure its correct performance. Hence, a series of different polarisation states, both linear and elliptical, were generated using the 2 LVCRs. The setup for these retarders was fairly simple, merely requiring the first LCVR to be oriented at 45° and the second one to remain horizontal. Through trial and error, a series of input signals were fed to each LCVR, ranging from 0 to 8 volts. While fixing one of the input voltages to a specific value, the second voltage would be varied gradually, until the desired voltages were obtained. These voltages were to vary in ellipticity while the orientation remained constant. These values were then to be applied to the retarders in order to characterise the finished instrument.

Furthermore, obtaining linear polarisations (ellipticity=0) at different orientations was desirable as well for the same reasons. Thus, the following values were obtained for each of the described state of polarisation:

Polarisation State	Voltage for LCVR 45° (V)	Voltage for LCVR 0° (V)
O=90°, e=-1	1.457	4.68
O=90°, e=-.9	1.451	4.448
O=90°, e=-.8	1.453	4.193
O=90°, e=-.7	1.455	3.979
O=90°, e=-.6	1.458	3.832
O=90°, e=-.5	1.461	3.639
O=90°, e=-.4	1.467	3.43
O=90°, e=-.3	1.476	3.248
O=90°, e=-.2	1.485	3.143
O=90°, e=-.1	1.55	2.935
O=90°, e=0	1.599	2.873
O=90°, e=.1	2.299	2.855
O=90°, e=.2	2	3.1
O=90°, e=.3	1.985	3.245
O=90°, e=.4	1.96	3.36
O=90°, e=.5	1.946	3.57
O=90°, e=.6	1.939	3.75
O=90°, e=.7	1.933	3.96
O=90°, e=.8	1.929	4.17
O=90°, e=.9	1.925	4.364
O=90°, e=.10	2.92	2.245
O = 0°, e=0	4.9	0.98
O=45°, e=0	5.25	2.227
O=-45°, e=0	5.4	4.75

Table 4.2. Applied voltages for generating various polarisation states used for the complete system characterisation. Note: "O" stands for orientation and "e" for ellipticity.

With these voltages established, and the second stage, i.e. the polarisation state analyser (PSA), completed, it was possible to verify the correct performance of both stages. It must be stated however, that the PSA was previously tested using other means to generate known polarisation states, such a linear polarisers and waveplate retarders. Once more, the ThorLabs™ Polarimeter was used as reference for such measurements. A picture of the optical setup for the PSA is shown in figure 4.5.

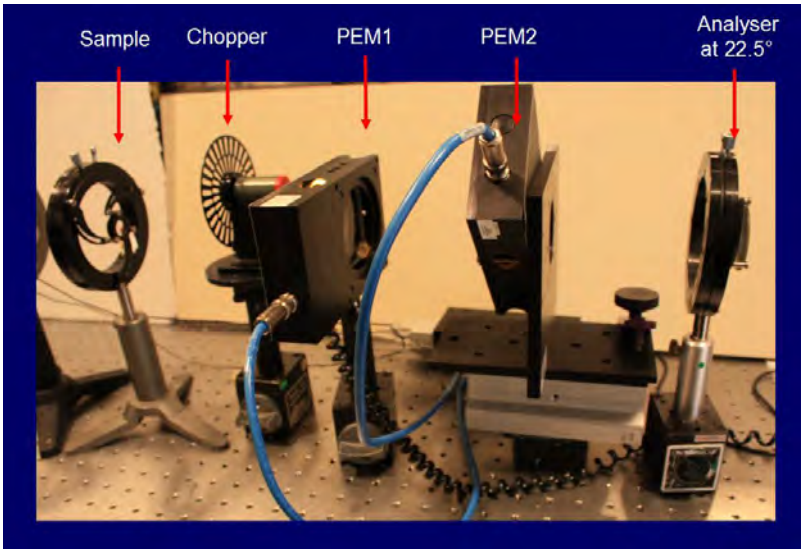

Figure 4.5. Experimental setup for the polarisation state analyser based on two photoelastic modulators

4.2 Characterisation of the system

With both stages working and by measuring a series of different states of polarisation, both linear and elliptical, it was possible to characterise the system. Firstly, a linear polarisation was generated using the two LCVRs. After each measurement, the polarisation was rotated by 10 degrees, going from 0° to 180°. The necessary calculations for determining the 4 Stokes parameters along with ellipticity and orientation were performed by the labview program and logged into a text file. The obtained results are shown in the table below.

Orientation	Ellipticity	S0	S1	S2	S3
0	-8.50E-04	1.00E+00	2.14E-01	3.03E-02	-1.70E-03
10	-8.40E-04	1.00E+00	2.15E-01	-2.37E-02	-1.68E-03
20	-7.69E-04	1.00E+00	2.03E-01	-7.47E-02	-1.54E-03
30	-5.33E-04	1.00E+00	1.72E-01	-1.30E-01	-1.07E-03
40	1.33E-04	1.00E+00	1.10E-01	-1.86E-01	2.65E-04
50	6.89E-04	1.00E+00	1.27E-02	-2.16E-01	1.38E-03
60	1.64E-03	1.00E+00	-4.40E-02	-2.11E-01	3.28E-03
70	2.71E-03	1.00E+00	-9.13E-02	-1.96E-01	5.42E-03
80	3.97E-03	1.00E+00	-1.54E-01	-1.52E-01	7.94E-03
90	5.19E-03	1.00E+00	-2.03E-01	-7.32E-02	1.04E-02
100	5.77E-03	1.00E+00	-2.10E-01	4.70E-02	1.15E-02
110	4.43E-03	1.00E+00	-1.60E-01	1.45E-01	8.86E-03
120	2.95E-03	1.00E+00	-1.03E-01	1.89E-01	5.90E-03
130	1.82E-03	1.00E+00	-5.43E-02	2.09E-01	3.63E-03
140	8.26E-04	1.00E+00	8.43E-03	2.16E-01	1.65E-03
150	4.42E-05	1.00E+00	8.63E-02	1.98E-01	8.83E-05
160	-1.02E-03	1.00E+00	1.99E-01	8.43E-02	-2.04E-03
170	-1.11E-03	1.00E+00	2.14E-01	3.02E-02	-2.22E-03
180	-1.10E-03	1.00E+00	2.14E-01	3.04E-02	-2.19E-03

Table 4.3. Stokes vectors for each of the generated orientations for the linear polarisations in the system

As we can see from table 3, the S1 parameter which in the first row ought to be approximately 1 is significantly smaller than S0. Nevertheless, S2 and S3, which ought to be close to zero, are in turn smaller than S1. Although further adjustments were still required at this point, the graph of these data shows that the behaviour of the results, at least, was the expected one.

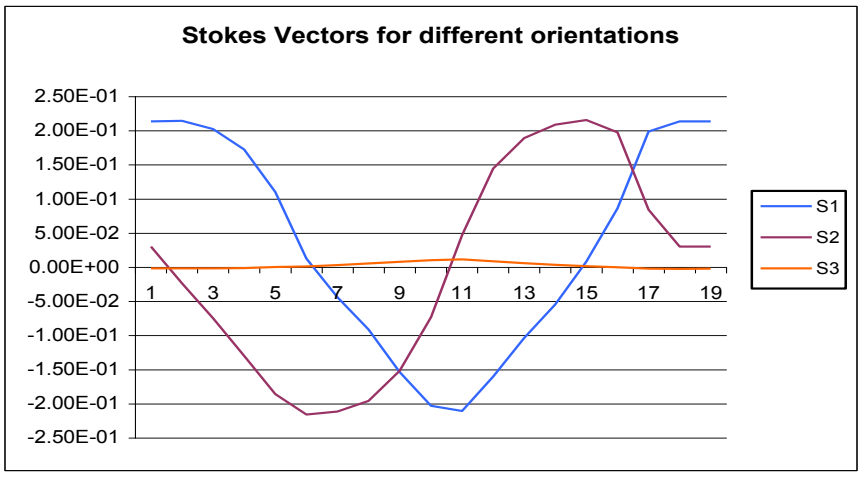

Figure 4.6. Curves representing the last three stokes vectors for each of the linear polarisations with varying orientation from 0° to 180°. The amplitude is given in millivolts.

As we can see in figure 4.6, S3 remains relatively constant, its value nearing zero, as ought to be the case for all linear polarisations, thus indicating that the input beam had a linear polarisations, regardless of the orientation. The parameter S0 was not included in the graph, since it always amounts to one once all four parameters have been normalised.

As for the elliptical polarisations, as stated above, the orientation was fixed at a specific angle, in this case 90° while the ellipticity was varied from -1 to 1 by .1 each time. The results are shown in the table below.

Ellipticity	S0	S1	S2	S3
-1.0	1.00E+00	-1.08E-01	-1.81E-01	-9.78E-01
-0.9	1.00E+00	-2.38E-01	-9.63E-02	-9.66E-01
-0.8	1.00E+00	-4.11E-01	-6.30E-02	-9.09E-01
-0.7	1.00E+00	-5.54E-01	-3.91E-02	-8.31E-01
-0.6	1.00E+00	-6.50E-01	-3.14E-02	-7.60E-01
-0.5	1.00E+00	-7.66E-01	-1.35E-02	-6.42E-01
-0.4	1.00E+00	-9.87E-01	7.69E-04	-1.62E-01
-0.3	1.00E+00	-9.93E-01	4.40E-03	-1.17E-01
-0.2	1.00E+00	-9.96E-01	5.93E-03	-8.95E-02
-0.1	1.00E+00	-1.00E+00	1.18E-02	-2.25E-02
0.0	1.00E+00	-1.00E+00	2.05E-02	-1.22E-02
0.1	1.00E+00	-9.99E-01	3.24E-02	1.93E-02
0.2	1.00E+00	-9.71E-01	4.79E-02	2.33E-01
0.3	1.00E+00	-9.30E-01	5.64E-02	3.64E-01
0.4	1.00E+00	-8.88E-01	5.08E-02	4.56E-01
0.5	1.00E+00	-7.89E-01	4.67E-02	6.13E-01
0.6	1.00E+00	-6.84E-01	4.18E-02	7.29E-01
0.7	1.00E+00	-5.44E-01	3.73E-02	8.38E-01
0.8	1.00E+00	-4.01E-01	3.23E-02	9.15E-01
0.9	1.00E+00	-2.65E-01	2.76E-02	9.64E-01
1.0	1.00E+00	-1.43E-01	-2.14E-01	9.66E-01

Table 4.4 - Stokes vectors for each of the generated ellipticities at 90°

It must be noted, that these results were taken after various adjustments had been made to the system, which is the reason why the normalised Stokes parameters are much closer to the ideal values than was the case for the linear polarisation results. These same results are graphed in figure 4.7.

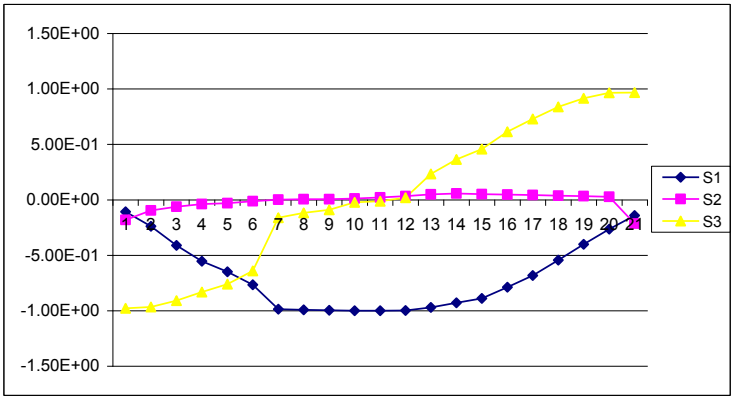

Figure 4.7. Curves representing the last three Stokes vectors for each of the elliptical polarisations oriented a 90° and ellipticities varying from -1 to 1.

Although the above curves do not display an ideal pattern, the behaviour and trend do match the expected results, thus ensuring that the system is indeed functioning adequately.

4.2.1 Results for different media and comparison to ideal response

Listed below are the Mueller Matrices for three different common media, air, quarter waveplate retarder and halfwave plate retarder. These media were selected to perform a series of test using the completed instrument in order to characterise the system and locate sources for inaccuracies and errors.

$$M_{AIR} = \begin{bmatrix} 1 & 0 & 0 & 0 \\ 0 & 1 & 0 & 0 \\ 0 & 0 & 1 & 0 \\ 0 & 0 & 0 & 1 \end{bmatrix} \tag{4.1}$$

$$M_{QWP}(\phi = \pi/2) = \begin{bmatrix} 1 & 0 & 0 & 0 \\ 0 & 1 & 0 & 0 \\ 0 & 0 & 0 & -1 \\ 0 & 0 & 1 & 0 \end{bmatrix} \tag{4.2}$$

$$M_{HWP}(\phi = \pi) = \begin{bmatrix} 1 & 0 & 0 & 0 \\ 0 & 1 & 0 & 0 \\ 0 & 0 & -1 & 0 \\ 0 & 0 & 0 & -1 \end{bmatrix} \tag{4.3}$$

Let us bear in mind however that these three matrices represent the **ideal** elements. Nevertheless, in reality as we know, no optical element is one hundred percent ideal. Along with this, the system is still bound to have a certain amount of error. It is for these two reasons, that the obtained results we present, although approximate to what was expected are not necessarily the best possible ones.

After a series of measurements, the averages of the obtained results are as follows:

$$M_{AIR} = \begin{bmatrix} 1 & 0 & 0 & 0 \\ -.0028 & .996 & 0.08175 & 0.007 \\ 0.0445 & -0.0033 & .92675 & 0.0775 \\ 0.027 & 0.04375 & -0.0698 & .9385 \end{bmatrix} \quad (4.4)$$

$$M_{QWP}(\phi = \pi/2) = \begin{bmatrix} 1 & 0 & 0 & 0 \\ -0.007 & .9824 & -0.193 & -0.3046 \\ -0.0234 & -0.089 & 0.0192 & -.9486 \\ -0.0052 & 0.0354 & .9886 & -0.0052 \end{bmatrix} \quad (4.5)$$

$$M_{HWP}(\phi = \pi) = \begin{bmatrix} 1 & 0 & 0 & 0 \\ -.0136 & .9638 & -.606 & -0.1768 \\ -.0646 & -0.211 & -0.7166 & 0.2332 \\ .0054 & -0.1464 & 0.0498 & -0.9718 \end{bmatrix} \quad (4.6)$$

If we compare the above matrices to the ideal ones, it is clear that the obtained results differ from the expected ones, though a tendency to either “0” or “1” is apparent in each case, none of the values, with the exception of those in the first row, actually reaches 0 or 1. This suggests, as stated above, a certain amount of inaccuracy both in the optical elements used for the analysis and the instrument itself.

4.2.2 Repeatability and Precision

Using the same three media as in the previous section, i.e. air, quarter wave plate retarder and half waveplate retarder, a series of 5 measurements for each of them was performed in order to test the repeatability and precision of the system. The graphed results for the three cases are shown on figures 8-10.

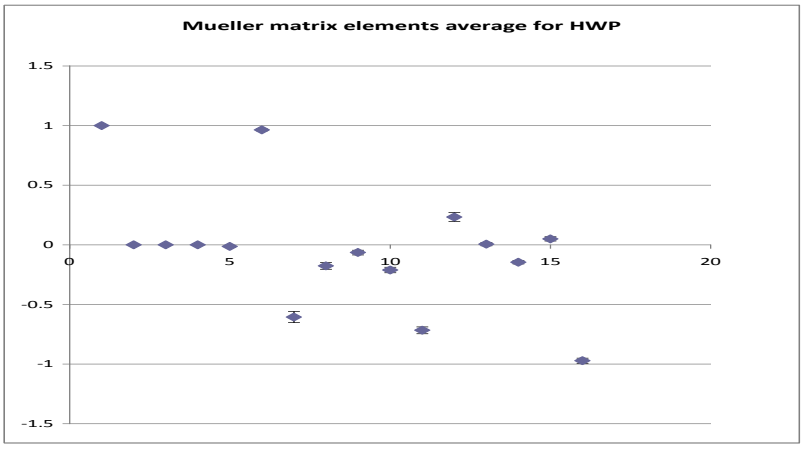

Figure 4.8. The sixteen Mueller Matrix elements, averaged throughout five different measurements, along with their respective error (in black) for a λ/2 retarder.

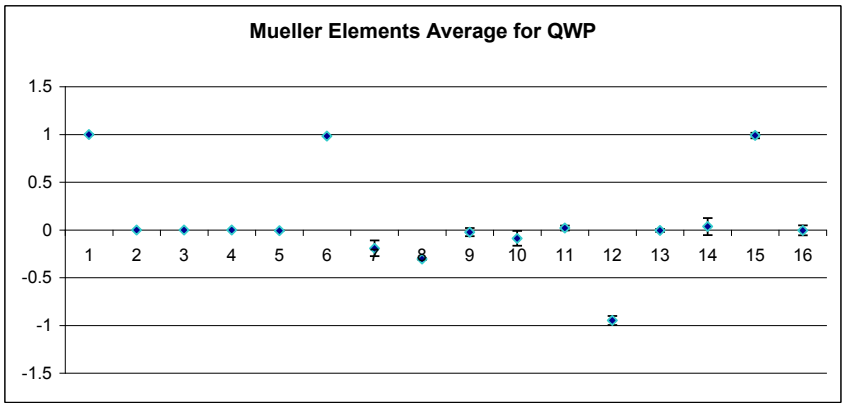

Figure 4.9. The sixteen Mueller Matrix elements, averaged throughout five different measurements, along with their respective error (in black) for a λ/4 retarder.

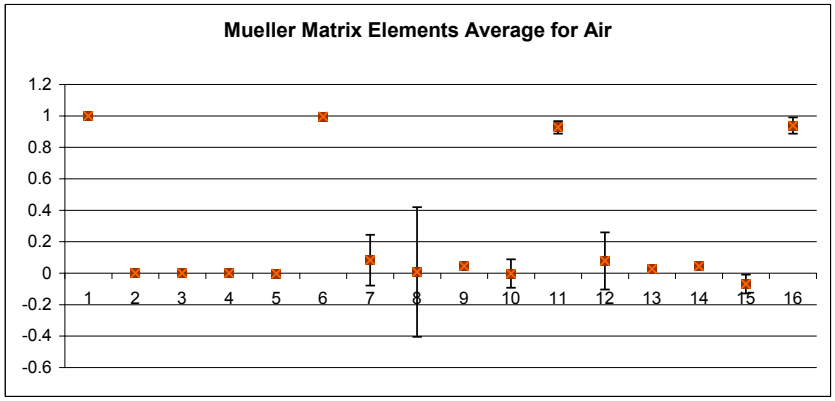

Figure 4.10. The sixteen Mueller Matrix elements, averaged throughout five different measurements, along with their respective error (in black) for Air.

From figures 8 - 10 it is evident that the repeatability for the three different measurement sets is not constant. For the case of the Half Waveplate (figure 6), the standard deviation, represented by a black line in all 16 points, remains the smallest of the three sets, whereas the measurements for air present a far greater deviation, particularly among the zero elements. The latter case might be due to variations in ambient factors among the different measurements, noting that they were performed on different days, as opposed to other two cases.

Nevertheless, it is also the half wave plate retarder measurement that presented a greater inaccuracy in all 16 elements, landing farther from either 0 or 1 (depending on the element) than was the case for the other two media. This may be caused by the superior thickness in this media when compared to the other two. The highest accuracy was obtained for the quarter waveplate retarder, whose values were far more proximate to 0 or 1, though a fairly decent accuracy was also achieved when measuring air.

4.2.3 Analysis of system performance through gradual variation of a single factor

In order to determine the system's susceptibility to changing surrounding conditions, a series of measurements varying the ambient light intensity were taken. Using a quarter waveplate retarder as a media, a simple light dimmer to control the illumination, and a radiometer to monitor the varying light intensity, the 16 Mueller matrix elements were obtained and recorded for eight different intensities. The obtained results are shown in the figure below.

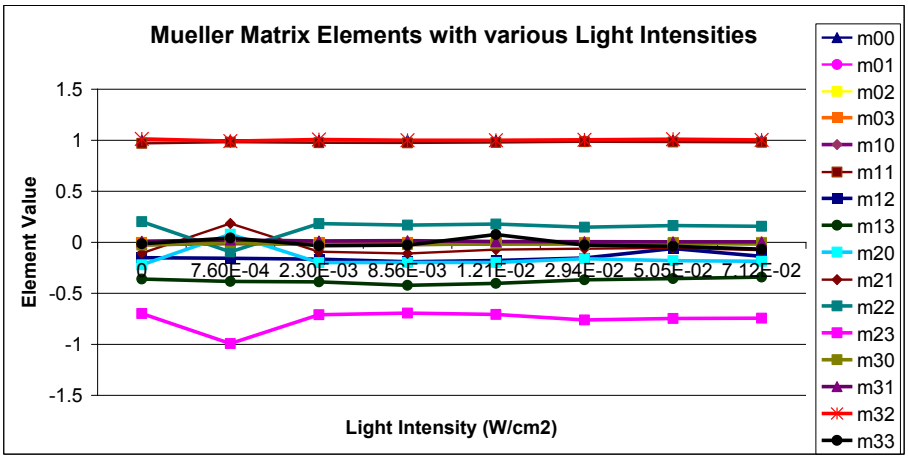

Figure 4.11. Elements for the Mueller matrix corresponding to a quarter waveplate retarder throughout a series of measurements with various light intensities

From figure 11, we can see that those elements that should be approximate to one present a relatively constant behaviour, with its values fairly close to 1. As for the elements that should ideally be zero vary somewhat among themselves, though they are all small. However, we may also notice that they don't share a

common sign either, some of them being negative and the other positive. This suggests a certain amount of inaccuracy in the measurements. Furthermore, although the curves do present a certain degree of consistency, their behaviour is not as constant as that of the elements that represent the value of 1.

Finally, the element m_{23}, which for this case should be close to the value of "-1", deviates from the ideal value by a significant amount except for the second measurement. Yet again, apart from the second value, the curve's behaviour is relatively constant.

Chapter 5
Conclusions

5.1 System performance

As the results from the previous section have shown, there is still work to be done in regard to the system's accuracy. In order to make a more robust instrument further adjustments and modifications ought to be implemented.

Nevertheless, the system proved to be working up to a certain point. The obtained Mueller matrices for different media do coincide with the predefined ones albeit with limited accuracy. The basic functions of the instrument however have been successfully implemented as were both stages, the polarisation state generator (PSG) and the polarisation analyser.

Endeavouring to make a fully autonomous instrument, a photoreceiver was designed and implemented, specifically design for the system and the frequency and amplitude of the signals to be read. Also, a switching system that would enable to automatically read all reference signals by turns to be fed to the lock-in system was made and, encompassed with digital commands controlled via the PC, enabled the measurement process to be automated.

As for the software, a program that allows the user to request a measurement, or manually control the measurement process, that for both cases logs and displays the obtained results was developed and is functioning correctly.

Finally, it must be noted, that the system may be used either as a laser transmission ellipsometer or a standard polarimeter which determines the state of polarisation (ellipticity, orientation, and stokes vector) of an incident light beam.

5.2 System limitations

From the system's characterisation, it remains clear that the system's accuracy and repeatability need to be improved. Also, the system's susceptibility to ambient factors must be minimised for it to be considered robust.

First off, all noise needs to be minimised. Although the photoreceiver was enclosed in a metal case, which indeed proved effective, the rest of the system remains in the open. In order to reduce the instrument's susceptibility to light changes as well as other sources of noise, it might be advisable to enclose the whole system, blocking as much ambient light as possible.

Another source for inaccuracy, as with all optical systems, is a faulty alignment. Try as one might to realign the constituting elements for each set of measurements, differences, however slight, in alignment are inevitable. Thus,

the retarders, modulators, polarisers, and the rest of the elements should be fixed in a specific position so as to guarantee a proper alignment during all measurements.

Another possible source for inaccuracies is the integration time constant that is being used. Although a time constant of 1ms was used, which, according to an ideal system's response ought to provide a minimum error in the lock-in's readings, it is possible that another value proves to be more effective. Thus further tests should be performed while trying other time constants, comparing the response in each case.

Finally, the system's speed must be addressed. The lock-in amplifier's response needs to be faster and the communication between amplifier and PC can be enhanced by changing the communication interface. The amplifier had an already developed communication interface via the serial port, RS232. However, by using the USB port instead, the communication speed could be increased and thus, the entire measurement process sped up. Another way of enhancing the system's response would be optimising the control program. An in-depth analysis of the code and functions must be done, which, when properly done, might lead to locating bottlenecks in the processing and finding more efficient and faster ways of carrying out certain functions.

5.3 Future work

Besides the proposed adjustments and enhancements necessary for the system, further work is required for a feasable, marketable instrument to be obtained.

5.3.1 Lock-In amplifier

Although the commercial amplifier was able to take the appropriate measurements, it takes up too much time to lock the signal, measure the amplitude and send the data to the PC. Since the amplifier is designed for measuring signals with a wide range of frequencies and amplitudes, it provides different time constants, cut-off frequencies, and various options that the user can manipulate according to the signal they are trying to measure.

Since we have specific frequencies and signals to measure, a lock-in amplifier specifically designed for the system and measurement requirements might speed up the process, since it would have a fixed time constant and cut off frequencies for the filters predefined, so there would be no need for in-the-moment adjustments to be performed via PC or manually.

A good option would be designing an amplifier for each of the four signals to measure, using each of the four reference signals. This would then enable, not only to have fixed parameters and save processing time, but it would allow for the four signals to be measured simultaneously without the need for switching

and waiting one signal at one frequency to be measured before the next one can be read, as is the case right now. This would undeniably enhance the instrument's response and make the system non-dependant from third party equipment by integrating it all in the same instrument.

It must be noted, that these quadruple lock-in amplifier was indeed contemplated, and its design and implementation begun. Nevertheless, due to time and budget limitations, the commercial one was used as a temporary measure, postponing the plans for the other one.

5.3.2 Data acquisition card

Another piece of equipment that must be replaced for the system to become autonomous is the data acquisition card. Now that the required number of signals to generate and acquire, the frequency and sampling requirements and voltage range have all been established, it is possible to design and implement an acquisition card solely dedicated to meeting this instrument's needs.

Another important detail is that since the control program was developed in Labview, it might be advisable to develop a user interface in the same platform so as to simplify the communication among all the elements in the system.

5.3.3 PEM based PSG

Two liquid crystal variable retarders (LCVR) are being currently used for the polarisation state generator. However, two photoelastic modulators (PEM) will replace these LCVRs in order to achieve a faster response.

5.3.4 Mechanical system

As stated in the previous section, the optical elements ought to be fixed down so that alignment problems do not ensue. Nevertheless, although the LCVRs, retarders, polarisers, and PEMs can be fixed in a certain position, a mount for all of these elements and the sample must be properly designed. This however, can only be done once the definite constituting elements are acquired.

Another aspect to consider is that the ellipsometer is expected to perform measurements in reflection as well as in transmission for future stages of the instrument. Finally, it must be determined whether a single point or a wide area is to be analysed. Thus, an appropriate mount for either laser or camera must also be implemented.

5.3.5 Readings for wider areas

As stated above, one possibility of future stages of the project is to analyse more than one point within the sample. That is a wider area in which different changes may be taken place in different points of the sample. A CCD camera is

to be bought and will be used instead of the photoreceiver. Image processing might thus be necessary in the future, and the control program and calculations should be modified accordingly.

5.3.4 Spectral range

Finally, the instrument is intended to work within a wide spectral range. At the moment, the instrument only detects red light at a wavelength of λ=632.8 nm. If the spectral range is to be widened, a white light source must be used along with a monochromatic, so that selection of wavelength is available. Furthermore, the camera which is to replace the photoreceiver must be sensitive to all the desired wavelengths so that measurements are possible.

References

Aspnes, D. (1976) *Rotating-compensator/analyzer fixed-analyzer ellipsometer: Analysis and comparison to other automatic ellipsometers*. Journal of Optical Society of America, Vol. 66, No. 9

Azzam, R. (1977) *Fourier Photoellipsometers and Photopolarimeters based on Modulated Optical Rotation*. SPIE Optical Polarimetry, Vol. 112

Carey, R. (1996) *Programmable liquid crystal waveplates in ellipsometric measurements*. IOP Publishing, Ltd.

Chabay, I. (1975) *Infrared Circular Dichroism and Linear Dichroism Spectrophotometer.* Applied Optics Vol. 14, No. 2

Collins, R. W, Chen, I. An, C. (2005). *Rotating polarizer and analyzer ellipsometry in Handbook of ellipsometry*. New York: Springer.

Corn, R. (1996) Rapid-scan Polarization-modulated Fourier-transform Infra-red Reflection Absorption Spectroscopy, Hinds Instruments Inc.

De Martino, A. (2003) Optimized Mueller polarimeter with liquid crystals, Optics Letters, Vol. 28, No. 8, Optical Society of America

Diner, J. D. (2007) *Dual-photoelastic-modulator-based polarimetric imaging concept for aerosol remote sensing.* Applied Optics, Vol. 46, No. 35

Fjarlie, E. (1977) *Photodiode preamplifier systems: low-noise positive-feedback*. Applied Optics Vol. 16, No. 2

Giudicotti, L. (2007) *Data analysis for a rotating quarter-wave, far-infrared Stokes polarimeter*. Applied Optics, Vol. 46, No. 14

Goldstein, D. (2003). *Polarized light* (2nd ed.). United States of America : Marcel Dekker.

Graeme, J. G. (1995) *Photodiode Amplifiers*, United States of America: McGraw Hill, Ch. 4

Guo, X. (2007) *Stokes polarimetry in multiply scattering chiral media: effects of experimental geometry*. Applied Optics, Vol. 46, No. 20.

Hinds Instrument (2005). *Dual PEM Stokes Polarimeter: Applications*. (http://www.hindspem.com/DUALPEMStokesPolarimeter/default.aspx)

Hinds Instruments (2007) PEM 100 Photoelastic Modulator User Manual, Hinds Instruments Inc.

J. G. Graeme. (1995) *Photodiode Amplifiers*, United States of America: McGraw Hill

Jellison, G. E., Modine, F. A. (2005). *Polarization modulation ellipsometry in Handbook of ellipsometry*. New York: Springer.

Johnson, M. (2004) *Photodetection and Measurement*, McGraw Hill, Ch. 1.

Jonasz, M. (2009) *Handbook of measuring system design: Light Sources and Detectors,* T.3, Ch. 91, Wiley Ed.

Jung, W. G. (2002) *Op Amp Applications*,: Analog Devices Inc.

Kim, Myeonghee (1987) Differential Polarization Imaging, II. Symmetry Properties and Calculations. Biophysical journal. Vol. 52

Kromer, P. Pc-Based Lock-In Detection of Small Signals in the Presence of Noise, Department of Physics, University of Texas, Austin

Meadowlark, (2009). *Polarization Control with Liquid Crystals*.

Neiswander, R. (1975) *Low-noise extended-frequency response with cooled silicon photodiodes.* Applied Optics Vol. 14, No. 11

Oakberg, T. (2005) *Magneto-Optic Kerr Effect*. Hinds Instruments Application Note.

Ord, J. (1977) *Self-Nulling Ellipsometer Design*. SPIE Optical Polarimetry, Vol. 112

Perkin Elmer Instruments (2000) Specifying Lock-in Amplifiers, Technical Notes TN 1001, Perkin Elmer Instruments

Pye, D., (2001). *Polarised Light in Science and Nature*. United Kingdom: Institute of Physics, London.

Rashid, M., (1999) *Circuitos Microelectrónicos*, Mexico : Thomson Editores, p. 297

Refrégiér, P. (2007) *Intrinsic Coherence: A New Concept in Polarization and Coherence Theory*. Optics and Physics News. Optical Society of America.

Signal Recovery (2005) The Incredible Story of Dr D.P. Freeze, Technical Note TN 1007

Signal Recovery (2008) The Analog Lock-In Amplifier, Technical Note TN 1002

Stanford Research Systems (2004) About Lock-In Amplifiers, Application Note #3

Tuchin, V. V., Wang, L. V., Zimnyakov, D. A. (2006). *Optical Polarization in Biomedical Applications.* Germany: Springer

Tuchin, V.V.(2009) Handbook of Optical Sensing of Glucose in biological Fluids and Tissues, CRC Press, Taylor & Francis Group

Urbena, R. (2006) New Polarisation generator/analyzer for imaging Stokes and Mueller polarimetry, The international Society for Optical Engineering, SPIE

W. G. Jung. (2002) *Op Amp Applications*, United States of America: Analog Devices Inc.

Wang, B. (2005) *Dual PEM Systems: Polarimetry Applications*. Hinds Instruments Application Note.

Appendix A

ANALYSIS FOR TRANSMITTED LIGHT INTENSITY FOR A DUAL PHOTOELASTIC MODULATOR SYSTEM

A. Torales-Rivera[1]
G. Martínez-Ponce
C. Solano
Centro de Investigaciones Óptica
Apdo. Postal 1-948, 37000 León, Guanajuato, México
[1]alitorales@cio.mx

INTRODUCTION

The construction of a photoelastic modulator based polarimeter has been motivated by the necessity to quantify the optical properties of photosensitive materials to a single wavelength. Such a system is able to measure the changes different polarisation states in a beam of light experiment while propagating through a material sample by means of the optical anisotropies it possesses.

A comparison between experimentally obtained signals and ideal ones is presented. Furthermore, an approximate of the ideal curved using Bessel functions is also compared in order to establish differences between all three curves.

Finally, a statistical analysis of 16 experimental curves was carried out, in each case randomly varying various factors that may influence the quality of the measurements, so as to determine the degree of impact of each one of them and thus enhance the system's performance.

THEORY

Suppose that a beam of polarised light $\mathbf{S}_i = \{S_{i,0}, S_{i,1}, S_{i,2}, S_{i,3}\}$ is cast upon a polarimetric system constituted by two photoelastic modulators $\mathbf{P}_1$ and $\mathbf{P}_2$ with their optical axes oriented at $\theta_1 = 0°$ y $\theta_2 = 45°$ respectively, followed by a polariser (i.e. analyser) **A** oriented at $\theta = 0°$ and a photoreceiver. The retardance values for $\mathbf{P}_1$ and $\mathbf{P}_2$ are designated as ϕ_1 and ϕ_2 respectively whilst the modulating frequencies are ω_1 and ω_2. Thus, the outcoming beam may be obtained from the product

$$\mathbf{S}_s = \mathbf{A}\mathbf{R}(\theta_2)\,\mathbf{P}_2\,\mathbf{R}(-\theta_2)\,\mathbf{P}_1\,\mathbf{S}_i\,, \tag{1}$$

where

$$\mathbf{A}=\begin{bmatrix}1&1&0&0\\1&1&0&0\\0&0&0&0\\0&0&0&0\end{bmatrix},\quad \mathbf{P}_i=\begin{bmatrix}1&0&0&0\\0&1&0&0\\0&0&\cos[\phi_i\sin(\omega_i t)]&\sin[\phi_i\sin(\omega_i t)]\\0&0&-\sin[\phi_i\sin(\omega_i t)]&\cos[\phi_i\sin(\omega_i t)]\end{bmatrix},\quad i=1,2$$

and **R**(x) is the rotation matrix

.The light intensity registered by the photoreceiver I_D is given by the first row of $\mathbf{S}_s$. That is,

.

$$I_D=S_{s,0}=\frac{1}{2}S_{i,0}+\frac{1}{2}\cos[\phi_1\sin(\omega_1 t)]S_{i,1}-\frac{1}{2}\sin[\phi_1\sin(\omega_1 t)]\sin[\phi_2\sin(\omega_2 t)]S_{i,2}+\frac{1}{2}\sin[\phi_1\sin(\omega_1 t)]\cos[\phi_2\sin(\omega_2 t)]S_{i,3} \quad (2)$$

In Mueller polarimetry, equation 2 is usually expressed in Bessel function terms as,

$$I_D=S_{s,0}=\frac{1}{2}S_{i,0}+\frac{1}{2}[J_0(\phi_1)+2J_2(\phi_1)\cos(2\omega_1 t)]S_{i,1}-\frac{1}{2}[2J_1(\phi_1)\sin(\omega_1 t)][2J_1(\phi_2)\sin(\omega_2 t)]S_{i,2}+\frac{1}{2}[J_1(\phi_1)\sin(\omega_1 t)][J_0(\phi_2)+2J_2(\phi_2)\cos(2\omega_2 t)]S_{i,3} \quad (3)$$

where $J_i(x)$ is the first degree polynomial *i*. This approximation is useful when choosing f1 and f2 and optimising the system for obtaining the Stokes vector from the incident light.

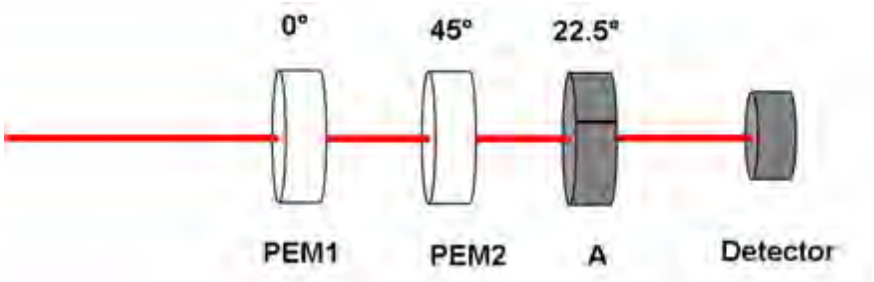

Fig.1 Polarimetric system based on photoelastic modulators (PEM_1 and PEM_2).

A is a linear polariser and D a photoreceiver.

EXPERIMENTAL SETUP

One of the modulator's optical axes is oriented at 45°, while the second one is set horizontally. The retardance value is considered as one of the values under study by comparing the ideal, experimental, and mathematically estimated curves. The detected signal is sent to a computer for processing by means of LabView™ software. The device that is being developed aims to obtain the transmission Mueller matrix of different materials with optical applications, thus providing information on various of its properties.

The obtained results present a root mean square error among the three compared data which varies from 10 to 20%. This value is related to the sampling frequency that was used during the experiment.

With the purpose of optimising the system's overall performance, the effect of different variables such as ambient light, distance between modulators, mechanical noise, metal encasing, input voltage for the photoreceiver and quality of the analyser.

By establishing 2 different levels for each of the afore mentioned factors and by means of a 2^{6-2} factorial design with a IV level resolution, a statistical analysis that allowed us to determine which of the six factors contributes more to the performance of the system, and which, if any, is crucial to its optimal response, was carried out.

The following table shows the two levels used for each of the factors analysed during the study:

Factor	High Level	Low Level
Ambient Light	1	0
Distance between modulators	6 cm.	12 cm.
Mechanical Noise	1	0
Metallic Encasing	1	0
Input Voltage	15 V	12 V
Analyser	Calcite	Glass

Table 1 – Varying factors during the experiments and their respective low and high values.

Note: The values shown as “0” and “1” represent the absence o presence of said factor respectively.

By using these values and randomly varying each factor a data matrix was generated, hence obtaining a total of 16 different tests, each with a different combination of values.

Furthermore, with the purpose of analysing the impact each of the modulator’s retardance value on the system, the experiment was carried out using a specific combination of retardance amplitudes for the modulators. The tests were made with retardance values of $\pi/2$ radians for the first PEM and π for the second one.

The resulting curves in each case were compared to the computer generated curve. A total of 62 values in each of the tests was obtained and a cubic interpolation was performed using a mathematical software, in this case Matlab. Next, the RMS error for each of the results was computed, having considered this the output variable in the experiment in order to analyse the variables and thus optimise the system based on the result from the corresponding statistical analysis.

In figure 2 one of the graphs (light intensity vs. time) is presented. The data for this graph was obtained from the experimental tests. The blue curve represents the ideal computer generated response, whereas the red curve represents the experimentally obtained data.

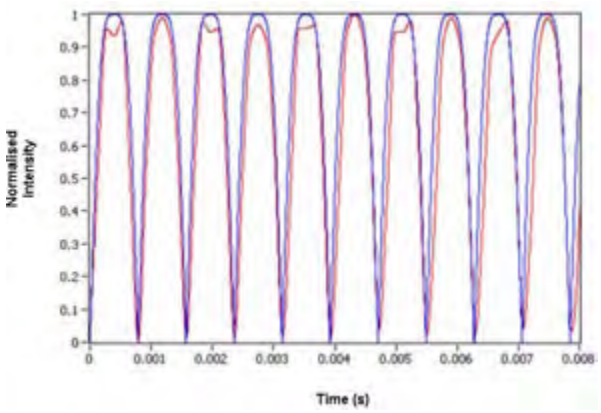

Figure 2 – Comparison between the experimental curves (red) and the computer generated ones by means of a mathematical software (blue).

From the obtained RMS error values , a statistical analysis was carried out with the aid of the statistical software Statgraphics™ with the purpose of establishing up to which point does each of the studied factors influence the performance of the system and hence minimise the error whilst striving to obtain the most reliable instrument possible.

In figure 3 a graph illustrating the impact of all the factors is presented. As it may be surmised, the two factors whose impact is the strongest are metallic encasing and analyser quality. It must be noted that the calcite polarisers have better quality and thus, are more costly than those of glass.

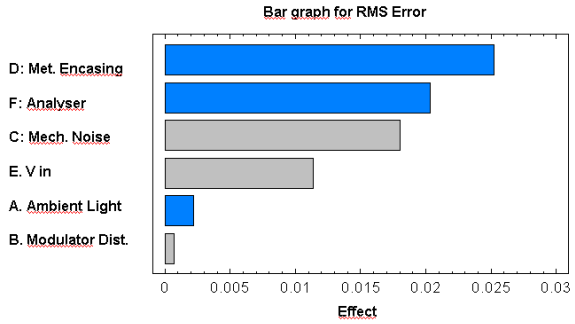

Figure 3 - Bar graph illustrating the amount of impact each factor has on the system, obtained from the results of the 16 first tests.

According to figure 4, which depicts the correlation between the most significant effects, it is possible to determine the optimal values for each of the factors so as to minimise the RMS error.

Figure 4 – Effect of both levels for each of the analysed factors on the other factors

From the above figure it can be seen that, for the case of ambient light, the ideal value to minimise the RMS error is “high”, i.e. with the lights on. The distance between modulators ought to be the “low” one, which in this case is 6 cm. Similarly, for the remaining factors, as was to be expected, it is best to keep the mechanical noise to a bare minimum, to have a metallic encasing for the circuitry and use the calcite analyser. Curiously, the corresponding result for input voltage (Vin) was

somewhat unexpected, resulting in a “low” level voltage, which is that of 12 volts as opposed to 15V, which it must be said, was the value recommended by the manufacturer.

In the following table, a summary of the results is presented.

Factor	Recommended Level
Ambient Light	High
Distance between modulators	Low
Mechanical noise	Low
Metallic Encasing	High
Input Voltage	Low
Analyser Type	High

Table 2 – Recommended values for each of the studied factors.

Now, based on the graph on figure 3, it is necessary to determine which of the factors will be maintained at the recommended level and which are not significant to the measurements, thus allowing us to select which level to use, not necessarily because it is recommended, but because it is more economical.

From figure 3, it is clear that the effect of both ambient light and distance between modulators is negligent. Therefore, it is possible to choose either level for these factors without significantly affecting the final result. It was then decided to encase the whole system, thus blocking the ambient light and simplifying the mechanical design for the system.

The distance between modulators will also be kept at a “low level”, since one of the purposes for the project is to keep the instrument as compact as possible.

Before validating any of these conclusions though, the data variance must be verified; ensuring that it is constant and the factors are independent.

First off, the term “residual” must be approached. A residual is defined as “the difference between the observed value in a test and the response that was initially predicted by the model for such test.” (Gutiérrez, 2008).

In order to verify that the variance condition is met, the residuals versus the predicted values must be graphed.

Figure 5 presents the resulting graph.

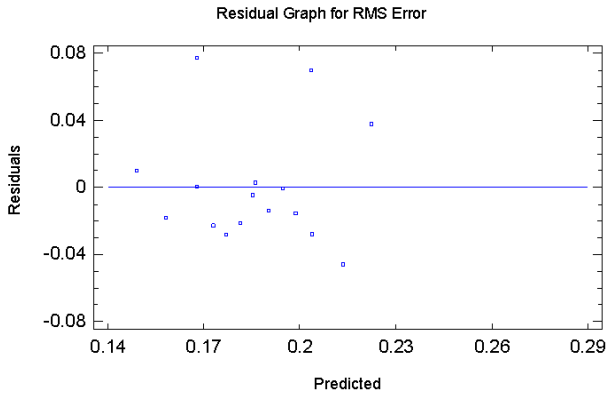

Figure 5 – Residual Graph for the experiments regarding the polarimeter's performance.

From the previous graph, one can see that the data points do not follow a specific pattern, that is, the ay appear to fall randomly, which enables us to conclude that the variance is indeed constant and thus, the conclusions gathered from the analysis are valid.

In order to verify the independence, the residuals for each of the tests are graphed in the same order in which they were obtained. Thus,

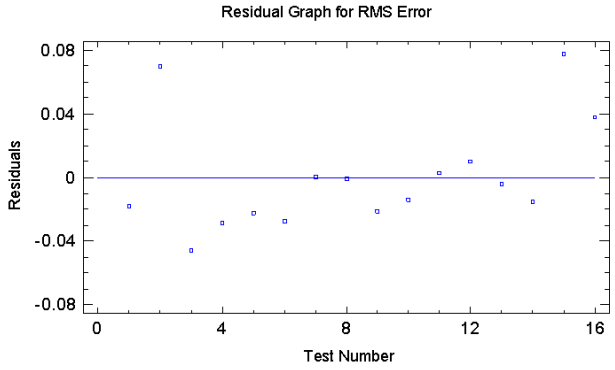

Figure 6 – Residuals vs. test number used for verifying independence.

Once again, if the residuals turn out to be independent, no definite pattern should be observable along the horizontal axis. If we look at figure 6, we can also conclude that this condition is also met, thus validating our results.

BIBLIOGRAPHY

1. R. W. Collins, I. An, C. Chen, “Rotating polarizer and analyzer ellipsometry” en *Handbook of ellipsometry*, Eds. H. G. Tompkins, E. A. Irene, William Andrew Pub. (Nueva York, 2005).
2. G. E. Jellison, F. A. Modine, “Polarization modulation ellipsometry” en *Handbook of ellipsometry*, Eds. H. G. Tompkins, E. A. Irene, William Andrew Pub. (Nueva York, 2005).
3. D. Goldstein, *Polarized light*, 2nd ed., Estado Unidos de América : Marcel Dekker, 2003, p. 562
4. H. Gutiérrez Pulido, R. De la Vara Salazar, *Análisis y diseño de experimentos*, 2a ed., México : McGraw Hill, 2008, p. 180-182

Appendix B

Transmission Laser Ellipsometer
Business Plan

Dr. Geminiano Martínez Ponce
Dr. Cristina Solano Sosa
Eng. Alicia F. Torales Rivera

October 5th 2009

I. Theory

Photoelastic Modulator (PEM)

A photoelastic modulator causes a phase shift to change sinusoidally as a function of time. This phase shift is obtained by making the two perpendicular components of light pass through a waveplate at different speeds. This is achieved by inducing a time-varying birefringence by way of a time-varying stress in a normally isotropic material. An isotropic material will become anisotropic when stressed and will thus induce the same kind of birefringence as an anisotropic crystal like calcite.

The construction of a photoelastic modulator is shown in figure I.1. A piezoelectric transducer is a block of crystalline quartz cut at a specific orientation (-18°, Xcut)[1]. A metal electrode is deposited on each of two sides and the transducer is cut in such a way that it resonates at a specified frequency f. The resonance is uniaxial and is directed along the long axis of the crystal. A block of fused quartz is cemented to the end of the transducer. The length of the fused quartz is such that it also has f as the fundamental longitudinal resonance. When both elements are cemented together, resonance of the transducer causes a periodic strain in the fused quartz.

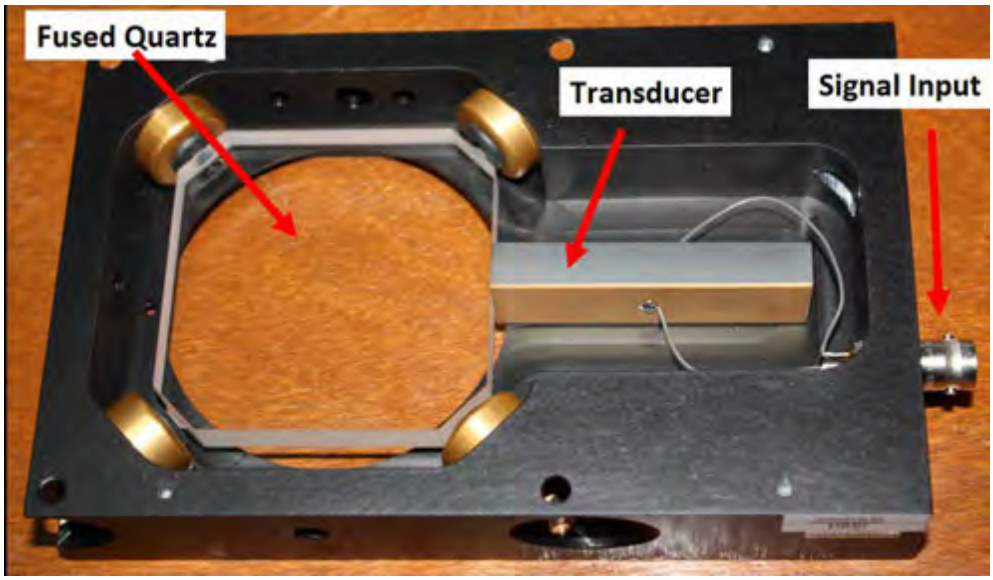

Figure I.1 – The components of a photoelastic modulator.

Dual PEM Systems in Polarimetry

A dual Photoelastic modulator system can obtain all four Stokes vectors simultaneously. The typical configuration for such an ellipsometer would be tuning the first PEM, P1, at frequency F1 and orientation of 0°, and the second PEM (P2) tuned at frequency F2 (where F2 is slightly different from F1). Furthermore, P2 must have an orientation of 45°. P2 is then followed by a linear polariser at 0°, as shown in figure I.2.

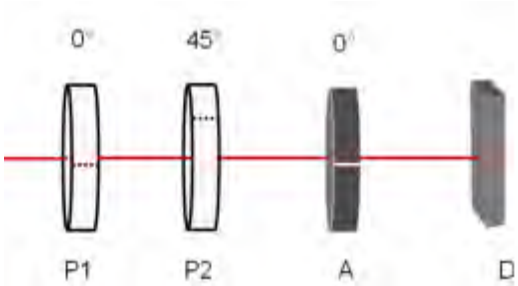

Fig. I.2 – Polarimetric system based on photoelastic modulators(P_1 y P_2).
A is a linear polariser (analyzer) and D is a photoreceptor.

II. Applications

Whether in transmission or reflection, certain materials can affect the polarisation state of light that interacts with them. This is due to intrinsic qualities and properties of said materials such as optical activity, chirality and reflectivity.

Applications for Dual PEM Systems range from the medical to the military.

Depending on the wavelength and other parameters, the system enables analysis and characterization of different materials (most of them organic in nature, but also certain reflecting materials). Such materials are used in medical analysis, holography, food processing and pharmaceutics, among others.

Properties and characteristics such as stress, defects, reflectivity, polarisation loss and polarisation mode of dispersion[2] may be determined with the instrument.

Other applications include thin film characterization and laser test and measurement.

III. Overview of the Device

The device is mainly composed out of two blocks: The polarisation generator block and the polarisation analysis block (see figure III-1).

The former is constituted by a linear polarizer (P1) with its transmission axis at 0°, followed by two liquid crystal retarders* (LCVR1 and LCVR2) oriented at 45° and 0° respectively.

Both LCVRs are controlled by means of a 2KHZ square wave signal of variable amplitude, generated by a function generator and controlled via software. Depending on the amplitudes of both signals, the LCVRs induce a retardation in the light, and hence, a change in polarization. Specific amplitude values are to be sent to the retarders in order to induce a known polarisation state.

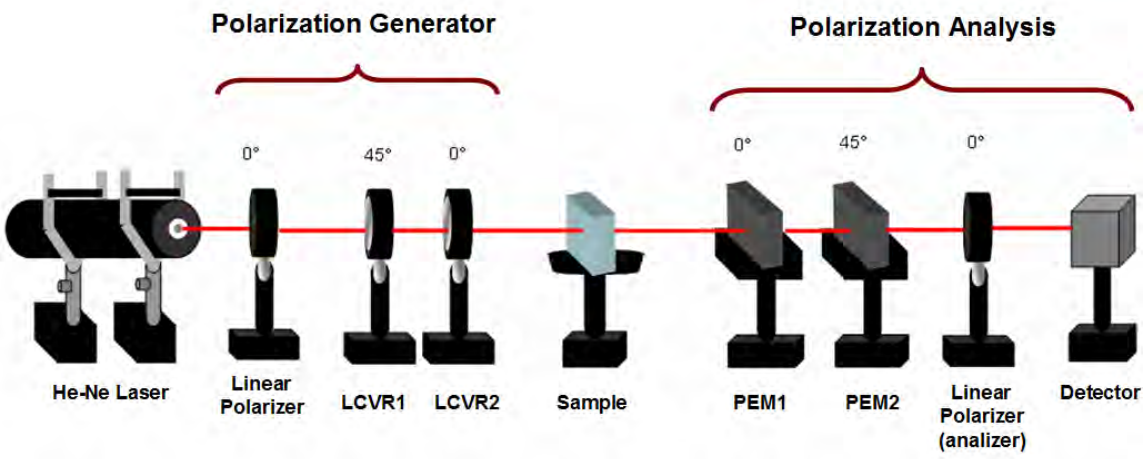

Figure III-1 : Element diagram of the device.

The second block, of polarisation analysis, is formed by two photoelastic modulators (PEM1 and PEM2), the first one being oriented at 0° and the second at 45°, followed by a second linear polarizer at 0° and a photodetector. Both modulators resonate at slightly different frequencies, and allow the incoming light to be modulated, thus sending a characteristic signal to the detector depending on the polarisation state of said light (figure III-2).

* Eventually, this pair of liquid cristal retarders will be replaced by a pair of photoelastic modulators, thus providing the system with a significantly greater speed response.

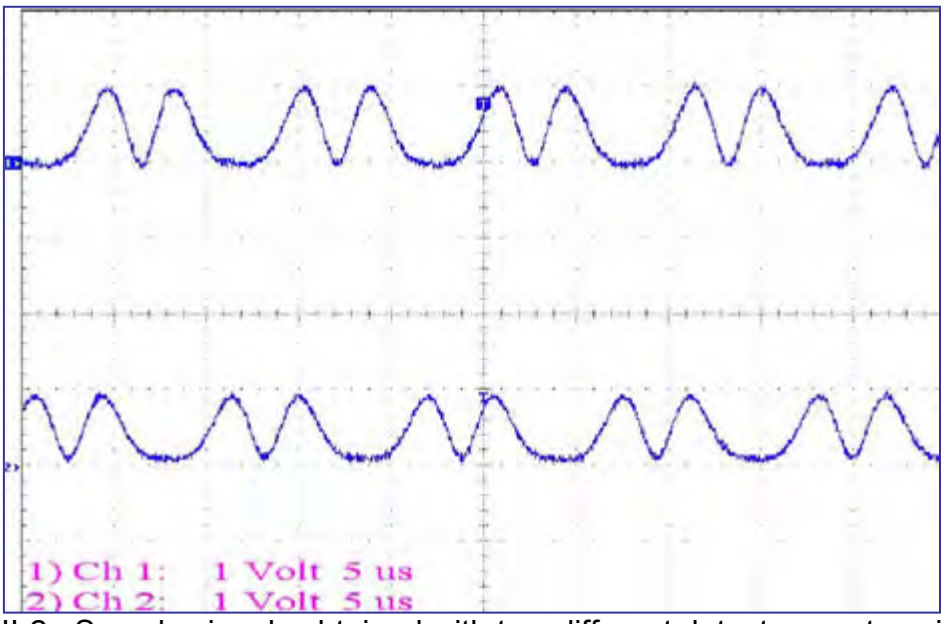

Figure III-2 : Sample signals obtained with two different detectors, outcoming from a dual modulator system.

The signal from the detector is then sent to a PC via an acquisition board, for analysis.

Using a Lock-In Amplifier, the obtained signal is analysed and the polarisation state is thus determined and displayed by the software.

With this knowledge, different characteristics about the sample may be obtained, such as composition and concentration.

In the final instrument, the detector will be replaced by a CCD camera, for analysis of a wider spectrum and variety of samples.

The device is to encompass as well a monochromator, enabling a wide selection of wavelengths, from ultraviolet to infrared, in order to broaden the scope of materials that can be studied.

Finally, a special mount will be designed to enclose all the constituting elements of the device and to provide mechanical mobility, both manual and automatic, to different parts so as to provide greater flexibility and versatility to the device.

IV. Justification: The need for this device

Although similar instruments are already available in the market, the instrument will enable analysis in both transmission and reflection, as opposed to most of those already on sale. Furthermore, what is probably the most attractive feature of this system, the instrument and proposed analysis will provide for a far more economic instrument, enabling easier access to the system. This way, we are confident

different areas of the industry and research fields will be interested in acquiring such an instrument. Lastly, we strive to produce a high speed response, capable of competing with other existing systems.

Lastly, a software user-friendly platform is being developed, which will enable the user not only to visualize the results in real-time, but also to control specific features of the system, such as mechanical rotation, start, pause and stop measurement, create a datalog for various successive measurements and specify the number of measurements for the system to make automatically without any needed intervention from the user.

V. STOW Analysis

Strengths	Opportunities	Weaknesses	Threats
Significantly lower cost compared to similar systems	Mexico and the rest of Latin America might prefer acquiring this system for its lower cost, shipping and customs expenses	System still under development	Continuous system upgrade for other instruments in the market
Works in both transmission and reflection	No similar system manufactured within the country	Lacking mechanical and electrical design of mount	Worldwide renown manufacturers as main competitors
Development of system not over costly	Food and pharmaceutics industry relatively strong in the Country	Lacking funding for equipment acquisition (i.e. CCD Camera)	People might prefer a much more costly system manufactured in the US or Europe
Mechanical mount for different types of samples and functioning modes	Medical instrumentation is getting stronger in the country among universities and hospitals	Dependence on another manufacturer regarding the modulators	The system is still years away from being launched into the market, by which time there may well be a similar yet affordable system already for sale
	Customers in Mexico wouldn't need to pay import taxes and the shipping would cost considerably less		

VI. Similar Products already on the Market

J.A. Woollam Co., Inc.

Ellipsometry Solutions
VASE®

According to the catalogue information, this ellipsometer can be used on materials research such as semiconductors, metals, and polymers. It has a spectral range of 193 to 2500 nm, which is achieved using a monochromator. Among the mentioned measurement capabilities there are reflection and transmission ellipsometry, depolarization and scatterometry. Furthermore, the device provides an acquisition rate of 0.1 to 3 seconds per wavelength, depending on reflectivity of sample, though for high accuracy measurements, in may take up to 20 seconds per wavelength.

J.A. Woollam Co., Inc.
Ellipsometry Solutions
M-2000®
According to the information provided by the manufacturer, this device is a spectroscopic ellipsometer mainly used for thin film characterization. It encompasses CCD detection for the entire spectrum (i.e. it is able to measure hundreds of wavelengths simultaneously) and offers different configurations.

One of the most attractive features of this device is its mechanical flexibility. The device's mount allows the incidence angle to be modified either manually or automatically. It also includes an automated focusing camera feature, for more accurate exploration of the sample.

Teledyne Judson Technologies
Policam II – Polarimetric Imaging Camera

Although still under development, this camera is already being promoted among the science community. Some of the main features this camera offers are CCD sensors, VGA or Megapixel sensor resolution, complete Stokes parameter measurement and a spectral bandwidth of 450-670 nm. The device will use a Firewire interface.

VII. Required resources and elements

As stated in the sections above, there are various elements constituting the whole device. In this section, we shall state both the main and complementary elements required for the system assembly and functioning, as well as experts and engineers to put the whole thing together and ensure its correct overall functioning.

Optical and electro optical elements:

Light Source (white, spectrum must include from UV to IR)
Monochromator
Dual System PEM modulators (1)

Dual System PEM modulators (2)
2 linear polarizers (select type)
Photodiode* (wavelength response : from UV to IR, high speed response
CCD Camera (wavelength response : from UV to IR)

Electronic Elements

Photodiode pre-amplifier (not purchased, but designed and manufactured by the research team)

- IC AD823AN
- 2 Identical Photodiodes
- (3) 33.2 KW resistors
- (2) 100 KW resistor
- 1pF capacitor
- 7.5 pF capacitor
- 100 nF capacitor
- Power Source (±15 V)
- Metallic encasing for the circuit in order to minimize noise

Acquisition and transmission card (currently under development)

This card is to be designed and manufactured by the research team, with two objectives in mind: first, to reduce the cost of the entire product and second, to make the system as independent from other companies as possible.

Additionally, this card will be designed specifically for the system, that is to say, it will be made to meet the particular needs of the instrument, including sampling rate, required signal outputs and inputs and voltage specifications.

This card will be controlled via the instrument's software, which is also under current development.

The list of components that will be used for the card is shown in the table below:

Element/System	Quantity
PIC18F4553	1
MASTER-PROG	1
SOCKET	1
QUARTZ CRYSTAL	1
USB CONNECTOR	1
USB CABLE	1
BREADBOARD	1
CABLE (mtr)	2

* Currently, the photodiode model 13 DSH 005 from Melles Griot is being used.

CONNECTORS	15
RED LEDS	2
GREEN LEDS	2
Micro switch	4
FENOLIC PLATES	3
PNP BLUE SHEETS	3
NE555	3
IC AD823AN	6
DIODES	6
DIODE BRIDGE.	1
TRANSF.	1
MC7912	1
MC7812	1
ZENER DIODE	2
FERRIC CLORIDE	1
CP. DE 100UF	5
CP. DE 4.7 UF	5
CAP DE 1NF	6
CAP 2200 UF A 25 VOLTS	2
CAP 33 PF	10
CAP 47 NF	10
CAP 10NF	10
CAP 470 PF	10
CAP 22 PF	10
CAP 470 PF	10
CAP 27 Pf	2
CAP 100mF	8
CAP .1mF	6
R 4.7 K	4
R 470 OHMS	10
R 1 K	10
R 22k OHMS	10
R 27k OHMS	10
R 15k OHMS	5
R 100k OHMS	5
R 33k OHMS	10

Software resources

As previously mentioned, the system is to be controlled via a computer and its own software. From among the different platforms that could enable the creation of this software, LabVIEW™, from National Instruments™ was chosen because of the ease of use, versatility and tools it offers. Furthermore, an acquisition card, also from National Instruments™, is currently being used for testing, while the system's own card is completed.

VIII. Manufacturing process

Mechanical Mount

The design and implementation of the mount must go through various stages in order for it to function.

The mount will have to modes of operation: Manual and Automatic.

This requirement encompasses the need for both a mechanical and an electrical design. Requirements for the subsystem are yet to be defined, but it will definitely be controlled via the same software, generated in LabView and make use of one or more stepper motors for automatic movement.

Data Acquisition and Transmission Card

This card will have essentially two constituent elements, the electronical and he programming.

The control of the data I/O will be controlled using a programmed microprocessor, which will in turn be implemented in the final circuit board. The signal generation, filtering and signal conditioning will be managed with operational amplifiers and other active and passive elements yet to be determined.

VIII. Cost analysis and comparison

The total cost for the circuits' elements is shown above. Both the detector circuits and the card circuits are considered.

Element/System	Cost per unit	Qty	Total	Details
IC AD823AN	$180.00	5	$900.00	Instrumentation Amplifier for better performance
Photodiodes (FDS010)	$558.83	4	$2,235.33	Must be identical
33.2 KW resistors	$1.00	6	$6.00	1/4 watt

100 KW resistor	$1.00	4	$4.00	1/4 watt
1pF capacitor	$3.00	2	$6.00	ceramic @ 60 V
7.5 pF capacitor	$3.00	2	$6.00	ceramic @ 60 V
100 nF capacitor	$3.00	2	$6.00	ceramic @ 60 V
Metallic encasing	$30.00	2	$60.00	For noise reduction
PIC18F4553	$120.00	1	$120.00	40-PIN PDIP
MASTER-PROG	$450.00	1	$450.00	universal programmer for Pics
SOCKET	$6.00	1	$6.00	40 PIN
QUARTZ CRYSTAL	$12.00	1	$12.00	20 MHZ
USB CONNECTOR	$12.00	1	$12.00	USB CONECTOR B TYPE
USB CABLE	$54.00	1	$54.00	I/O A & B
BREADBOARD	$93.00	1	$93.00	
CABLE (mtr)	$12.00	2	$24.00	UTP
CONNECTORS	$8.00	15	$120.00	w/screws
RED LEDS	$3.00	2	$6.00	3mm.
GREEN LEDS	$3.00	2	$6.00	3mm.
Micro switch	$4.00	4	$16.00	Switch 2 termin.
FENOLIC PLATES	$16.00	3	$48.00	10x15cm
PNP BLUE SHEETS	$64.00	3	$192.00	For printing circuit boards
NE555	$7.00	3	$21.00	Linear signal generator
IC AD823AN	$180.00	6	$1,080.00	AD823AN
DIODES	$2.00	6	$12.00	1N4004
DIODE BRIDGE.	$10.00	1	$10.00	
TRANSF.	$130.00	1	$130.00	12 VOL. 1.2 AMP
MC7912	$10.00	1	$10.00	VOLTAGE REGULATOR
MC7812	$10.00	1	$10.00	VOLTAGE REGULATOR
ZENER DIODE	$6.00	2	$12.00	ZENER DIODE ½ WATT
FERRIC CLORIDE	$71.00	1	$71.00	930 ML
CP. DE 100UF	$3.00	5	$15.00	ceramic @ 60 V
CP. DE 4.7 UF	$3.00	5	$15.00	ceramic @ 60 V
CAP DE 1NF	$3.00	6	$18.00	ceramic @ 60 V
CAP 2200 UF A 25 VOLTS	$3.00	2	$6.00	ceramic @ 60 V
CAP 33 PF	$3.00	10	$30.00	ceramic @ 60 V
CAP 47 NF	$3.00	10	$30.00	ceramic @ 60 V
CAP 10NF	$3.00	10	$30.00	ceramic @ 60 V
CAP 470 PF	$3.00	10	$30.00	ceramic @ 60 V

CAP 22 PF	$3.00	10	$30.00	ceramic @ 60 V
CAP 470 PF	$3.00	10	$30.00	ceramic @ 60 V
CAP 27 Pf	$3.00	2	$6.00	ceramic @ 60 V
CAP 100mF	$3.00	8	$24.00	25 VOLTS MIN.
CAP .1mF	$3.00	6	$18.00	25 VOLTS MIN.
R 4.7 K	$1.00	4	$4.00	1/2 Watt
R 470 OHMS	$1.00	10	$10.00	1/2 Watt
R 1 K	$1.00	10	$10.00	1/2 Watt
R 22k OHMS	$1.00	10	$10.00	1/2 Watt
R 27k OHMS	$1.00	10	$10.00	1/2 Watt
R 15k OHMS	$1.00	5	$5.00	1/2 Watt
R 100k OHMS	$1.00	5	$5.00	1/2 Watt
R 33k OHMS	$1.00	10	$10.00	1/2 Watt
Total Cost			**$6,084.33**	

Note: Prices are in Mexican Pesos

The system will include its own function generator, power supply and some other necessary equipment for the instrument to function properly. However, for comparison purposes only, we consider the cost of the equipment should it be acquired separately, as will be the case of some of the following components:

Element/System	Cost per unit	Qty	Total	Details
Power Supply (±15)	$6,497.12	1	$6,497.12	3 Amperes
Function Generator	$8,816.55	3	$26,449.64	
Monochromator	$29,596.47	1	$29,596.47	
Light source	$23,424.89	1	$23,424.89	White light (from UV to NIR)
Polarizer (Glan-Thompson)	$5,886.74	2	$11,773.48	
Beam Splitter	$3,730.08	1	$3,730.08	
Photoelastic Modulators (Dual Syst.)	$209,070.87	2	$418,141.74	
Data Acquisition Card (National Instruments)	$26,110.55	1	$26,110.55	
CCD Camera (Edmund Optics)	$47,812.82	1	$47,812.82	
Total			**$593,536.79**	

Note: Prices are in Mexican Pesos

As a whole a system like this in the market, including shipping expenses and taxes would cost around US$126,636.39 (see attached quotation) which translates to $1,717,685.86 in mexican pesos.

As for the system we propose, the approximate costs would be as follows,

Power Supply (±15)	$1,000.00	1	$1,000.00	3 Amperes
Lock-in Amplifier	$300.00	3	$900.00	
Monochromator	$29,596.47	1	$29,596.47	
Light source	$23,424.89	1	$23,424.89	White light (from UV to NIR)
Polarizer (Glan-Thompson)	$5,886.74	2	$11,773.48	
Beam Splitter	$3,730.08	1	$3,730.08	
Photoelastic Modulators (Dual Syst.)	$209,070.87	2	$418,141.74	
Data Acquisition Card (Manufactured)	$3,000.00	1	$3,000.00	
CCD Camera (Edmund Optics)	$47,812.82	1	$47,812.82	
Total			**$539,379.48**	

Note: Prices are in Mexican Pesos